



저작자표시-비영리-변경금지 2.0 대한민국

이용자는 아래의 조건을 따르는 경우에 한하여 자유롭게

- 이 저작물을 복제, 배포, 전송, 전시, 공연 및 방송할 수 있습니다.

다음과 같은 조건을 따라야 합니다:



저작자표시. 귀하는 원저작자를 표시하여야 합니다.



비영리. 귀하는 이 저작물을 영리 목적으로 이용할 수 없습니다.



변경금지. 귀하는 이 저작물을 개작, 변형 또는 가공할 수 없습니다.

- 귀하는, 이 저작물의 재이용이나 배포의 경우, 이 저작물에 적용된 이용허락조건을 명확하게 나타내어야 합니다.
- 저작권자로부터 별도의 허가를 받으면 이러한 조건들은 적용되지 않습니다.

저작권법에 따른 이용자의 권리는 위의 내용에 의하여 영향을 받지 않습니다.

이것은 [이용허락규약\(Legal Code\)](#)을 이해하기 쉽게 요약한 것입니다.

[Disclaimer](#)

**Doctor of Philosophy**

**An experimental study on the enhancement of mechanical properties of glass fiber reinforced polyester composite based on optimum conditions and adding multi-walled carbon nanotubes**

**The Graduate School  
of the University of Ulsan  
Department of Mechanical Engineering  
Van-Tho Hoang**

**An experimental study on the enhancement of mechanical properties of glass fiber reinforced polyester composite based on optimum conditions and adding multi-walled carbon nanotubes**

**Supervisor: Professor Young-Jin Yum**

**A Dissertation**

**Submitted to**

**the Graduate School of the University of Ulsan**

**In partial Fulfillment of the Requirements**

**for the Degree of**

**Doctor of Philosophy**

**by**

**Van-Tho Hoang**

**Department of Mechanical Engineering**

**Ulsan, Korea**

**May, 2018**

Van-Tho Hoang 의  
공학박사 학위 논문을 인준함

심사위원장

주석재

주석재

심사위원

유희

유희

심사위원

이경식

이경식

심사위원

천두만

천두만

심사위원

염영진



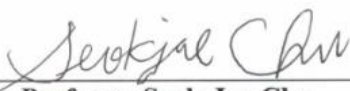
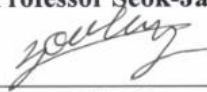
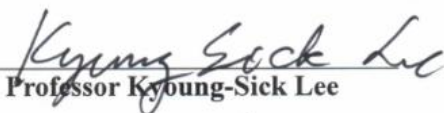
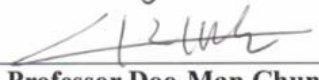
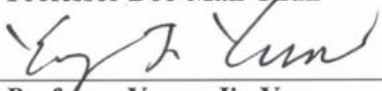
울산대학교 대학원

기계자동차공학과

2018 년 5 월

**An experimental study on the enhancement of mechanical properties of glass fiber reinforced polyester composite based on optimum conditions and adding multi-walled carbon nanotubes**

**This certifies that the dissertation  
of Van-Tho Hoang is approved.**

<b>Committee Chairman</b>	 <b>Professor Seok-Jae Chu</b>
<b>Committee Member</b>	 <b>Doctor Hee You</b>
<b>Committee Member</b>	 <b>Professor Kyung-Sick Lee</b>
<b>Committee Member</b>	 <b>Professor Doo-Man Chun</b>
<b>Committee Member</b>	 <b>Professor Young-Jin Yum</b>

**Department of Mechanical Engineering**

**Ulsan, Korea**

**May, 2018**

## ACKNOWLEDGEMENTS

First of all, I would like to express my deepest gratitude to my advisor Professor Young-Jin Yum for his guidance and support throughout my Ph.D. study, especially his kindly encouragement in not only doing research but also in my daily life. It cannot be denied that he virtually recovers and refreshes my mind in even some tremendous circumstances from his mild and positive thinking.

I would like to thank the Professors in the school of Mechanical Engineering at the University of Ulsan for their great knowledge that I have learned. I would also express my gratitude to the doctoral committee members: Prof. Seok-Jae Chu, Doctor Hee You, Prof. Kyoung-Sick Lee, and Prof. Doo-Man Chun for their helpful feedback, suggestions and comments to evaluate my work.

My acknowledgement is also sent to all of my friends who are always heartfelt in their sharing, advice, and help me. They are indispensable to make me stronger and more confident. Besides, thank you my colleagues in my own country as well as my lab mates for their kindly helps.

The last but not least thank is for all of my family members. Words cannot express my gratitude for everything they have done to make me into who I am. I hope I have made them proud. I am thankful to my wife for love, care, and sharing with me every moment of this incredible journey. I am looking forward to our better life.

Ulsan city, Republic of Korea

May, 2018

**Van-Tho Hoang**

## **ABSTRACT**

Glass fiber reinforced polymer composites have been utilized as alternative materials for many decades to avoid exhausting natural resources. In addition, the applications of this material have been increasing widely. Thus, improving mechanical properties of composite materials plays a critical role in satisfying needs in real-life situations. Nowadays, adding multi-walled carbon nanotubes (MWCNTs) has been showing as a high potential method due to their superlative mechanical properties. Motivated by this tendency, the optimum conditions were found beside adding MWCNTs to increase mechanical properties and fracture toughness of conventional composites. First of all, the simple dispersion method was chosen to mix MWCNTs into unsaturated polyester resin (UPR). Some optimal conditions were proposed such as mixing temperature, initial curing temperature, hardener content, fiber changes, composite fabrication methods, and MWCNTs content. Higher mechanical properties of separated UPR and glass fiber reinforced UPR composites were obtained. Furthermore, some other test methods were performed to verify the effects of optimum factors and adding MWCNTs such as exothermic temperature measurement, thermal gravimetric analysis (TGA), density measurement, and field emission scanning electron microscope (FE-SEM). The higher mechanical properties and simple fabrication method can be recommended to develop efficiently the properties of mass products.

# CONTENTS

ACKNOWLEDGEMENTS .....	v
ABSTRACT .....	vi
CONTENTS .....	vii
LIST OF FIGURES .....	xii
LIST OF TABLES .....	xv
ABBREVIATIONS .....	xvi
<b>CHAPTER 1: Introduction</b> .....	1
1.1 Materials .....	5
1.1.1 Unsaturated polyester resin (UPR).....	5
1.1.2 Glass fibers.....	8
1.1.3 Multi-walled carbon nanotubes (MWCNTs) .....	11
1.2 Application of glass fiber reinforced polymer (GFRP) .....	11
1.3 Literature review .....	14
1.3.1 The methods of increasing mechanical properties and fracture toughness of GFRP composite materials.....	14
1.3.2 Composite structure modification .....	14
1.3.3 Dispersion method.....	15
1.4 Objectives and contents of dissertation .....	15
1.4.1 Objectives of dissertation .....	15
1.4.2 Thesis outline .....	16
<b>CHAPTER 2: Optimization of fabrication conditions</b> .....	17
2.1 Introduction.....	18
2.2 The effect of mixing temperature .....	19



2.2.1 Materials and evaluation method .....	19
2.2.2 Experiment .....	20
2.2.3 Results and discussion.....	21
2.2.4 Conclusions .....	23
2.3 The effect of hardener ratio .....	23
2.3.1 Materials and evaluation methods.....	23
2.3.2 Experiment .....	23
2.3.3 Results and discussion.....	24
2.3.3.1 <i>Compression properties</i> .....	24
2.3.3.2 <i>Exothermic temperature</i> .....	26
2.3.4 Conclusions .....	27
2.4 The effect initial curing temperature .....	28
2.4.1 Materials and evaluation methods.....	28
2.4.2 Experiment .....	28
2.4.3 Results and discussion.....	29
2.4.3.1 <i>Curing behavior of UPR</i> .....	29
2.4.3.2 <i>Density of UPR</i> .....	31
2.4.3.3 <i>Thermo-gravimetric analysis of UPR</i> .....	32
2.4.3.4 <i>Tensile properties of GFPR composites</i> .....	32
2.4.4 Conclusions .....	33
2.5 The potential of combining CSM and woven .....	34
2.5.1 Materials and evaluation methods.....	34
2.5.2 Experiment .....	34
2.5.3 Results and discussion.....	34

2.5.3.1	<i>Thermo-gravimetric analysis of various fibers composites</i> .....	34
2.5.3.2	<i>Tensile properties of various fibers composites</i> .....	36
2.5.4	Conclusions .....	37
2.6	The effect of fabrication method of GFRP composites .....	37
2.6.1	Materials and evaluation methods.....	37
2.6.2	Experiment .....	38
2.6.3	Results and discussion.....	38
2.6.3.1	<i>Density of composite structures</i> .....	38
2.6.3.2	<i>Thermo-gravimetric behavior of composite structures</i> .....	39
2.6.3.3	<i>Tensile properties of composite structures</i> .....	41
2.6.4	Conclusions .....	43
<b>CHAPTER 3:</b>	<b>Effect of multi-walled carbon nanotubes on tensile properties of</b>	
	<b>unsaturated polyester resin</b> .....	<b>43</b>
3.1	Introduction.....	44
3.2	Experiment.....	45
3.2.1	Materials.....	45
3.2.2	Fabrication of MWCNTs/ UPR specimens.....	45
3.2.3	Measurements.....	47
3.2.3.1	<i>Tension testing</i> .....	47
3.2.3.2	<i>Observation of fracture surfaces</i> .....	47
3.3	Results and discussion .....	48
3.3.1.	Tensile properties of nanocomposite.....	48
3.3.2	Fracture surface observation results .....	51
3.4	Conclusions.....	54

<b>CHAPTER 4: Effect of multi-walled carbon nanotubes on tensile properties of various glass fibers/ unsaturated polyester resin composites .....</b>	<b>55</b>
4.1 Introduction.....	56
4.2 Experiment.....	59
4.2.1 Materials.....	59
4.2.2 Fabrication.....	60
4.2.2.1 <i>Matrix modification</i> .....	60
4.2.2.2 <i>Composite structure fabrication</i> .....	60
4.2.3 Measurements.....	61
4.3 Results and discussion .....	61
4.4 Conclusions.....	64
<b>CHAPTER 5: Fracture toughness of neat UPR and various glass fibers composites.....</b>	<b>65</b>
5.1 Introduction.....	66
5.2 Experiment.....	68
5.2.1 Materials.....	68
5.2.2 Fabrication.....	68
5.2.2.1 <i>Single-edge-notch bending (SENB) specimen for UPR</i> .....	68
5.2.2.2 <i>Double cantilever beam (DCB) and end-notched flexural (ENF) specimen for composites</i> .....	71
5.2.3 Testing.....	72
5.3 Calculations .....	73
5.3.1 Plane-strain fracture toughness $K_{IC}$ of UPR (ASTM D5045-99).....	73
5.3.2 Mode I interlaminar fracture toughness of various glass fibers reinforced UPR composites (ASTM D5528-13).....	75

5.3.3 Mode II interlaminar fracture toughness of various glass fibers reinforced UPR composites (ASTM D7905/D7905M-14) .....	78
5.4 Results and discussion .....	80
5.4.1 Effect of pre-crack method on the behavior of UPR.....	80
5.4.1.1 Morphology .....	80
5.4.1.2 Plane-strain fracture toughness $K_{IC}$ and $G_{IC}$ of UPR .....	84
5.4.2 Effect of different fibers on interlaminar fracture toughness of composites.....	85
5.4.2.1 Mode I.....	85
5.4.2.2 Mode II .....	88
5.5 Conclusions.....	89
<b>CHAPTER 6: Conclusions and future works.....</b>	<b>90</b>
6.1 Conclusions.....	91
6.2 Future works .....	92
REFERENCES .....	93
RESEARCH ACTIVITIES .....	101

## LIST OF FIGURES

Figure 1-1: The families of engineering materials .....	3
Figure 1-2: Strength versus density of engineering materials .....	3
Figure 1-3: Evolution of engineering materials until 2020 .....	4
Figure 1-4: Unsaturated polyester resin (UPR) .....	7
Figure 1-5: Methyl ethyl ketone peroxide (MEKP) .....	7
Figure 1-6: Specific properties of metals and composites.....	8
Figure 1-7: Effect of fiber volume fraction of different fibers on mechanical properties and cost of their composites. ....	9
Figure 1-8: Woven roving .....	10
Figure 1-9: Chopped strand mat .....	10
Figure 1-10: Multi-walled carbon nanotubes (CM-130).....	11
Figure 1-11: GFRP products .....	13
Figure 2-1: The shape of compression specimen .....	20
Figure 2-2: Compressive stress-strain behavior of UPR at various mixing temperatures... 21	
Figure 2-3: Compression specimens of UPR fabricated at different mixing temperatures. 22	
Figure 2-4: Monitoring exothermic reaction .....	24
Figure 2-5: Compression stress-strain relation of UPR with different MEKP contents. .... 25	
Figure 2-6: Variation of curing temperature of UPR with different MEKP contents .....	27
Figure 2-7: Curing behavior for different initial curing temperatures .....	30
Figure 2-8: Tensile properties of CSM/woven/CSM/woven for the different fabrication temperatures.....	33
Figure 2-9: Effect of fibers on the thermo-gravimetric behavior of the composites.....	36
Figure 2-10: Tensile properties of composite structures with different of fiber components .....	37
Figure 2-11: Effect of vacuum on the density of composite structures.....	39
Figure 2-12: Effect of vacuum on the thermo-gravimetric behavior of GFRP composites 41	
Figure 2-13: Effect of vacuum on the tensile strength of composite structures .....	42

Figure 2-14: Effect of vacuum on the elastic modulus of composite structures .....	43
Figure 3-1: Tensile test specimen parameters (unit: mm) .....	46
Figure 3-2: Hot and stir machine .....	46
Figure 3-3: Aluminum casting mold .....	47
Figure 3-4: Tensile behavior of nanocomposite with difference MWCNTs ratios .....	50
Figure 3-5: Dispersion of MWCNTs in UPR .....	51
Figure 3-6: Morphology of fracture surfaces .....	53
Figure 4-1: Effects of MWCNTs on the tensile strength of various fibers composite .....	63
Figure 4-2: Effects of MWCNTs on the elastic modulus of various fibers composite .....	63
Figure 5-1: Aluminum mold for casting UPR .....	69
Figure 5-2: The shape and parameter of SENB specimen .....	69
Figure 5-3: UPR after casting in aluminum mold .....	70
Figure 5-4: Configuration of mode I and mode II specimens .....	71
Figure 5- 5: Configuration of mode I and mode II specimens .....	73
Figure 5-6: Load-displacement curve of UPR .....	74
Figure 5-7: Determination of correcting delamination length (Figure 4, Ref. 103) .....	76
Figure 5-8: Linear regression function of cube root of compliance and delamination length .....	77
Figure 5-9: Load, displacement, and delamination length of mode I test .....	77
Figure 5-10: Load - displacement curve of different crack length in fracture test .....	79
Figure 5-11: Linear regression function of compliance and delamination length cubed ....	79
Figure 5-12: The notch of SENB specimen after curing .....	80
Figure 5-13: The configuration and surfaces of specimen after fracture test .....	83
Figure 5-14: Fracture surface of UPR after fracture test: (a) 2D model and (b) 3D model	83
Figure 5-15: Critical stress intensity factor of different pre-crack methods .....	84
Figure 5-16: Delamination resistance curves with different fibers composites .....	86

Figure 5-17: Mode I interlaminar fracture toughness of various glass fibers composite ....	87
Figure 5-18: Fiber bridging of different glass fibers composite.....	87
Figure 5-19: Mode II fracture toughness of different glass fibers composite .....	88
Figure 5-20: The specimens after mode II fracture test.....	89

## LIST OF TABLES

Table 2-1: Compression properties of UPR at various mixing temperatures.....	22
Table 2-2: Compression properties of UPR based on the difference of hardener ratios .....	26
Table 2-3: Density of the materials. ....	31
Table 2-4: Density of UPR for the different initial curing temperatures.....	31
Table 2-5: Thermal behavior of UPR for the different initial curing temperatures. ....	32
Table 4-1: Fiber weight fraction in different cases.....	61
Table 5-1: The shape of pre-crack with different methods. ....	81
Table 5-2: The surface of pre-crack after fracture test. ....	81
Table 5-3: The difference in pre-crack method. ....	85
Table 5-4: $G_{IC}$ of the different pre-crack methods. ....	85



## **ABBREVIATIONS**

- PMCs : Polymer matrix composites
- FRP : Fiber reinforced plastic
- GFRP : Glass fiber reinforced plastics
- UPR : Unsaturated polyester resin
- MEKP : Methyl ethyl ketone peroxide
- CSM (M): Chopped strand mat (Mat)
- W : Woven (Roving)
- CNTs : Carbon nanotubes
- SWCNTs: Single-walled carbon nanotubes
- DWCNTs: Double-walled carbon nanotubes
- MWCNTs: Multi-walled carbon nanotubes
- FE-SEM: Field emission scanning electron microscopy
- ASTM : American Society for Testing and Materials
- SENB : Single-edge-notch bending
- CT : Compact tension
- DCB : Double cantilever beam
- ENF : End-notched flexural
- LEFM : Linear elastic fracture mechanics

# **CHAPTER 1:**

## **Introduction**

The first composite materials were used at around the 1,500 B.C. by mixing mud and straw to create strong and durable buildings. The definition of composite materials has been likely started from that time and has not changed until now [1]. The objectives of composite materials are almost conserved historically in order to obtain the better mechanical and physical properties, light weight etc. The improvement can be obtained from each component or all of them as long as improved reinforcement and/or improved matrix combined.

The time has been going with so many events in all over the world such as World War 1, 2. The composite materials have been also improving to adapt the specific purposes. In the early 1,900s, some plastics were found as vinyl, polystyrene, phenolic, and polyester [2]. In 1935, the first glass fiber were known when it was combined with a plastic polymer by Owen Corning [2]. From that time fiber reinforced polymers (FRP) became well-known in industry as well as in military aircraft due to the lightweight and strong alternative materials [2]. In 1946, FPR was used in boat hull commercially after lower demand from military products [2]. And, nowadays, it is a common materials with other wider applications such as electronics, home and furniture, medical, automobile etc. [3, 4]. Indeed, FRP has been used as alternative materials to avoid exhausting natural resources and it also exhibits the desirable characteristics including low density, high specific strength, high specific modulus, high corrosion resistance, and low cost [1]. Additionally, Michael F. Ashby [5] has listed the families of engineering material (Figure 1-1), their mechanical strength (Figure 1-2), and the evolution until 2020 (Figure 1-3) for the selection in mechanical design. It is not only convenient for design procedure but also helpful to understand easily the role of composite materials in the material world.

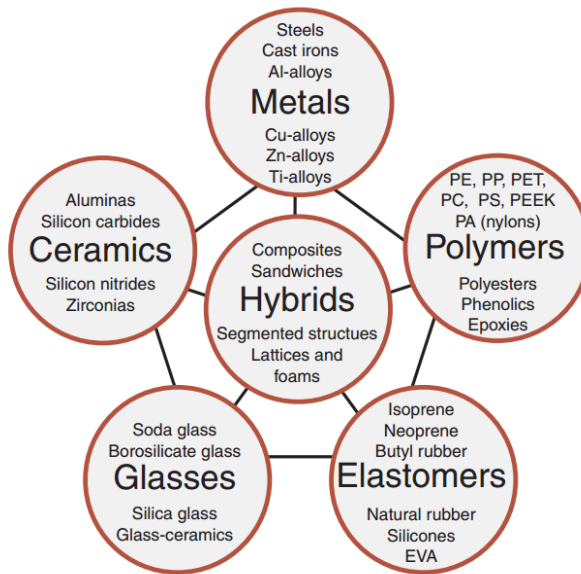


Figure 1-1: The families of engineering materials [Figure 3.1, Ref. 5]

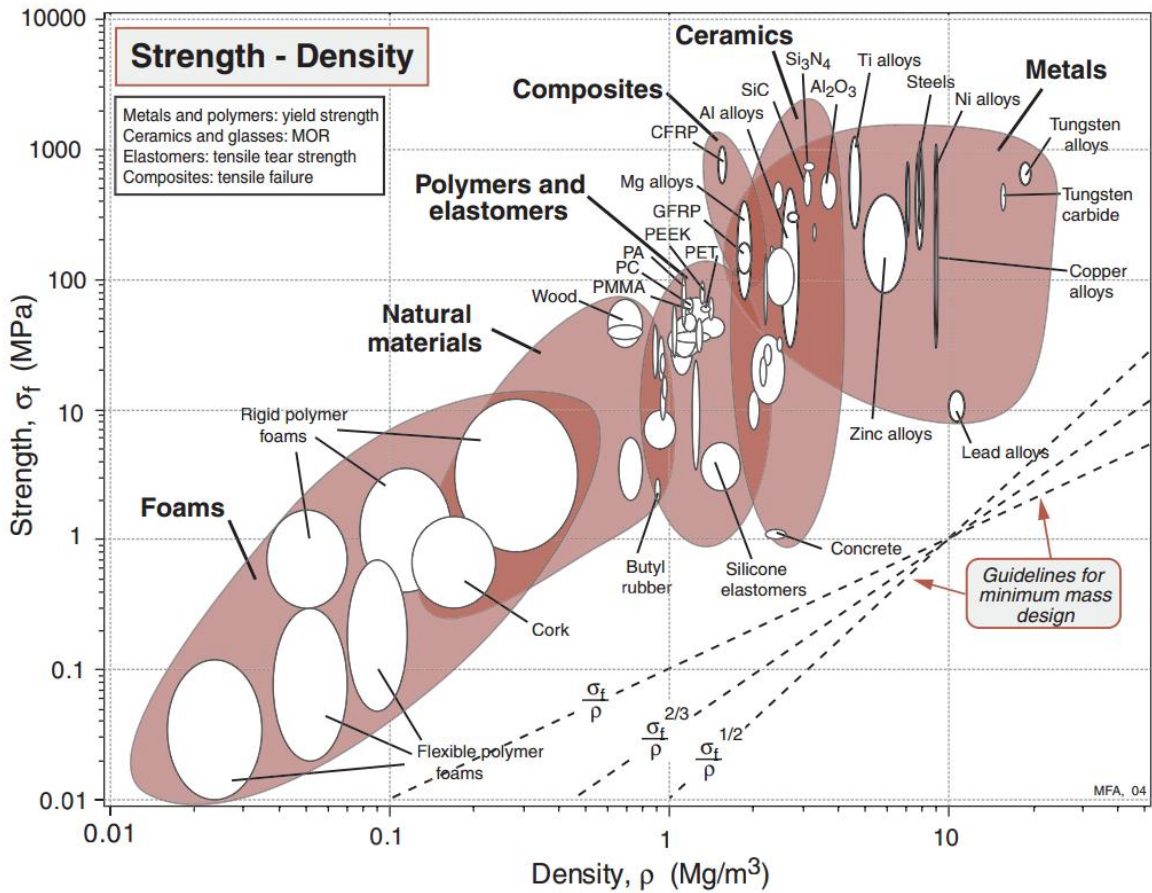


Figure 1-2: Strength versus density of engineering materials [Figure 4.4, Ref. 5]

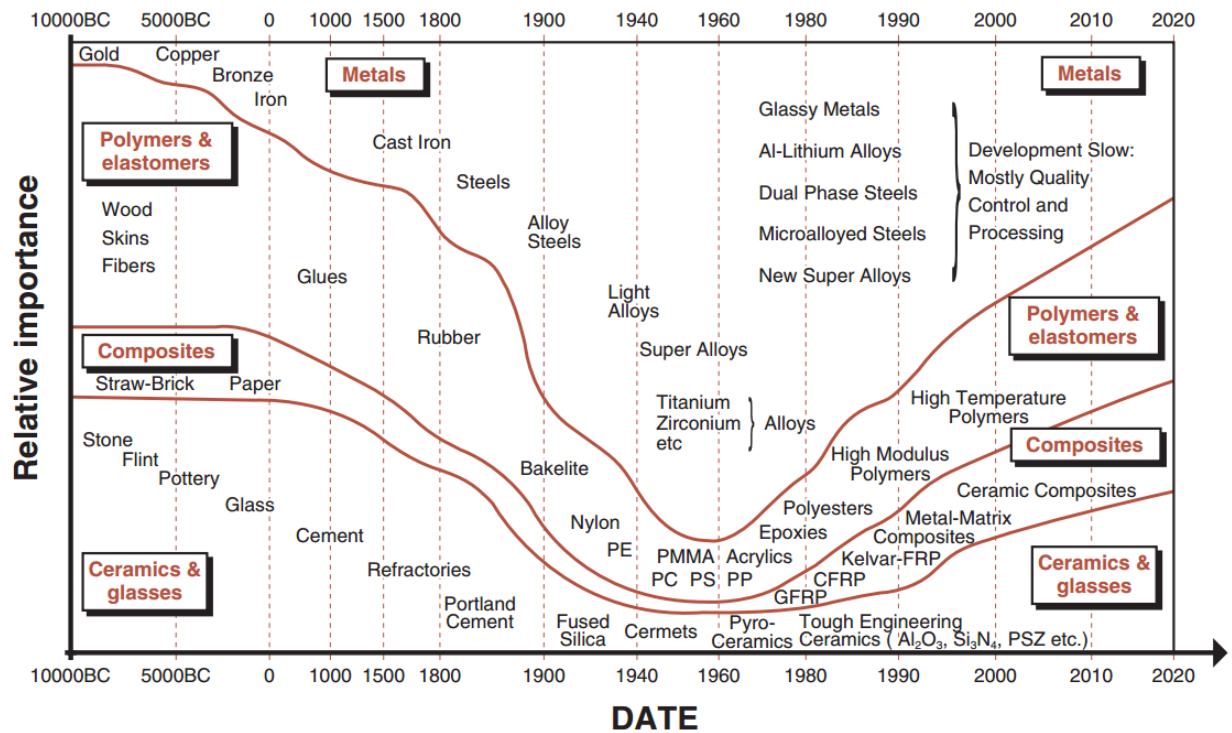


Figure 1-3: Evolution of engineering materials until 2020 [Figure 1.1, Ref. 5]

There are totally four classes of matrix materials, they are polymers, metals, ceramics, and carbon while polymer matrix composites (PMCs) are by far the most widely used types [6]. Thermosets and thermoplastic are two major classes of polymers. And thermosetting polymers are by far the most widely used matrix resins for structural applications due to its advantages. The main characteristic of thermosetting polymers is to undergo a curing process, after that they are rigid and cannot be reformed. On the other hand, thermoplastics can be reused by application of heat [6]. FRP has been known well as fibers reinforced thermosetting resin composites. Many manufacturing methods were born not only to adapt the vital applications and their scale in industry but also to improve the properties and quality of composites [3, 7]. For the open mold process, hand lay-up and spray up methods are commonly used to fabricate FRP [7]. The quality of "second surface" of products can be provided better by closed mold process including matched-die, resin

injection molding, compression molding, transfer molding (vacuum bag molding/ resin transfer molding/ vacuum infusion), press molding, autoclave molding methods [7]. Vacuum assisted hand lay-up method is combined manual stacking method and vacuum, that is not a current method but it can produce a appropriate quality and mechanical properties of composites.

The demand of increasing mechanical and physical properties of composite materials is unstoppable. The complicated working environment of various applications has been motivated to find better products. Nowadays, fabrication technology is strongly developing that can promote to create better composite material generations. Especially, the appearance of graphene and carbon nanotubes (CNTs) that have been expressed the superlative properties in mechanical, electrical, and chemical prospects. There are many related researches that have been utilizing these subjects to build nano-composite materials.

In this dissertation, tensile properties of thermosetting resin (unsaturated polyester resin) and various glass fiber/ unsaturated polyester resin are focused. To understand fully mechanical behavior and fracture toughness of FRP composites, multi-walled carbon nanotubes were also used based on some optimum fabrication conditions without any chemical treatment.

## **1.1 Materials**

### **1.1.1 Unsaturated polyester resin (UPR)**

Unsaturated polyester resin is the solutions of unsaturated polyester and vinyl monomers (reactive diluents) in form of three dimensional network backbone [8]. The viscosity of UPR is reduced from the high range  $10^3 - 10^5$  (mPa.s or cps) of unsaturated

polyester to much lower range of 100 - 500 cps due to the reactive diluents. Compared to the Newtonian fluid (water) with 1 cps, we can see UPR has so high viscosity.

The curing behavior is the specific characteristic of UPR, that was presented deeply in the reference [8] as follows: The curing reaction of UPR is a free radical chain growth cross-linking polymerization between the reactive diluents (styrene monomers) and unsaturated resin. While, polyester molecules are the cross-linkers and reactive diluents work as agent to link the adjacent polyester molecules. At the room temperature, methyl ethyl ketone peroxide (MEKP) is used as initiator for large hand lay-up structures. The curing of UPR leads to volume shrinkage. When the reaction starts, the initiator decomposes to form free radicals initiating polymerization which link adjacent unsaturated resin chains through connecting styrene monomers by both inter- and intra-molecular reactions (three dimensional network). As the polymerization continues, the temperature and degree of polymerization increases causes shrinkage. The polymerization shrinkage of UPR phase causes a large stress in monomer phase leading to formation of micro-voids. The polymer coils get tightened up to form the so-called "micro-gel" structure. The concentration of the micro-gel increase continuously leading to macro-gelation. The curing process of UPR can be divided into four stages: induction, micro-gel formation, transition, and macro-gelation. In the induction period, the free radicals are consumed by the initiator and very little polymerization takes place. In the second stage, spherical structures (micro-gel particles) with high cross-link density are formed. In transition stage the (C=C) double bonds buried inside the micro-gel undergo intra-molecular cross-linking while those on surface react with micro-gels. This results in growth of micro-gel. Finally macro-gelation takes place by inter-molecular micro-gels and micro-gel clusters including a sharp increase in viscosity of UPR.

The commercial UPR and MEKP are shown in figure 1-4 and 1-5, respectively that were made by Aekyung chemical company in South Korea.



Figure 1-4: Unsaturated polyester resin (UPR)



Figure 1-5: Methyl ethyl ketone peroxide (MEKP)



### 1.1.2 Glass fibers

From reference [8], there are many type of artificial synthesis fibers in the world of fiber reinforcement composites such as glass fibers, carbon (graphite) fibers, kevlar (aramid) fibers, boron fibers, etc. They have been showing the better candidate in comparison with metal because of their high specific strength, high specific modulus, high corrosion resistance, low cost, low density etc. Among them, glass fibers are responsible for majority of FRP composites because an acceptable manufactured cost although they have lower specific properties. The adequate mechanical properties, suitable cost, good specific electrical insulation purpose can be applied by glass fiber reinforced polymer (GFRP) composites. The comparison in specific strength and modulus of some fibers in their composites can be seen at Figure 1-6.

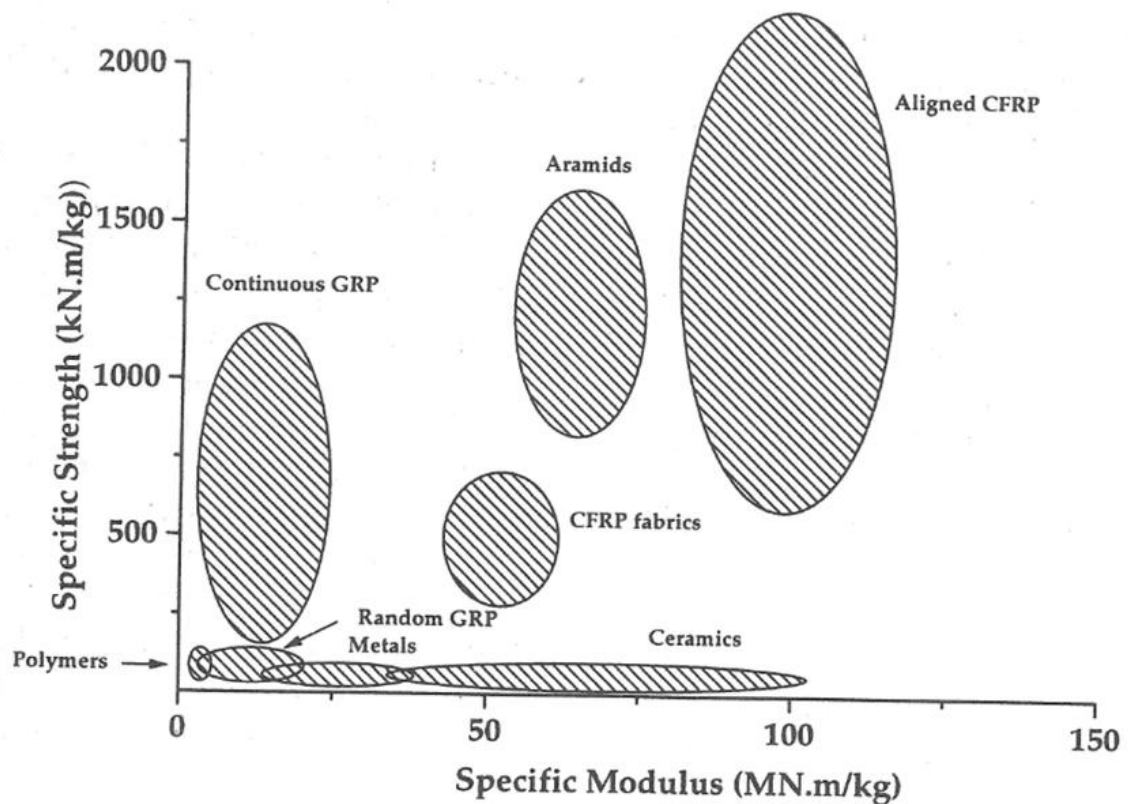


Figure 1-6: Specific properties of metals and composites [Figure 1, part 2.05, Ref. 8]

In the group of GFRP, there are many classes such as E glass, S glass, S-2 glass, C glass, D glass, A glass, prepreg, chopped strand mat (CSM), woven roving etc. They were synthesized for specific purpose with the different mechanical and physical behaviors. As other fiber composites, GFRP also can be aligned to reinforce in specific direction to improve local strength of structures. In composite structures, fibers contribute as reinforcement component while polymers play as matrix binder role. Consequently, for GFRP, to obtain the desirable mechanical properties, the fiber orientation and the fiber volume fraction can be changed. The fiber volume fraction could be chosen in range of 60-70% in fabrication as long as composite structures can be formed. The difference fiber types and fiber volume fractions represent difference properties and prices as Figure 1-7.

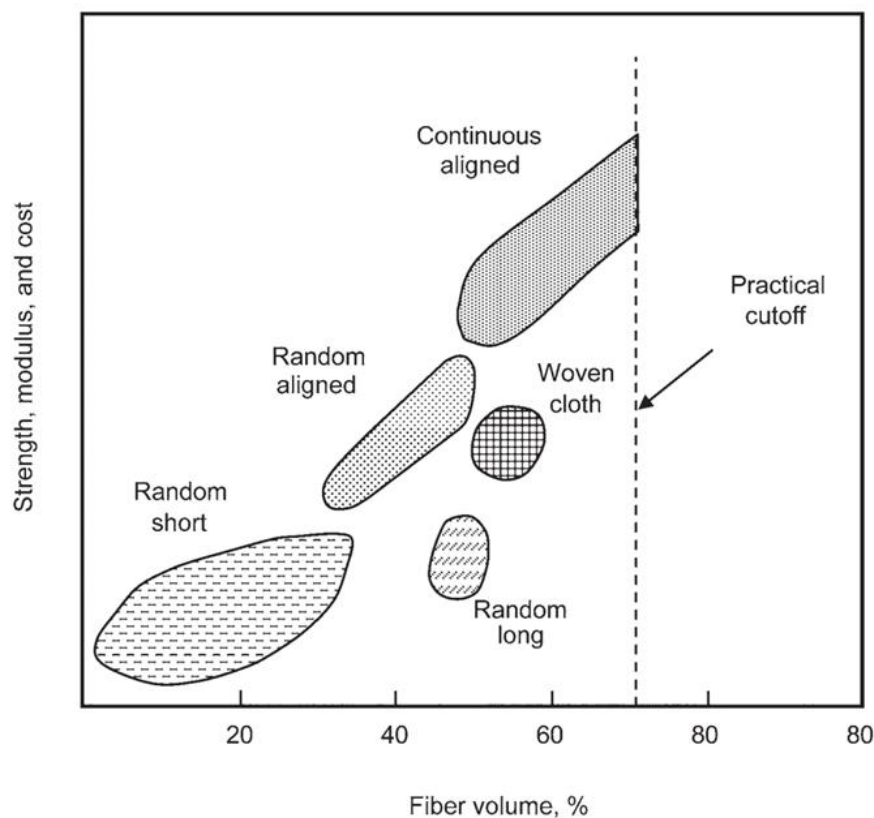


Figure 1-7: Influence of reinforcement type and quantity on composite performance

[Figure 1.2, Ref. 9].

The commercial glass fibers include woven (roving) and chopped strand mat (CSM) are seen in Figure 1-8 and Figure 1-9 respectively, that were purchased from Kimchon plant company in South Korea.

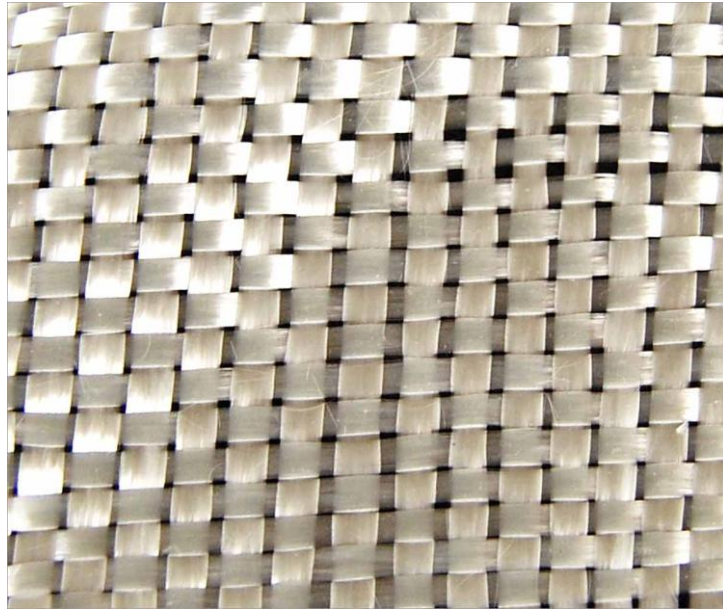


Figure 1-8: Woven roving



Figure 1-9: Chopped strand mat

### 1.1.3 Multi-walled carbon nanotubes (MWCNTs)

The carbon nanotubes were discovered by Iijima [10] in 1991. Some later generations that have been known as single-walled carbon nanotubes, double-walled carbon nanotubes and multi-walled carbon nanotubes. They all have outstanding electronic, physical, and mechanical properties.

Figure 1-10 shows the multi-walled carbon nanotubes (CM-130) which are supplied by the Hanwha Chemical Company in South Korea. From specifications of the manufacturer, MWCNTs were synthesized in aligned form using a chemical vapor deposition (CVD) method and were 10-30  $\mu\text{m}$  in length with a 10-15 nm outer diameter, a 5-10 nm inner diameter, a high aspect ratio ( $\sim 2 \times 10^3$ ), about 90 wt.% purity, a bulk density of approximately  $0.04 \text{ g/cm}^3$ , and the true density of MWCNTs is  $1.80\text{-}1.95 \text{ g/cm}^3$ .

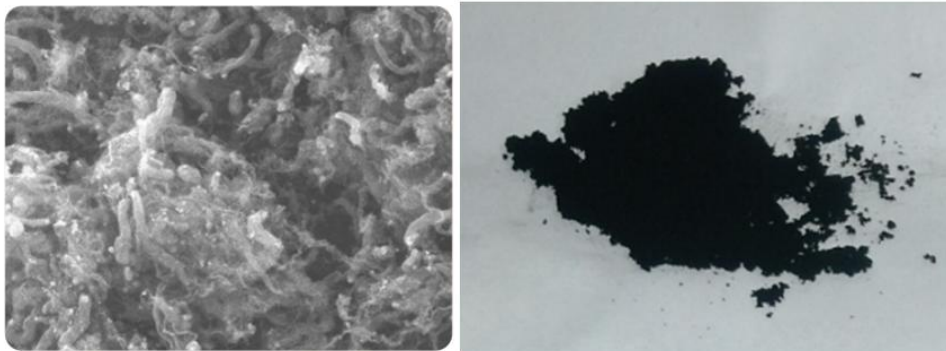


Figure 1-10: Multi-walled carbon nanotubes (CM-130)

### 1.2 Application of glass fiber reinforced polymer (GFRP)

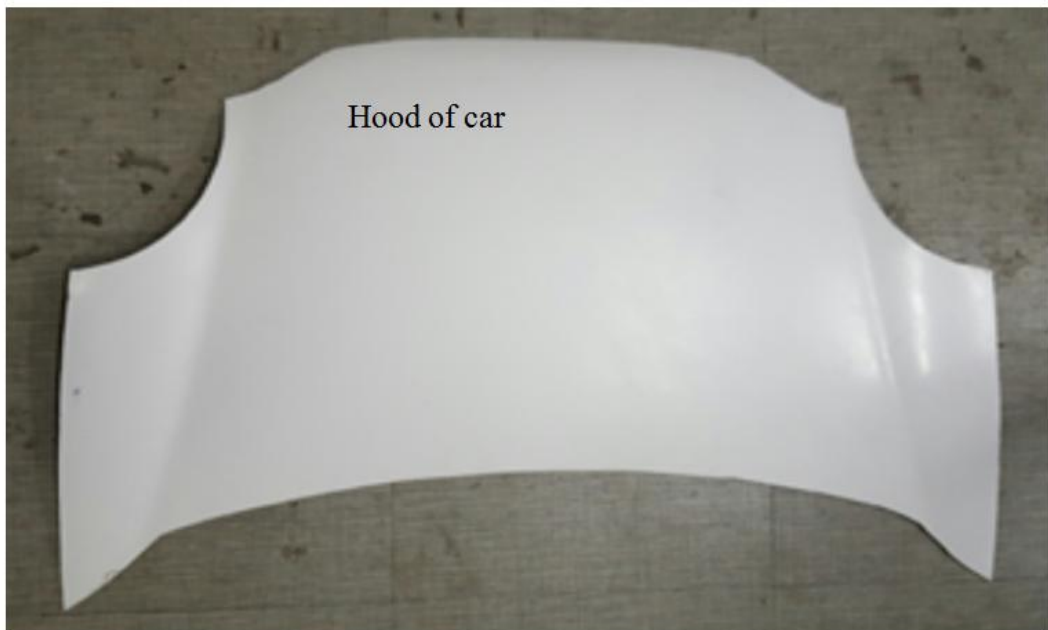
From the above discussion, there are so many applications of GFRP in the industry such as aerospace, transportation, construction, marine goods, sporting goods due to their good properties. In this part, some available fabricated parts are introduced at Figure 1-11.



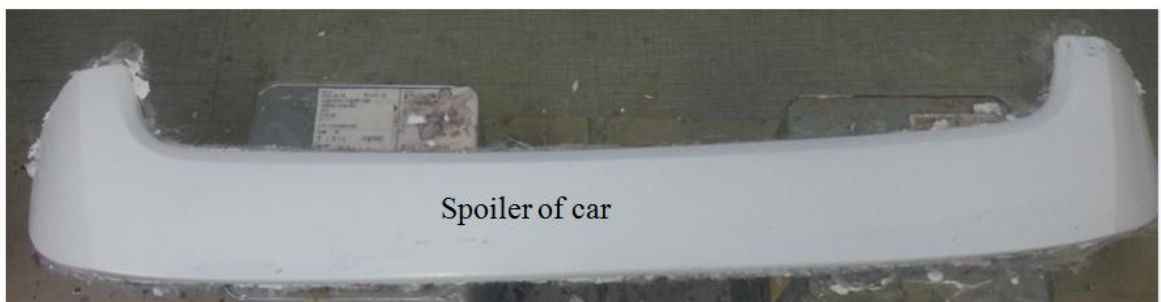
Door of car



Wheel of car



Hood of car



Spoiler of car

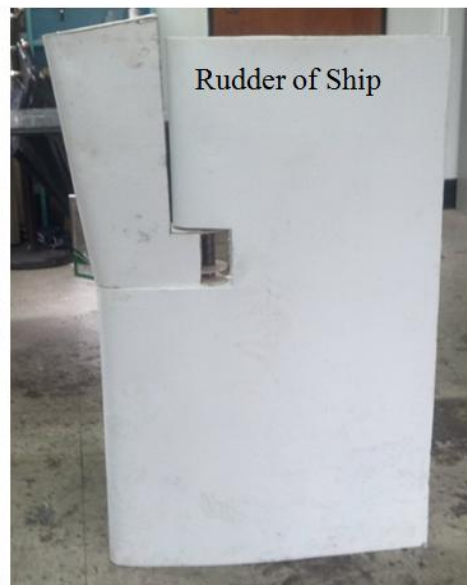


Figure 1-11: GFRP products

### **1.3 Literature review**

#### **1.3.1 The methods of increasing mechanical properties and fracture toughness of GFRP composite materials.**

The mechanical properties, fracture toughness of composite materials are strongly dependent on the mechanical properties of each component as well as the bonding strength between them [11]. Some predictable methods can be used to improve the properties of composite materials such as enhancing the properties by dispersing MWCNTs into matrix and growing MWCNTs on the surface of reinforcement. Those methods not only propose better properties of all composite components but also raise the bonding strength by bridging MWCNTs. In addition, the interaction of fibers and matrix also can be changed according to fiber arrangement, fiber length, and fabrication method. Therefore, those factors could be considered to increase mechanical properties and fracture toughness of composites.

#### **1.3.2 Composite structure modification**

The composite materials can be modified by modifying matrix, or reinforcement, or both of them at the same time. Each method has its own advantages and disadvantages. Fibers can be treated by growing MWCNTs on their surface via chemical vapor deposition (CVD), physical vapor deposition (PVD), or a simple chemical method. For matrix, MWCNTs can be defused into UPR by some ways such as stir mixing, sonication, 3-roll mill, or combination of at least two above methods with and without chemical treatment.

### **1.3.3 Dispersion method**

From above modification methods, the performance of each method was evaluated [12, 13]. Fiber modification has been expressed as the best solution and matrix had a little bit lower effect. While, the combination modification methods resulted in the worst form according to the assessment of mode I fracture toughness ( $G_{IC}$ ), thermal expansion coefficient etc. Compared to the pristine composite materials, the modified composites indicated obviously better results. In addition, among those methods, modifying matrix is known as the simple method. Therefore, it is focused in this dissertation.

## **1.4 Objectives and contents of dissertation**

### **1.4.1 Objectives of dissertation**

The effort in this dissertation is finding a better GFRP composites based on the evaluation of tensile properties and fracture toughness. In the thermosetting polymer group, epoxy have been investigated mostly while UPR has not been considered appropriately. As a consequence, some characteristics of UPR is studied carefully and optimized its curing behavior based on the content of MEKP and initial curing temperature. From those factors, mixing condition of MWCNTs into UPR is also optimized. The simple mixing method is chosen without chemical treatment of MWCNTs and fibers. The composite fabrication methods and fiber changes are also considered to improve mechanical properties and fracture toughness of new materials. All above optimum conditions and adding MWCNTs are applied to obtain higher tensile properties and fracture toughness GFRP/ MWCNTs + UPR composites. Moreover, the expectation from the better performance of new composites as well as simple mixing method is applied in mass production so far.



### 1.4.2 Thesis outline

In **Chapter 2**, some optimum conditions are introduced based on the mixing temperature, hardener (MEKP) ratio, initial curing temperature, fiber changes, and vacuum.

After the optimum conditions of mixing temperature and hardener ratio are estimated, MWCNTs will be dispersed into UPR to find the optimum weight content via tensile properties of UPR and FE-SEM result of fracture surfaces in **Chapter 3**.

Other fabrication factors will be applied into GFRP composite materials combining with optimum MWCNTs weight fraction of UPR. **Chapter 4** presents the results of tensile test that will be conducted to access the effect of MWCNTs on the GFRP/ modified UPR composites.

**Chapter 5** will focus on the various fracture toughness of modified UPR as well as GFRP/ modified composites with most of optimum conditions.

**Chapter 6** summaries the result of whole dissertation and plan of future works.

## CHAPTER 2:

# Optimization of fabrication conditions

*Based on:*

1. Van-Tho Hoang and Young-Jin Yum, "**Optimization of mixing process and effect of multi-walled carbon nanotubes on tensile properties of unsaturated polyester resin in composite materials**", *Journal of Mechanical Science and Technology*, vol. 31, pp. 1621-1627, 2017.
2. Van-Tho Hoang and Young-Jin Yum, "**Optimization of the fabrication conditions and effects of multi-walled carbon nanotubes on the tensile properties of various glass fibers/ unsaturated polyester resin composites**", *e-Polymers*, (accepted) 2018.

## 2.1 Introduction

MWCNTs are wrapped in graphene sheets as tubes with large surface area and they attract each other via the Van der Waals force [14]. MWCNTs normally aggregate and stack together as micro particles, so it is a challenge to evenly disperse nanoparticles in a polymer. Practically, good dispersion represents a uniform distribution of MWCNTs in a polymer [15]. A more homogeneous dispersion can enhance interfacial strength of the fiber and matrix [16] and reduce concentrated stress and improve uniform stress distribution [17]. On the other hand, agglomeration may produce slippage between MWCNTs and porosity in the nanocomposite [15, 18].

In order to overcome those difficulties, several solutions have been suggested, such as optimum physical blending, in situ polymerization, and chemical functionalization [18]. For a thermosetting polymer, dispersion and bonding of MWCNTs within the matrix plays a prevailing role in the improvement of mechanical properties of nanocomposite materials. Therefore, various mechanical methods were introduced, such as ultrasound [18-20] with bath type [21] and horn type [22]; 3-roll mill [19, 20, 23]; stir or shear mixing [19, 20, 24, 25]. Another efficient method to prevent aggregation relies on the functionalization of nanofillers. This technique has shown many promising results and is based on the modified structure of MWCNTs [14, 18-20, 26-28]. From a mechanical engineering point of view, each of the physical methods have both advantages and disadvantages for inducing dispersion in nanocomposite materials. Here, shear mixing shows less influence on dispersion than other methods [25], while 3-roll mill provides better dispersion than sonication techniques [23]. The higher input power of the sonicator may obstruct the degree of dispersion [22]. Controlling the evaporated weight of the mixture during mixing with the 3-roll mill method is a challenge [23]. The straightforward technique of manual

mixing falls short of the degree of dispersion of the nanocomposite provided by other methods [29].

Most of the above results are focused on epoxy, even though unsaturated polyester resin (UPR) is a very popular thermosetting matrix used in composite materials. A few of researchers interested in the behavior of UPR and MWCNTs, but their mixing methods are different. For instance, Mahmoud M Shokrieh et al. [30] combined stirrer and sonicator for mixing MWCNTs into UPR, while M. D. H. Beg et al. [31] or A. K. M. Alam et al. [32] improved the mixing method by pre-mixing MWCNTs with Tetrahydrofuran (THF) before dispersed them into UPR. In addition, there are many other factors that have an effect on the dispersion of MWCNTs in polymer of nanocomposites such as mixing temperature, hardener ratio, etc.

In this dissertation, a stir mixing was used to disperse MWCNTs in the UPR. It has been known as very simple dispersion method. Therefore, some optimum conditions should be considered carefully to enhance the dispersion quality of MWCNTs in UPR. In addition, to understand more clearly the behavior of UPR and GFRP composite materials, some optimum factors such as mixing temperature, hardener ratio, initial curing temperature, fiber change, and vacuum will be presented in this chapter. Those conditions are expected to apply for enhance mechanical properties and fracture toughness of UPR separately and GFRP/ modified UPR as well that can be seen in some later chapters.

## **2.2 The effect of mixing temperature**

### **2.2.1 Materials and evaluation method**

The unsaturated polyester resin (EC-304) and methyl ethyl ketone peroxide (MEKP) are made by the Aekyung chemical company in South Korea.

Compression test was carried out to evaluate the effect of mixing temperature on compressive properties of UPR.

### 2.2.2 Experiment

The mixing temperature of UPR and MWCNTs were changed in range of 20 °C-100 °C with 20 °C interval. Hot and stir machine was used to raise the mixing temperature to the expected values by the hot plate. The magnet was rotated at 2,000 rpm to transfer uniformly the heat inside the beaker for a certain time. The box was used to cover around the beaker with heat insulation foil to avoid heat consumption by surrounding environment.

After heating to the expected temperatures, pure UPR (20 g) was mixed immediately with 1 wt.% hardener (MEKP) for a short time (~ 30 seconds), then poured into a jar. The curing was held at 25 °C for 24 hours. Afterward, specimens were post-cured in an oven at 80 °C for 3 hours. The resulting cylindrical compression specimens were an average 30 mm in diameter and 20 mm in height after polishing (Figure 2-1).

The compression test was conducted by a universal testing machine (DTU-900MHN) at 2mm/min test speed.



Figure 2-1: The shape of compression specimen

### 2.2.3 Results and discussion

As mentioned from the **section 2.2.2**, in this study we dispersed MWCNTs into the UPR using only the hot and stir machine. The stirring process has shown suboptimal effects [25], but is an important starting point for analysis of dispersion of nanotubes in UPR. In addition, the effect of the temperature of resin during such experiments has not been thoroughly investigated. The viscosity of resin is obviously reduced at higher temperatures, but it converges at a certain high temperature due to its Newtonian fluid behavior. Surprisingly, the compression behavior of each temperature-controlled specimen was different (Figure 2-2). Table 2-1 shows more detailed compression testing results, in which the ultimate strength and modulus reach the highest values at a resin temperature of 60 °C. Specimens fabricated at 20 °C and 40 °C are more ductile than at those mixed at 80 °C and 100 °C due to the higher strain at the ultimate strength. The ultimate strength and modulus degradation of UPR at 80 °C and 100 °C is attributed to the liquid evaporation phenomenon that occurs at high temperatures. Thus, mixing temperature at 60 °C should be referred in experiments.

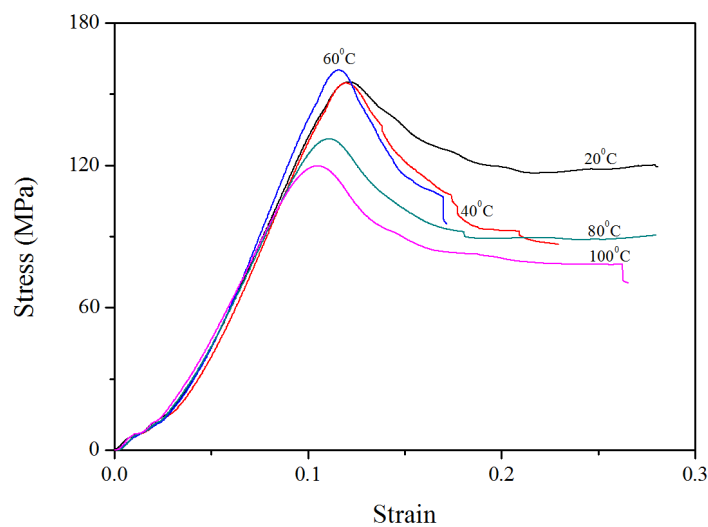


Figure 2-2: Compressive stress-strain behavior of UPR at various mixing temperatures

Table 2-1: Compression properties of UPR at various mixing temperatures.

Specimen name	Mixing temperature (°C)	Ultimate strength (MPa)	Modulus (MPa)	Strain at ultimate strength
T-1	20	155.20	1,690.63	0.1212
T-2	40	154.73	1,644.07	0.1194
T-3	60	160.26	1,694.86	0.1160
T-4	80	131.24	1,443.99	0.1109
T-5	100	119.87	1,367.15	0.1046

Figure 2-3 provides another evidence to see the obtained compression specimens. The different color can be seen easily at different mixing temperature.

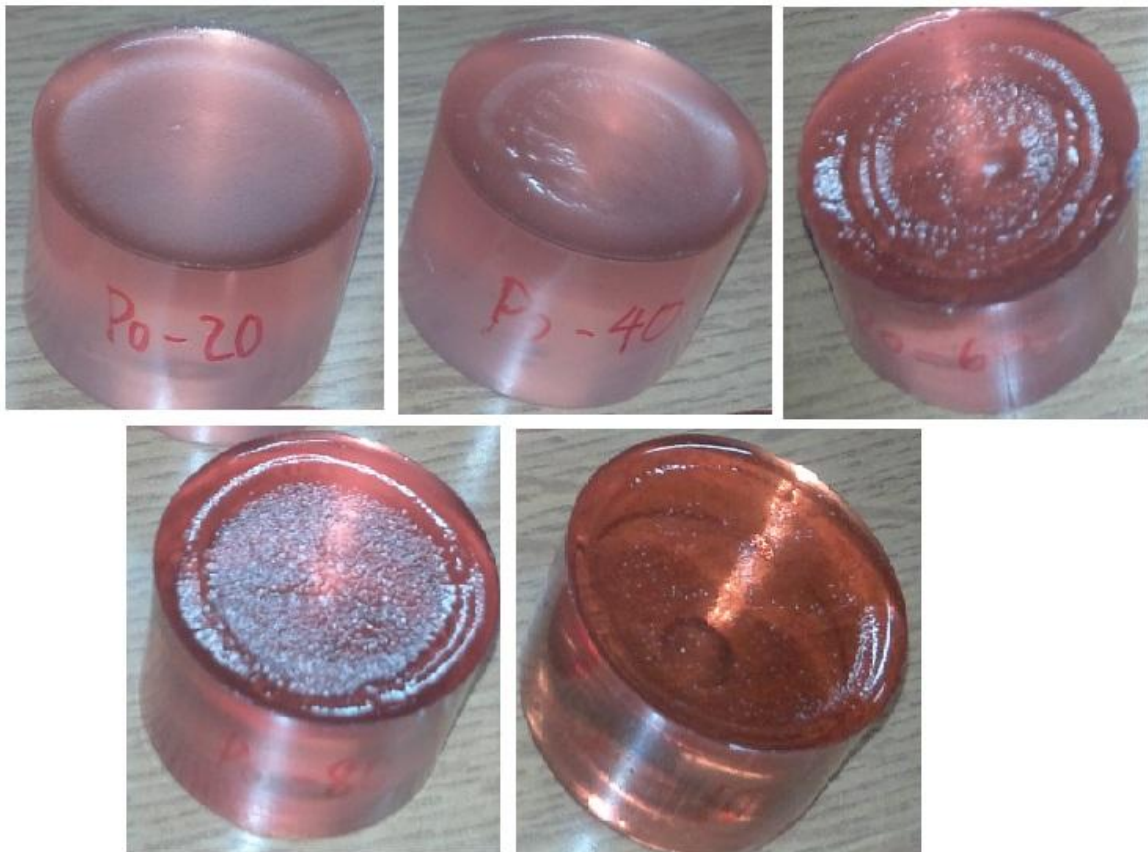


Figure 2-3: Compression specimens of UPR fabricated at different mixing temperatures

## 2.2.4 Conclusions

From the compression behavior of UPR that was fabricated at different mixing temperature, we can see 60 °C represents the higher compression strength, modulus and average strain. Therefore, it can be used as one of the optimum condition during mixing MWCNTs into UPR.

## 2.3 The effect of hardener ratio

### 2.3.1 Materials and evaluation methods

The unsaturated polyester resin (EC-304) and methyl ethyl ketone peroxide (MEKP) are made by the Aekyung chemical company in South Korea that also can be seen from **Chapter 1**.

Compression properties, exothermic temperature, and curing time of UPR were monitored to extract the proper hardener ratio in the range of 1-3 wt.%.

### 2.3.2 Experiment

The mechanism of curing of UPR was described in **Chapter 1** based on the reference [8]. The chemical reaction between unsaturated polyester resin occurs when adding the initiator (hardener) namely methyl ethyl ketone peroxide (MEKP) that is an exothermic reaction due to cross linking [8, 33]. Thus, the cure rate of polyester can be determined based on temperature and curing time using a thermometer (FLUKE 568). Here, the UPR (20 g) was mixed with different hardener ratios (1, 2, and 3 wt.%) inside the jar. The thermocouple probe was set at the center of the mixture (Figure 2-4), the position at which the temperature is maximized.

The compression test was also conducted by a universal testing machine (DTU-900MHN) at 2mm/min test speed.



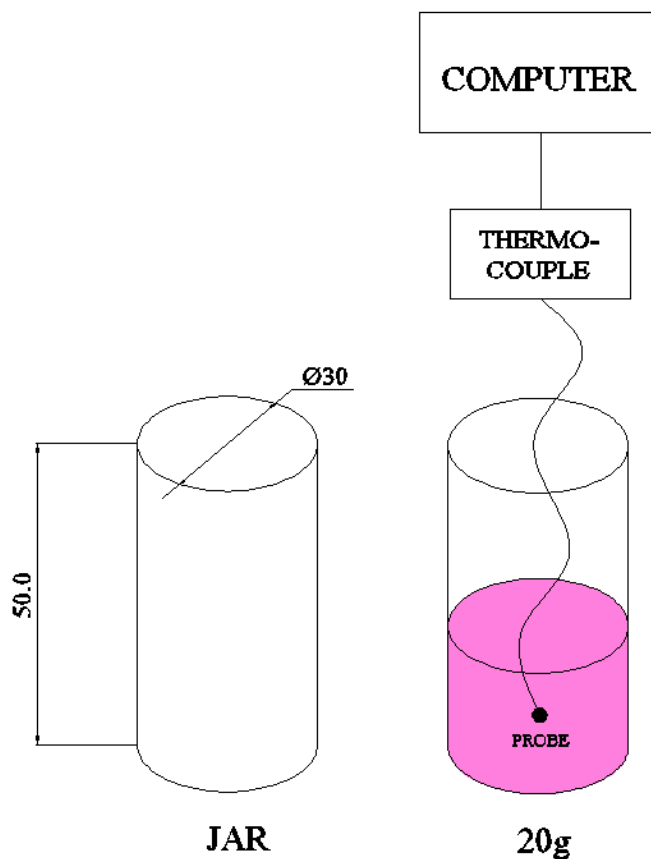


Figure 2-4: Monitoring exothermic reaction

### 2.3.3 Results and discussion

#### 2.3.3.1 *Compression properties*

Because the UPR is the principle binder in composite materials, the hardener is the all-important catalyst. Previously, J. R. M. d'Almeida and S. N. Monteiro [34] showed that the tensile strength and elastic modulus were largest at a stoichiometric ratio of hardener/epoxy, and that over a phr of 13 (13 parts of hardener per hundred parts of resin), some initial cracks are formed. Using this study as motivation, compression specimens were fabricated with the same parameters and process as in section 2.2.2, but the hardener concentration was varied from 1 to 3 wt.%. Figure 2-5 shows that UPR has the best

compression properties in terms of strength, modulus and strain at ultimate strength when we used 1 wt.% of hardener to construct the specimen. The polymer network structure tends to become weaker with higher catalyst concentration. For example, in comparison with 1% mixed hardener, ultimate strength of UPR was reduced by 14.39% and 22.89%; elastic modulus of UPR was also decreased by 3.99% and 10.41%; or strain of UPR had similar tendency with 8.27% and 11.72% lower values at 2% and 3% mixed hardener, respectively. The comparison values can be seen in Table 2-2. The two types of specimens, T-3 and H-1, have different names but were fabricated at the same conditions and had a similar hardener concentration, so their compression results are similar in terms of strength, modulus and strain (Table 2-1 and 2-2).

The exothermic temperature and gelation rate can be nonlinearly extrapolated to increase with higher MEKP concentration from the results in section 2.3.3.2. Practically, at high hardener ratio, chemical reaction of UPR occurred quickly and burned including smoke and harmful smell. Thus, crack was created and bonding of polymer chain was destroyed that lead to reduce compression properties of UPR.

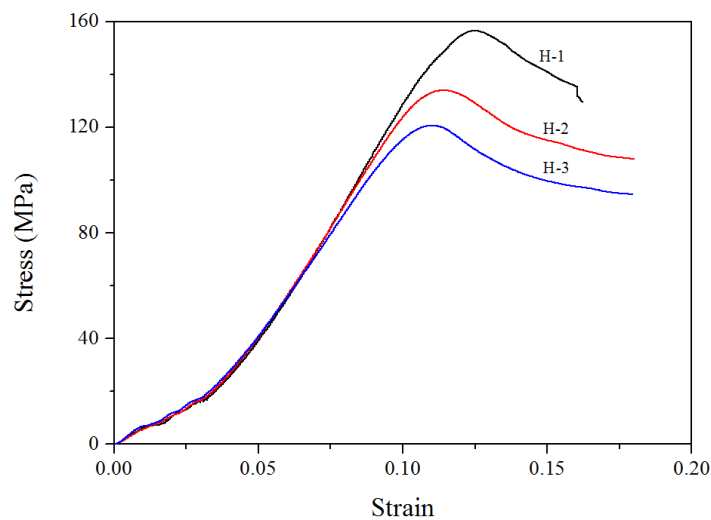


Figure 2-5: Compression stress-strain relation of UPR with different MEKP contents.

Table 2-2: Compression properties of UPR based on the difference of hardener ratios

Specimen name	Hardener (%)	Ultimate strength (MPa)	Modulus (MPa)	Strain at ultimate strength
H-1	1.0	156.60	1,712.51	0.1246
H-2	2.0	134.06	1,644.16	0.1143
H-3	3.0	120.76	1,534.20	0.1100

### 2.3.3.2 Exothermic temperature

Using the same range for the mixed hardener ratio (1 to 3 wt.%), the curing temperature of the UPR was monitored from room temperature through the exothermic reaction, and then back to room temperature. As can be seen from Figure 2-6, the peak exothermic temperature ( $\theta_{\text{peak}}$ ) and the time to peak ( $t_{\text{peak}}$ ) are significantly dependent on the concentration of MEKP. Generally, a higher exothermic temperature and shorter time to peak can be obtained when we add a greater percentage of MEKP. This indicates that the gelation rate is faster at a higher catalyst concentration. At a 3 wt.% concentration of MEKP,  $\theta_{\text{peak}}$  and  $t_{\text{peak}}$  were 186.3 °C and 602 seconds, respectively. With the reduction of MEKP to 1 wt.%,  $\theta_{\text{peak}}$  was reduced to its smallest value (144 °C), but  $t_{\text{peak}}$  increased to 1,491 seconds. The relation between MEKP concentration with  $\theta_{\text{peak}}$  and  $t_{\text{peak}}$  was not linear because  $\theta_{\text{peak}}$  and  $t_{\text{peak}}$  at 2 wt.% of hardener (176 °C and 722 seconds) were close in value to those at 3 wt.%, but were far from those at 1 wt.%. Figure 2-6 also shows that the essential time for curing and cooling at all of hardener ratios is almost 4,500 seconds, at that time the solid UPR was totally cooled to room temperature. Moreover, gelation rate and cooling rate almost similar at lower hardener ratio (H1), but they are different at higher

hardener ratios (H1, H2). Consequently, the cooling rate at higher hardener content is also higher than at lower content.

In fact, by increasing the percentage of hardener, we can save time for fabrication, but it is more dangerous working in the high temperature condition and the cost may increase simultaneously. Additionally, a higher catalyst concentration may prevent execution of other processes such as casting into the mold because the gelation time is too short and the mechanical properties degrade, as presented in section 2.3.3.1.

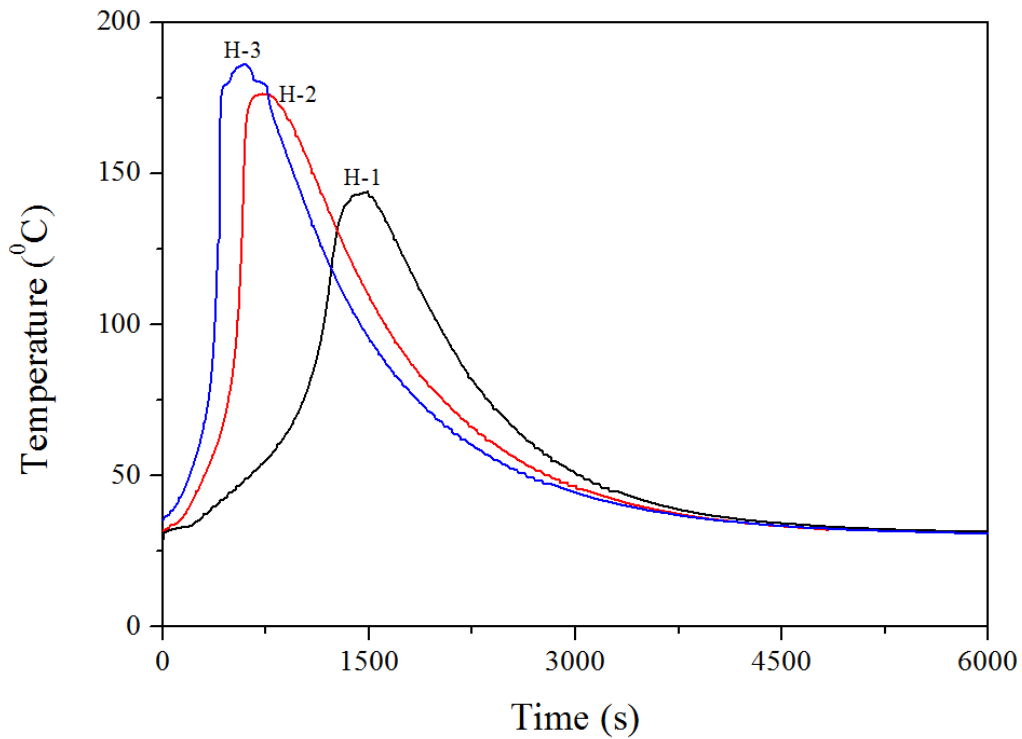


Figure 2-6: Variation of curing temperature of UPR with different MEKP contents

### 2.3.4 Conclusions

Consequently, by considering all of the benefits discussed in sections 2.2 and 2.3, 1 wt.% of MEKP and 60 °C mixing temperature should be used as the optimal conditions.

## **2.4 The effect initial curing temperature**

### **2.4.1 Materials and evaluation methods**

The unsaturated polyester resin (EC-304) and methyl ethyl ketone peroxide (MEKP) are made by the Aekyung chemical company in South Korea, while the commercial glass fibers include woven and CSM were purchased from Kimchon plant company that also can be seen from **Chapter 1**.

Exothermic temperature and curing time of UPR were also monitored. In addition, density of UPR, thermo-gravimetric analysis of UPR, and tensile properties of GFRP composite were carried out to find the proper initial curing temperature for composite fabrication.

### **2.4.2 Experiment**

From the results in section 2.2 and 2.3, we found that the curing behavior of UPR was also affected by initial curing temperature. In addition, from the weather forecast, the temperature can be significantly changed in some nations. For instance, it may be varied daily in range of 20 °C in the some seasons in South Korea. Furthermore, some other reports also showed the detail curing process by other techniques [33, 35, 36]. The curing behavior of UPR was investigated as the same procedure in section 2.3.2 and Figure 2-4. Here the initial curing temperature change from 10.9 °C to 45.5 °C, the exothermic temperature and curing time were recorded.

The composite laminate was fabricated with 4 layers of the fiber and matrix using a roller in a hand lay-up fabrication method. The stacking sequence was fixed as CSM/woven/CSM/woven to survey the effect of initial curing temperature. Five tensile specimens in rectangular shape were cut by a diamond cutter for each plate (the length was 200 mm, the width was 20 mm, and the thickness was about 3 mm) without a tab.

The thermal characteristics were evaluated using a TGA Q50 in a nitrogen environment (40 ml/min balance purge flow). The temperature was maintained under isothermal conditions for 5 minutes before it was increased to 800 °C at a rate of 10 °C/min. Roughly 10 mg specimens were prepared before test.

Tension test was conducted by a universal testing machine at 2 mm/min test speed of according to ASTM D 3099. An extensometer with a 50 mm gauge length was used.

### **2.4.3 Results and discussion**

#### ***2.4.3.1 Curing behavior of UPR***

Figure 2-7 shows the curing behaviors of UPR for different initial temperatures. Generally, the viscosity of UPR increased during the chemical reaction between polyester and the hardener while the temperature increased simultaneously. Gelation formation occurred until the mixture was converted fully to the solid stage. It is clear that the total curing time at higher initial curing temperatures is shorter than that at lower temperatures. The maximum exothermic temperature generated was 165.5 °C at an initial temperature of 45.5 °C with the shortest time (594 seconds) to reach the maximum temperature. On the other hand, the lowest initial curing temperature (10.9 °C) had the lowest exothermic temperature (124.8 °C) and took the longest time (3,561 seconds) to reach the maximum temperature. With initial temperatures of 28.5 °C and 35.2 °C, the exothermic temperatures were 132.6 °C and 138.9 °C and the times to reach these peaks were 1,980 seconds and 1,687 seconds, respectively. The differences of the exothermic temperatures and curing times were not significantly different for initial temperatures in the range of 28.5 °C to 35.2 °C. In comparison with the results of Huang YJ and Leu JS [35], 30 °C was lower temperature and rate of reaction, even higher tensile properties were received [36]. Indeed, the exothermic temperature decreased slightly in both cases of initial temperatures of 28.5

$^{\circ}\text{C}$  and  $35.2^{\circ}\text{C}$  because the chemical reaction was not immediately held after mixing the hardener. Therefore, the mixture was automatically cooled down because the heat was transferred to the room temperature environment. However, in the case of an initial curing temperature of  $10.9^{\circ}\text{C}$  (lower than room temperature), the exothermic temperature nonlinearly increased at the beginning. After curing, the temperatures in all cases were reduced similarly to room temperature ( $25^{\circ}\text{C}$ ) after different times. This means that the cooling rate also changed depending on the initial curing temperature.

In another research, Zhang J. et al. [37] found the maximum exothermic temperature and the time to reach the peak temperature of another thermosetting resin (epoxy) were approximately  $175^{\circ}\text{C}$  and 150 minutes, respectively. In comparison with the current result, epoxy has much lower curing rate that means the solidification procedure is much longer than UPR. It can result in some limitations of fabrication methods using vacuum for UPR such as vacuum bagging and resin infusion methods because the resin flow cannot transfer after the gelation time. Consequently, a vacuum should be applied as fast as possible to ensure UPR completely filled into fibers. It is also very important to consider thoroughly the curing time in mass production using UPR and vacuum.

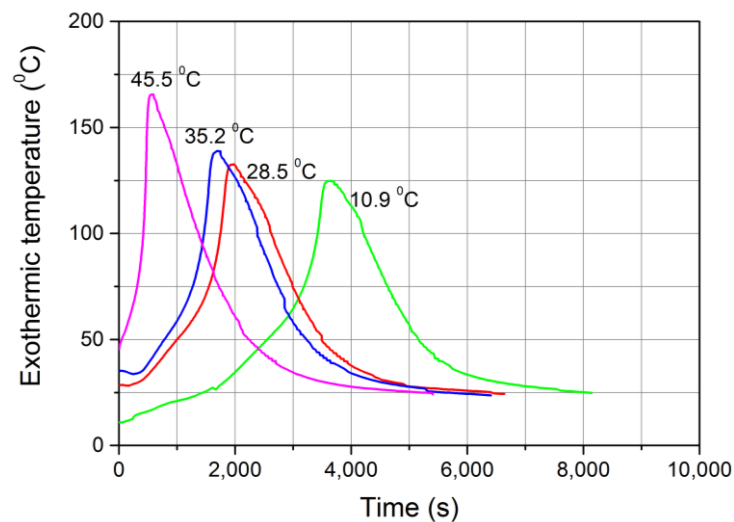


Figure 2-7: Curing behavior for different initial curing temperatures

### 2.4.3.2 Density of UPR

Unsaturated polyester resin (UPR) is a thermosetting resin. Thus, theoretically, the volume of the specimen should shrink after curing [38]. This was confirmed in the value of the density of UPR obtained in this study. The specimens from curing behavior investigation were reused to figure out density and thermo-gravimetric analysis (TGA). In the liquid stage, the density of UPR is 1.15 (g/cm<sup>3</sup>) (Table 2-3) and it is changed to 1.22 (g/cm<sup>3</sup>) in the solid stage (Table 2-4). The same mass of UPR was obtained in both the liquid and solid stages but the density changed, which means the volume was smaller in the solid stage. Interestingly, for all initial curing temperatures, the density of UPR was almost the same. Thus, the volume shrinkage of polyester does not depend on the initial curing temperature.

Table 2-3: Density of the materials.

Number	Material name	Density
1	Woven	570 (g/m <sup>2</sup> )
2	Chopped strand mat (CSM)	300 (g/m <sup>2</sup> )
3	Unsaturated polyester resin (UPR)	1.15 (g/cm <sup>3</sup> )
4	Multi-walled carbon nanotubes (MWCNTs)	Bulk: 0.04 (g/cm <sup>3</sup> )

Table 2-4: Density of UPR for the different initial curing temperatures.

Number	Initial curing temperature (°C)	Density (g/cm <sup>3</sup> )
1	10.9	1.218
2	27.5	1.22
3	35.2	1.22
4	45.5	1.22



### 2.4.3.3 Thermo-gravimetric analysis of UPR

There is some valuable information that can be provided by TGA measurements, such as the filler content of materials, composition of multi-component materials, decomposition kinetics, moisture and volatile content. Table 2-5 shows the behavior of UPR under elevated temperatures. It is clear that the degradation procedure was similar for the different specimens. The degradation started at about 287 °C with ~5.7% mass loss and most of the UPR was gone at around 541.2 °C (~1.1% mass remained). The small amount of mass reduction before degradation may be due to water absorption and/or volatile contents, while the mass retention after degradation (up to 800 °C) is possibly due to the impurities of UPR.

Table 2-5: Thermal behavior of UPR for the different initial curing temperatures.

No.	Initial curing temperature (°C)	Onset of degradation		Residue	
		Temperature (°C)	Mass (%)	Temperature (°C)	Mass (%)
1	10.9	288.9	93.6	542.1	1.2
2	27.5	286.8	94.2	541.1	1.3
3	35.2	288.7	94.9	542.0	1.2
4	45.5	283.4	94.5	539.6	0.7

### 2.4.3.4 Tensile properties of GFPR composites

From section 2.4.3.1 to section 2.4.3.3, the optimum curing temperature could be started approximately in the range of 25-35 °C. In addition, Belloul N. et al. [36] showed the different optimum temperatures of resin (30 °C) and composite (40 °C) based on their tensile properties. Practically, the initial curing temperatures were indicated by the probe of

the thermocouple at the center of specimens in the previous section that may be a little bit different with surrounding temperatures. Therefore, composite structures were fabricated to verify the effect of initial curing temperature range on the tensile properties. The initial curing temperatures were 22 °C (MC1), 30 °C (MC2), and 32 °C (MC3). In this case, the initial curing temperature can be known as making temperature or fabrication temperature. The tensile properties of materials are shown in Figure 2-8. It is clear that tensile properties of composite materials are also sensitive to environmental temperature. Higher tensile strength (20.88%) and elastic modulus (18.16%) were obtained when initial curing temperature raised from 22 °C to 32 °C.

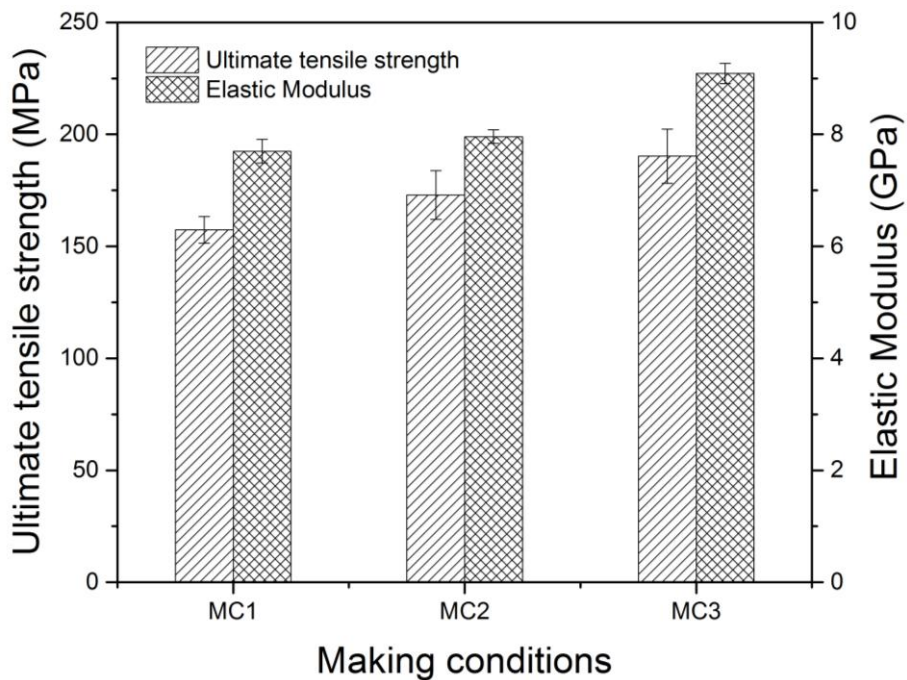


Figure 2-8: Tensile properties of CSM/woven/CSM/woven for the different fabrication temperatures

#### 2.4.4 Conclusions

The results of from section 2.4.3.1 to 2.4.3.4 show a good agreement with the results of Belloul N. et al. [36]. Thus, it can be concluded that initial curing temperature should be held in range of 25 °C -35 °C.

## **2.5 The potential of combining CSM and woven**

### **2.5.1 Materials and evaluation methods**

The unsaturated polyester resin (EC-304) and methyl ethyl ketone peroxide (MEKP) are made by the Aekyung chemical company in South Korea, while the commercial glass fibers include woven and CSM were purchased from Kimchon plant company that also can be seen from **Chapter 1**.

Thermo-gravimetric analysis and tensile test were performed to find the thermal and tensile behavior of CSM, woven and their combination.

### **2.5.2 Experiment**

The composite laminate was fabricated with 4 layers of the fiber and matrix by hand lay-up fabrication method using a roller. The fibers were changed as CSM/ UPR, woven/ UPR, and fiber combination/ UPR. CSM weight fraction was 25% and woven weight fraction was 50%. Five tensile specimens in rectangular shape were cut by a diamond cutter for each plate (the length was 200 mm, the width was 20 mm, and the thickness was varied based on using fiber) without a tab.

The thermal characteristics and tensile properties were evaluated as the same procedure in section 2.4.2.

### **2.5.3 Results and discussion**

#### ***2.5.3.1 Thermo-gravimetric analysis of various fibers composites***

Glass fibers are the main reinforcement components for composite materials in this study. The CSM has random directions and shorter length of fibers, while woven has orthogonal structures and longer fiber length. Therefore, the thermal gravimetric analysis was carried out to examine the thermal resistance with the appearance of different fibers.

Figure 2-9 (solid lines) indicates a higher thermal resistance of composite materials due to the addition of glass fibers. Similarly, Budai Z. et al. [39] also reported that the decomposition of UPR is delayed by adding glass fibers. Besides, the degradation rates of the materials are described by the dashed lines. The woven structure was the toughest candidate in this fiber group, as demonstrated by its highest onset degradation temperature and the lowest rate of decomposition. That means the longer fiber and specific fiber structures in woven really affect on thermal resistance of composite materials. In addition, the residual masses remaining at high temperatures (from 500 to 800 °C) were different in each case. For example, at 700 °C, the mass retentions of UPR, UPR/CSM, UPR/woven, and UPR/combination of fibers were about 1.27%, 23.42%, 46.51%, and 33.83%, respectively. The parallel nature of both the solid and dashed lines in the high temperature range (500-800 °C) also indicates good thermal stability of the fibers. The mass retention represents the exact fiber content of composite structures. In comparison to the 25% and 50% in section 2.5.2, the mass of the fibers was mostly conserved, except the small amounts of moisture and volatiles. It can be concluded that the chemical compositions of CSM and woven are almost similar and the thermal degradation is slightly dependent on the fiber structure and significantly dependent on the fiber concentration in composite materials.

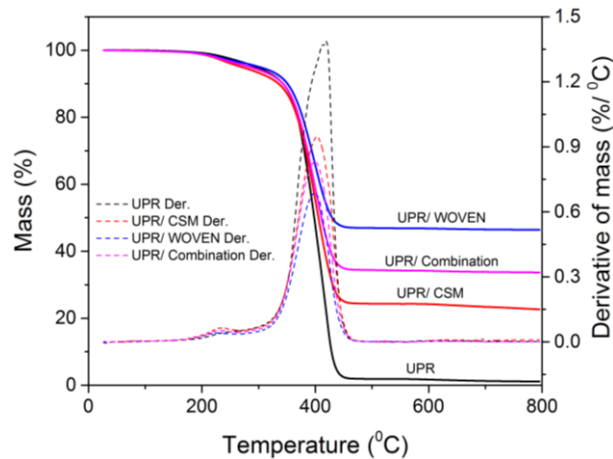


Figure 2-9: Effect of fibers on the thermo-gravimetric behavior of the composites

### 2.5.3.2 Tensile properties of various fibers composites

According to the rule of mixtures [1], the mechanical properties of a fiber composite can be calculated based on volume fractions. Thus, the 2 times higher weight fraction of woven than CSM (section 2.5.2) that can be estimated that mechanical properties of woven relatively are two times higher than CSM. In fact, the ultimate tensile strength and elastic modulus of CSM/UPR were 87.92 MPa and 7.09 GPa, respectively (Figure 2-10). Meanwhile, the tensile strength of woven/UPR was almost 2.8 times higher than that of the CSM composite, but Young's modulus of the woven composite was only 17.84% higher than that of CSM/UPR. Even though both fibers have almost similar chemical compositions (section 2.5.3.1), woven composite has much higher mechanical properties than CSM that can be attributed to the higher fiber length [40] and orthotropic fiber arrangement of woven.

Practically, woven has higher surface density than CSM (Table 2-3), but there are some gaps on the surface of layer and fibers are bundled together as shown at the Figure 1-8 and Figure 1-9. In comparison, woven may absorb less resin than CSM. In composite structures, CSM should be fabricated with more amount of UPR to ensure that the resin is fully filled into the fibers. As a consequence, woven fiber fraction is always higher than

CSM that can be resulted in a heavier product. In addition, woven has the native waviness surface that can be formed a rough surface composite structures. A composite laminate was fabricated by combining both of them as a CSM/woven/CSM/woven structure to obtain the best function of fibers. As a result, the combination of fibers can obtain an acceptable tensile properties as shown at the Figure 2-10. The CSM/woven/CSM/woven composite had a 79.02% higher ultimate tensile strength and a 8.54% higher elastic modulus than the CSM composite.

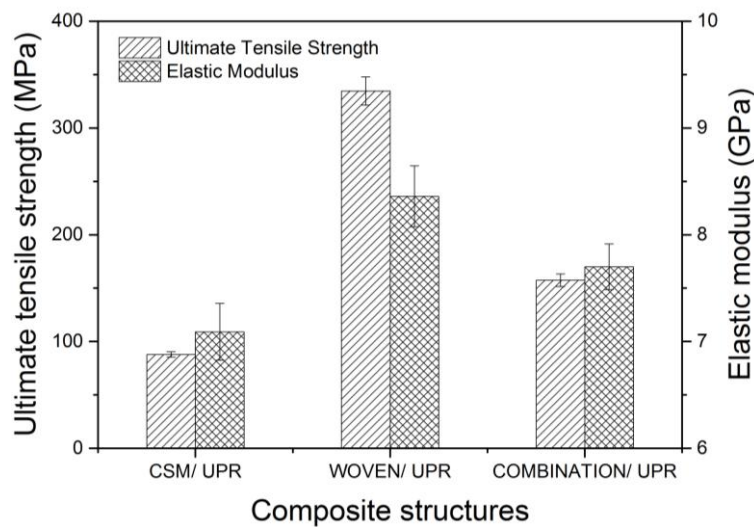


Figure 2-10: Tensile properties of composite structures with different of fiber components

## 2.5.4 Conclusions

The results from this section confirm that the types glass fibers do not have much effect on the thermal resistance, but affect significantly tensile properties of their composites.

## 2.6 The effect of fabrication method of GFRP composites

### 2.6.1 Materials and evaluation methods

The unsaturated polyester resin (EC-304) and methyl ethyl ketone peroxide (MEKP) are made by the Aekyung chemical company in South Korea, while the

commercial glass fibers include woven and CSM were purchased from Kimchon plant company that also can be seen from **Chapter 1**.

Density, thermo-gravimetric analysis, and tensile properties of GFRP composites were performed to find the effect of vacuum.

## **2.6.2 Experiment**

Different 4 layers of the fiber and matrix were also laminated by hand lay-up fabrication method using a roller. The fibers changed and fiber weight fraction were the same at section 2.5.2. After finished laminating, peel ply, bleeder, vacuum bag were applied immediately. As a consequence, curing of these specimens were cured at room temperature for 24 hours, under vacuum for 5 hours. The post-curing was also held in an oven at 80 °C for 2 hours. Five tensile specimens in rectangular shape were also cut by a diamond cutter for each plate (the length was 200 mm, the width was 20 mm, and the thickness was varied based on using fiber) without a tab.

The thermal characteristics and tensile properties were evaluated as same as the procedure in section 2.4.2. Besides, density of materials was measured by AND (GF-200) apparatus at atmospheric pressure and 22 °C.

## **2.6.3 Results and discussion**

### ***2.6.3.1 Density of composite structures***

The vacuum was used after hand lay-up fabrication, which has been known as hybrid fabrication method [41]. Specific structures were fabricated by this method to achieve higher density (lower void content) and mechanical properties. Vacuum is useful in isolating specimens with the surrounding environment and removing the unnecessary resin from specimens to bleeder, peel ply and even to the hose. In comparison to the compression molding method, vacuum may have less of an effect on the mechanical

properties but it is a simple method, more flexible and convenient with a variety of product geometries. In fact, the effect of vacuum is strongly dependent on the polymerization process. Vacuum may have not much influence if it is applied after the transition formation period because polymer cannot be transferred at much higher viscosity. Fortunately, the density of composite structures increased due to the longer curing time employed based on the optimum fabrication conditions. As can be observed in Figure 2-11, the density increased by 7.09%, 10.51%, and 11.63% in CSM/UPR, woven/UPR, and combination/UPR, respectively. The density of CSM and woven were 2.494 and 2.546 g/cm<sup>3</sup> in the experiment. They are much higher than the density of composite structures and UPR. Therefore, the reason for increasing density at Figure 2-11 may be attributed to the removing of a significant amount of UPR.

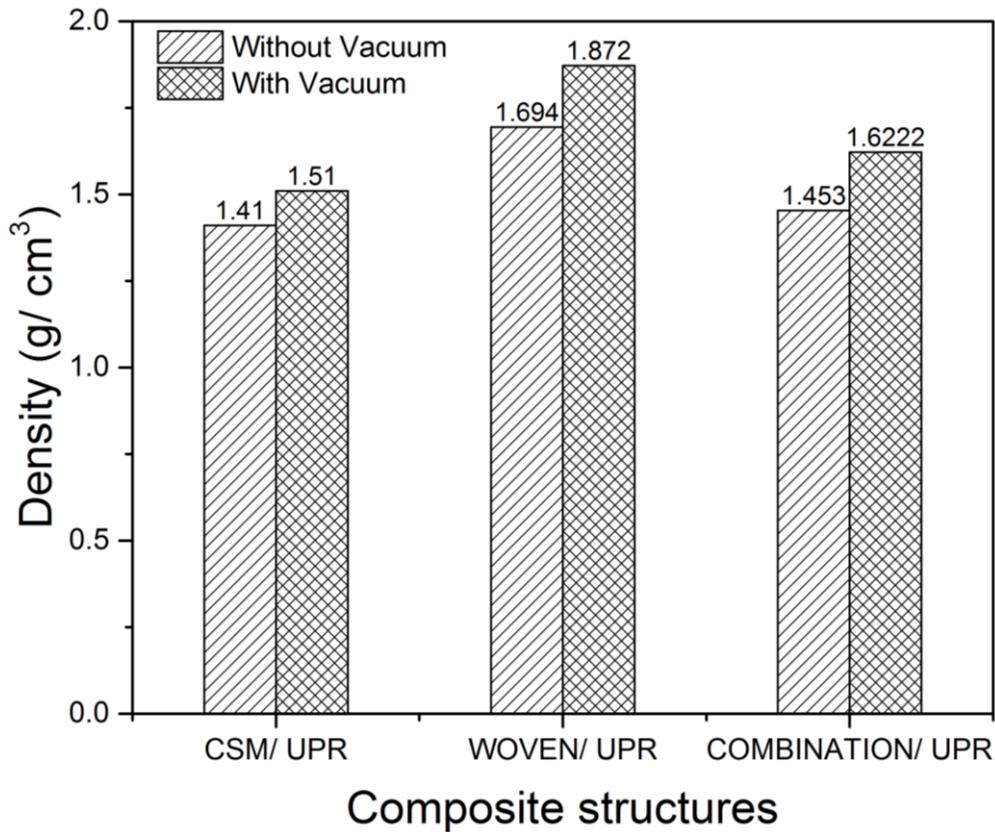


Figure 2-11: Effect of vacuum on the density of composite structures

### 2.6.3.2 Thermo-gravimetric behavior of composite structures



The contents of the fibers in the composite structures with and without vacuum are presented at Figure 2-12. It confirms that vacuum has influenced on removing UPR in composite structure from TGA results. For instance, around the onset of degradation, a vacuum can reduce the mass loss by 1.41%, 2.18%, and 2.49% for CSM, woven, and fiber combination, respectively. Especially, more than twice the CMS and fiber combination contents were obtained, while 60.09% woven fiber was obtained with heating up to 800 °C.

It also can be seen that the mass loss rates are lower under vacuum following the slope of curves at Figure 2-12 that means the better thermal stability of composite structures. If the mass retention represents the input fiber weight fraction, then it is recommended that less of UPR can be used for composites fabrication under the certain vacuum conditions. The almost linear increment of mass retention from CSM, woven, and their combination can be emphasized that thermal resistance and decomposition of composite structure are mainly dependent on the utilized fiber ratios. The little higher UPR removing in CSM composite displayed the better effect from vacuum pressure because woven is stiffer under the bundled form and UPR may be confined between woven gaps.

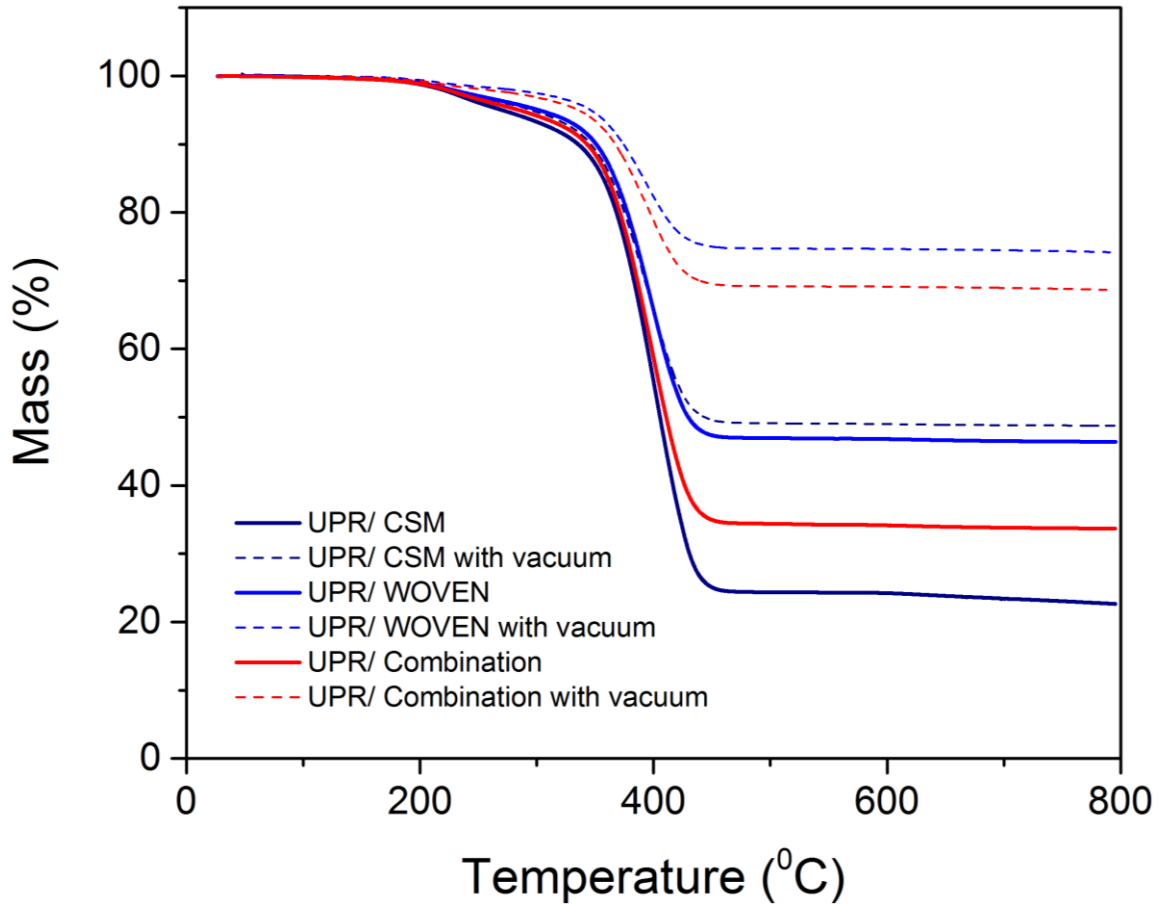


Figure 2-12: Effect of vacuum on the thermo-gravimetric behavior of GFRP composites

### 2.6.3.3 Tensile properties of composite structures

The leaving extra UPR and compressive conditions can make the cross-sectional area of the composite structures decreased when the vacuum was applied. Therefore, the tensile properties of the composite structures could be increased proportionally in the elastic region [41, 42]. Generally, the ultimate tensile strength and elastic modulus of composite structures were positively influenced by vacuum (Figures 2-13 and 2-14). Indeed, the tensile strengths of CSM/UPR, woven/UPR and combination/UPR increased from 87.92 to 125.36 MPa, from 351.67 to 402.96 MPa and from 190.26 to 258.14 MPa, respectively. Furthermore, the elastic modulus also increased by 38.63% in CSM/UPR,

24.31% in woven/UPR and 42.46% in combination/UPR. These results can be also attributed to the continuous vacuum pressure which can remove most of the flaws and voids of the specimens.

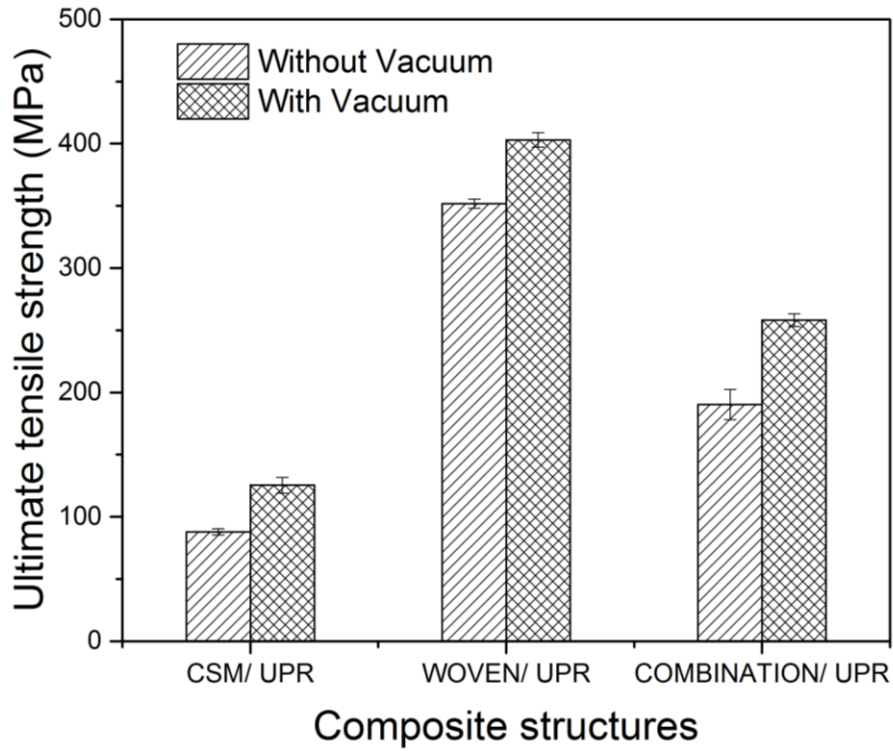


Figure 2-13: Effect of vacuum on the tensile strength of composite structures

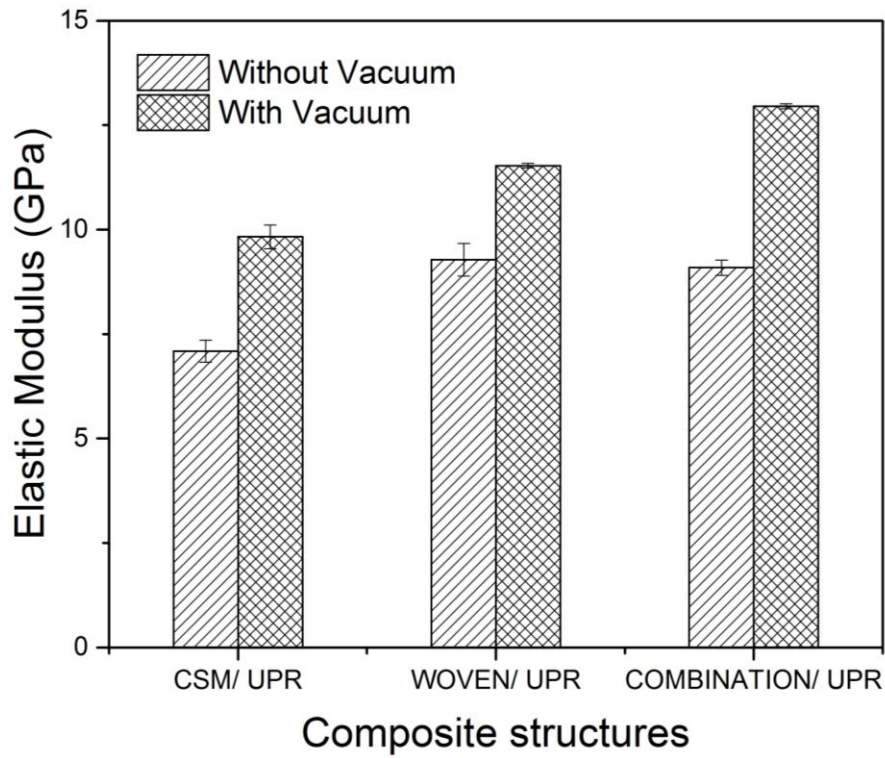


Figure 2-14: Effect of vacuum on the elastic modulus of composite structures

#### 2.6.4 Conclusions

The positive effect of vacuum on density, thermal resistance, and tensile properties is very clear. All type of fibers have almost similar effects by applying vacuum.

## **CHAPTER 3:**

# **Effect of multi-walled carbon nanotubes on tensile properties of unsaturated polyester resin**

*Based on:*

Van-Tho Hoang and Young-Jin Yum, "**Optimization of mixing process and effect of multi-walled carbon nanotubes on tensile properties of unsaturated polyester resin in composite materials**", *Journal of Mechanical Science and Technology*, vol. 31, pp. 1621-1627, 2017.

### 3.1 Introduction

There is a vital and growing demand for glass fiber reinforced polymers in composite materials, especially in many important industries such as aerospace, marine structures, etc. In fact, most of the applications (airplanes, ships) involve working under complex environmental stresses. Thus, improving mechanical properties of composite materials plays a critical role in satisfying needs in real-life situations. Fortunately, carbon nanotubes (CNTs) were found in 1991 [10] that may be one of expected solution due to their superlative properties in mechanical, electrical, and chemical prospects. Carbon nanotubes have attracted many researchers as a very promising reinforcement for thermoplastic and thermosetting plastic matrices of composite materials [15-17, 30, 43]. Most results show remarkable effects on the mechanical properties of nanocomposites with a very small addition of CNTs. For instance, A. Allaoui et al. [15] obtained a 100% and 200% increase in Young's modulus and yield strength respectively, when they added 1 wt.% of multi-walled carbon nanotubes (MWCNTs) into epoxy; Mahmoud M Shokrieh et al. [30] showed a 6% increase in tensile strength and a 20% increase in flexural strength with 0.05 wt.% MWCNTs mixed into epoxy; while Peng Guo et al. [44] used well-dispersed MWCNTs with 8 wt.% and reached 69.7 MPa tensile strength (about 60% higher than neat epoxy).

However, the critical MWCNT content is not coincident and a higher weight fraction of MWCNTs does not show higher mechanical property values. This is attributed to the dispersion state and alignment of MWCNTs in the polymer matrix [18, 45]. In this study, some optimum conditions that have been analyzed in the second chapter such as mixing temperature and hardener ratio for the simplest stirrer mixing to disperse MWCNTs

into UPR were utilized. Afterward, modified UPR was characterized by tensile properties and fracture surfaces to find the optimum MWCNTs weight fraction.

## **3.2 Experiment**

### **3.2.1 Materials**

The unsaturated polyester resin (EC-304) and methyl ethyl ketone peroxide (MEKP) are made by the Aekyung chemical company in South Korea. The multi-walled carbon nanotubes (CM-130) are supplied by the Hanwha Chemical Company in South Korea. From specifications of the manufacturer, MWCNTs were synthesized in aligned form using a chemical vapor deposition (CVD) method and were 10-30  $\mu\text{m}$  in length with a 10-15 nm outer diameter, a 5-10 nm inner diameter, a high aspect ratio ( $\sim 2 \times 10^3$ ), about 90 wt.% purity, and a bulk density of approximately  $0.04 \text{ g/cm}^3$ . The density of UPR is around  $1.15 \text{ g/cm}^3$  and the true density of MWCNTs is  $1.80\text{-}1.95 \text{ g/cm}^3$ .

### **3.2.2 Fabrication of MWCNTs/ UPR specimens**

Tensile specimens (Figure 3-1) of MWCNTs/UPR composite materials were fabricated according to ASTM D 638–03 [46]. Firstly, the different contents of MWCNTs were dispersed into the UPR with a hot and stir machine (HY-HS11, Figure 3-2) at  $60 \text{ }^\circ\text{C}$  and 2,000 rpm for a period of 1 hour. Then, the mixing temperature was reduced to room temperature before pouring 1 wt.% of hardener (MEKP) into the mixture. Next, the MEKP was quickly mixed with the mixture for 30 seconds. During the dispersion time, an aluminum casting mold (Figure 3-3) was cleaned using a cleaning agent. After that, the whole mixture was casted into the mold and cured at  $25 \text{ }^\circ\text{C}$  for 24 hours. In order to remove air voids and to improve cross-linking of the matrix in MWCNTs/UPR [16], specimens were post-cured in an oven at  $80 \text{ }^\circ\text{C}$  for 3 hours. Finally, five tensile specimens were obtained, each with a different MWCNT ratio.

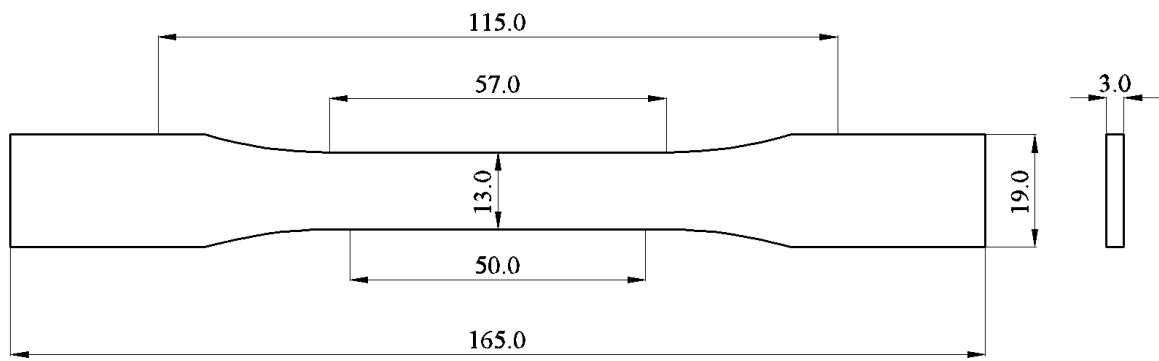


Figure 3-1: The parameters of tensile specimen according to ASTM D638-03 (unit: mm)



Figure 3-2: Hot and stir machine



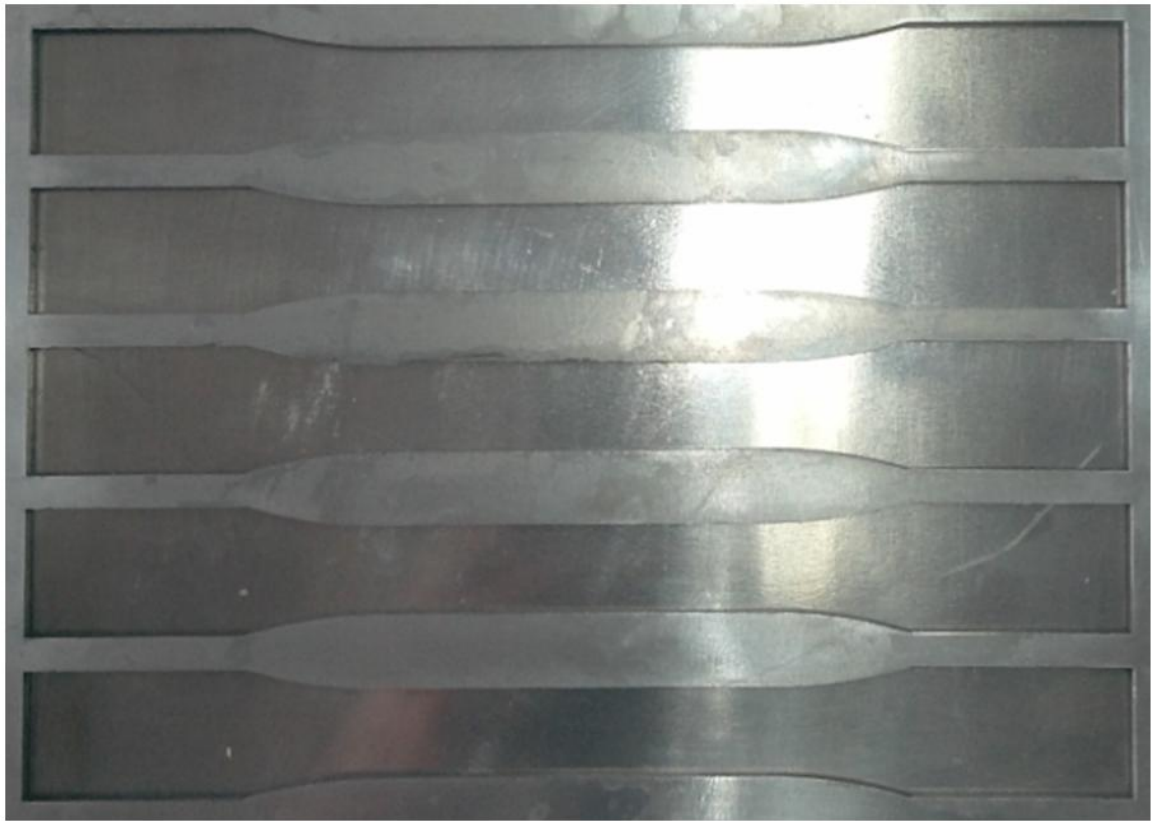


Figure 3-3: Aluminum casting mold

### **3.2.3 Measurements**

#### ***3.2.3.1 Tension testing***

Tension test was conducted with a universal testing machine (DTU-900MHN) to examine mechanical properties of the UPR and MWCNTs/UPR composite according to ASTM D 638–03. The testing speed was 2 mm/min for both tests.

#### ***3.2.3.2 Observation of fracture surfaces***

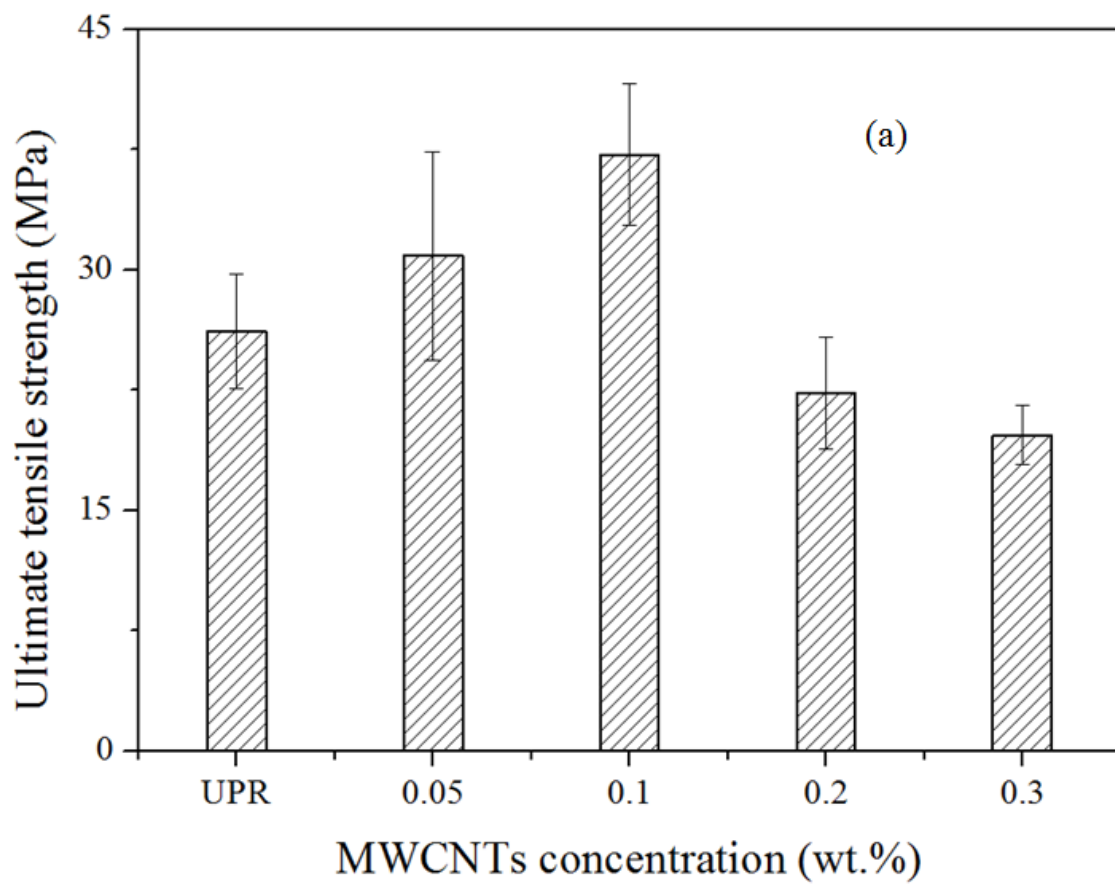
Fracture surfaces of composite materials were scanned with a field emission scanning electron microscope (FE-SEM), JSM-6500F. Degrees of dispersion and bonding of the fiber and matrix are discussed alongside the FE-SEM results.

### **3.3 Results and discussion**

#### **3.3.1. Tensile properties of nanocomposite**

Tensile specimens were fabricated by aluminum casting mold at optimum conditions (60 °C of mixing and 1 wt.% hardener). The enhancement of tensile properties of nanocomposite can be explained based on the uniquely advantageous properties of MWCNTs. Previously, Z. W. Pan et al. [47] showed that the elastic modulus and tensile strength of MWCNTs fluctuate around  $0.45\pm 0.23$  TPa and  $1.72\pm 0.64$  GPa respectively; Min-Feng Yu et al. [48] presented these values as 270-950 GPa and 11-63 GPa (for a set of 19 MWCNTs), respectively. According to load (stress) transfer mechanisms [21, 49], we can conclude that adding MWCNTs plays the important role of improving tensile properties of UPR in composite materials. Normally, mechanical properties of composite materials may be improved with higher reinforcement content. However, the viscosity of the mixture increases at high concentrations of MWCNTs, which impedes dispersion during the mixing process. Therefore, some defects such as air voids and bubbles may appear around MWCNTs inside tensile specimens. Even stress concentration may occur due to fiber agglomeration (poor dispersion). These are the primary reasons for the degradation of tensile properties at a higher weight fraction of MWCNTs. Figure 3-4 shows that tensile strength, Young's modulus and fracture strain increased simultaneously with an increase in the fraction of MWCNTs until 0.1 wt.%. Thus, this tendency strongly agrees with the results of Peng Guo et al. [44] that the fracture toughness of composites was improved by increasing MWCNT fraction. In more detail, the improvement was greatest with 0.1 wt.% MWCNTs added, yielding in increase 42.14%, 13.33%, and 37.17% of tensile strength, elastic modulus, and fracture strain, respectively. Adding 0.05 wt.% MWCNT showed a lesser effect than 0.1 wt.% MWCNT, but tensile properties of the

nanocomposites were still higher than neat UPR. On the other hand, adding higher weight percent of MWCNTs (from 0.2 to 0.3 wt.%) had a negative impact on the properties of material due to the lower distribution quality that is presented in **section 3.3.2**. Finally, the experiment results indicated that 0.3 wt.% MWCNTs is the worst concentration and provides the most unfavorable tensile properties.



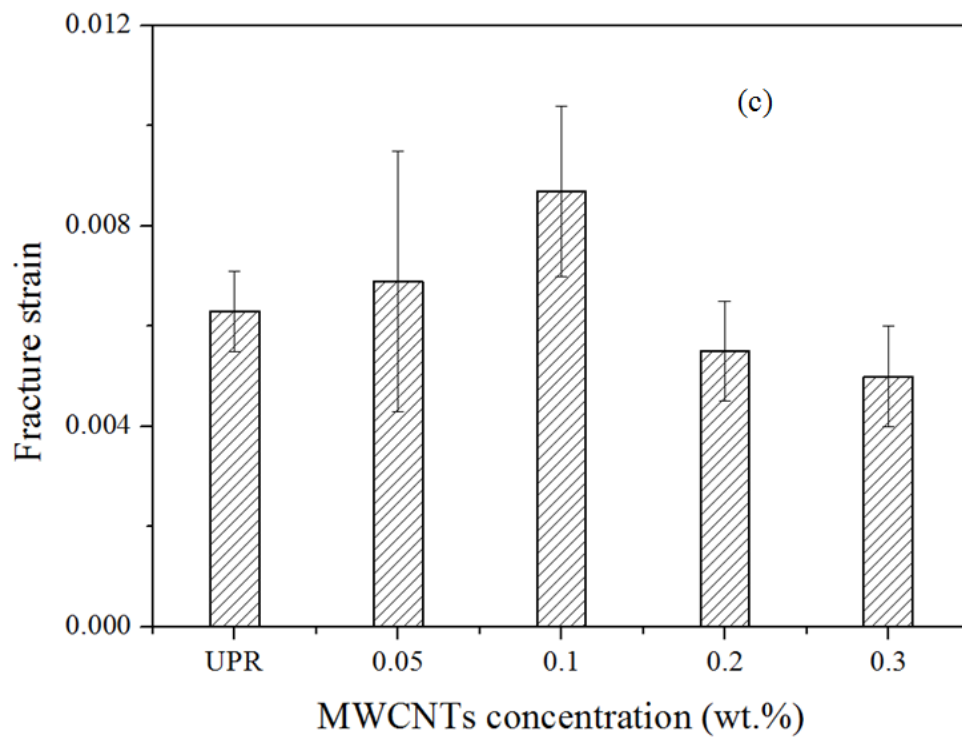
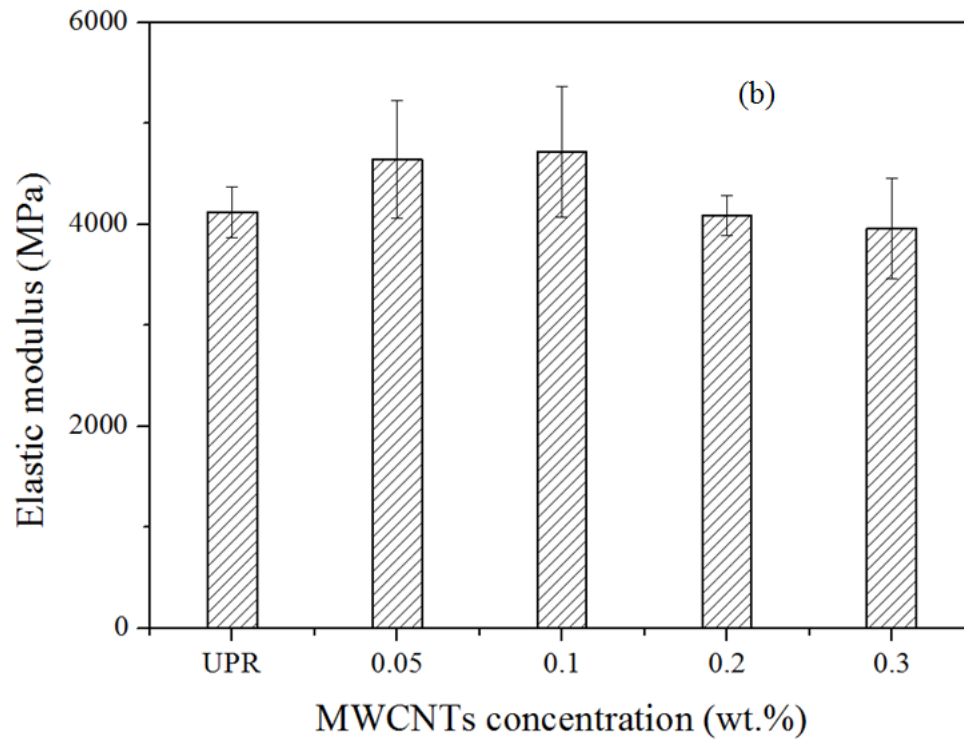


Figure 3-4: Tensile behavior of nanocomposites with different MWCNTs ratios

(a) Tensile strength, (b) Young's modulus, and (c) fracture strain

### 3.3.2 Fracture surface observation results

Several reports have shown that the dispersion of nanowires is an important factor contributing to the mechanical properties of nanocomposite materials. As can be seen from Figure 3-5, the color of the UPR changed from light pink (Figure 3-5a) to dark (Figures 3-5b-e) when MWCNTs were added. This color change indicates good infusion of MWCNTs into the liquid using the previously mentioned mixing conditions.



Figure 3-5: Dispersion of MWCNTs in UPR

(a) Pure UPR, (b) 0.05 wt.% MWCNTs, (c) 0.1 wt.% MWCNTs,  
(d) 0.2 wt.% MWCNTs, and (e) 0.3 wt.% MWCNTs.

The dispersion state and arrangement of MWCNTs are shown in Figure 3-6 based on fracture surfaces of tensile test specimens. All of the images were scanned at the same

scale and magnification by a field emission scanning microscope (FE-SEM). Firstly, Figure 3-6a denotes the smooth surface of neat thermosetting polymer, while others show rougher surfaces. This indicates that adding MWCNTs may make materials more ductile. The second observation is a more crowded distribution of nanowires from Figure 3-6b to Figure 3-6e due to the increase of weight fraction of MWCNTs. Figure 3-6b and Figure 3-6c show strongly uniform nanoparticle distributions in the polymer, which implies a robust mixing process with lower addition of nanotubes. Meanwhile, Figure 3-6d and Figure 3-6e indicate a non-uniform distribution of MWCNTs, and even show nanotubes aggregated in tangles. This aggregation can explain the stress concentration and the deterioration of the tensile properties at higher fiber concentrations. In addition, these agglomerations may more easily allow for the creation of defects around MWCNTs.

Focusing on Figure 3-6b and Figure 3-6c, we can see that fiber direction was randomly distributed, but most MWCNTs emerged perpendicularly with different fiber lengths on fracture surfaces. The fracture surfaces did not have any pits or holes with the approximate diameter with MWCNTs, which means that stresses are transferred from the matrix to fiber mostly via axial stress. Such stress transfer is one of the reasons that the addition of nanofibers increases tensile strength. Consequently, a greater number of emerged fibers on the fracture surface indicates a higher strength of the composite material. Furthermore, the different lengths of fibers prove that the fracture strength also improved because the underlying matrix can be broken early, but confined fibers are broken layer by layer over the critical load of the UPR.

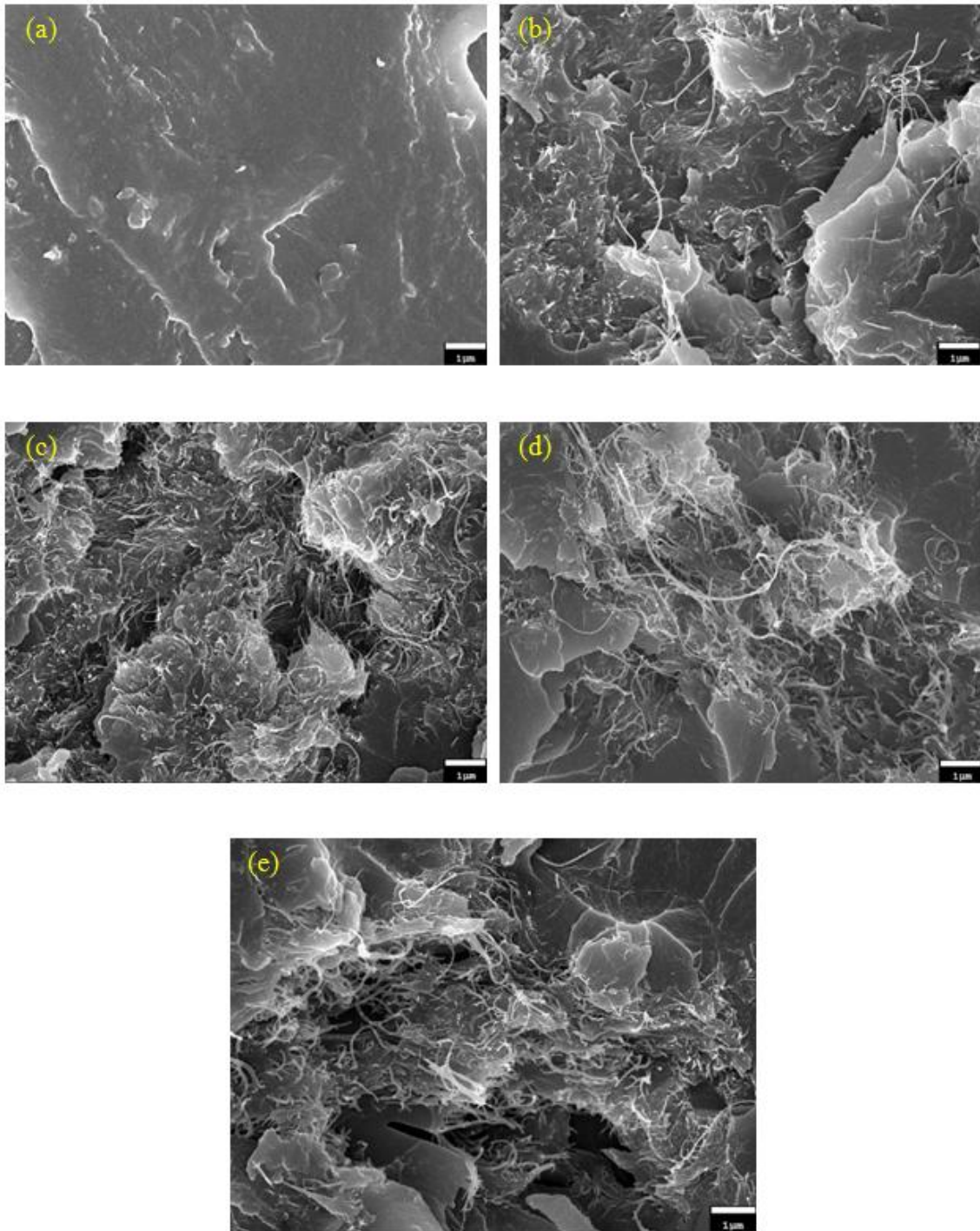


Figure 3-6: Morphology of fracture surfaces

(a) Pure UPR, (b) 0.05 wt.% MWCNTs, (c) 0.1 wt.% MWCNTs,

(d) 0.2 wt.% MWCNTs, and (e) 0.3 wt.% MWCNTs.

### **3.4 Conclusions**

MWCNTs were successfully mixed with UPR using the stir method based on the optimum conditions of 60 °C during mixing and 1 wt.% of MEKP. Tensile properties of the polymer matrix were significantly improved and 0.1 wt.% of MWCNTs is proved to be the best choice of fiber weight fraction, yielding a higher strength (42.14%), elastic modulus (14.33%) and fracture strain (37.17%). FE-SEM results also strongly agree with the tensile properties of 0.1 wt.% of MWCNTs for further applications. Mixing conditions are almost similar to the practical processes used in the industry, and they not only show improved mechanical properties, but are also exhibit safe working conditions. Therefore, the results in this study may be applied in future applications to obtain better products.



## **CHAPTER 4:**

# **Effect of multi-walled carbon nanotubes on tensile properties of various glass fibers/ unsaturated polyester resin composites**

*Based on:*

Van-Tho Hoang and Young-Jin Yum, " **Optimization of the fabrication conditions and effects of multi-walled carbon nanotubes on the tensile properties of various glass fibers/ unsaturated polyester resin composites** ", *e-Polymers*, (accepted) 2018.

## 4.1 Introduction

Polymer composites have been utilized as alternative materials for many decades to avoid exhausting natural resources. Among them, glass fiber reinforced thermosetting resin is a common material due to its use in electronics, home and furniture, aerospace, boats and marine, medical, and automobile applications [3, 4]. This material can show desirable characteristics including low density, high specific strength, high specific modulus, high corrosion resistance, and low cost [1]. In particular, glass fiber/polyester composite materials have represented excellent behavior to reinforce the specifically expected direction of structures compared to conventional metals.

The enhancement of material characteristics has attracted a wide range of researchers to improve fuel efficiency, reduce carbon dioxide emissions in the equipment industry [50], and increase the displacement of ships, particularly to satisfy the strength criteria for transport systems. Composite fabrication methods for thermosetting polymer composites have been improved to partially meet the above trends. Hand lay-up is a manual technique, while vacuum-assisted resin transfer molding has been considered the most efficient fabrication method because of its higher volume fraction, low void contents, low weight, low operating cost, low production rates, being less harmful, and ability to accommodate complex shapes [51].

In fact, the mechanical properties of composite materials are strongly dependent on the strengths and moduli of the matrix and fiber as well as the bonding strength between the matrix and fiber [11]. Therefore, modifying the fiber or matrix has increased by simply adding high potential candidates. Multi-walled carbon nanotubes (MWCNTs) have been widely applied due to their slightly lower properties but much lower cost compared to

single-walled carbon nanotubes in the series of carbon nanotubes since 1991 when Iijima [10] first discovered the unique structure of carbon nanotubes. Several researches have focused on dispersing MWCNTs into thermosetting resins including epoxy [44, 52-54], phenolic [55], and unsaturated polyester [56]. Some issues were encountered and compared to determine the best choice for dispersion quality between MWCNTs and the thermosetting polymer [57, 58]. In addition, based on the strong development of nanotechnology, reinforcement components were also treated by growing MWCNTs on their surfaces [59-65]. Some methods have been proposed to add MWCNTs on the surface of fibers such as chemical vapor deposition (CVD), physical vapor deposition (PVD) [61], and a simple chemical method [62], where CVD is the most widely used [59-61, 63-65]. Actually, MWCNTs impart different positive effects in each fabrication method. Thus, the mechanical properties of novel composite materials based on MWCNT-coated fibers/neat resins [66-75], MWCNT-dispersed resin/neat fibers [76-84], or a combination of both treated fibers and a treated matrix [12-13] have been considered to determine the optimum modification conditions. According to the load transfer mechanism [85] and stress transfer theory [49], axial stress and the interfacial shear strength (IFSS) of composite structures can be improved with an appropriate content of added MWCNTs. The basic mechanical behavior was mainly concentrated on the IFSS of a single fiber and matrix by fragmentation, tensile, and micro-droplet (pull-out) tests in most studies. Some significant influences of the MWCNTs on the material properties were observed such as a 69% higher tensile strength [72], 94% higher IFSS [73], 80% higher fracture toughness ( $G_{IC}$ ), and ~32% smaller coefficient of thermal expansion [77]. Ashish Warriar et al. [12] and A. Godara et al. [13] showed that the best performance was achieved from fiber treatment, and polymer treatment was slightly less effective than fiber treatment, while the

combination resulted in the lowest effect in the view of the  $G_{IC}$ , thermal expansion coefficient, crack propagation, and IFSS results.

On the other hand, J. Dai et al. [71] presented some drawbacks, difficulties, and challenges regarding both the MWCNT-modified matrix and fibers. For example, it is not easy to obtain high quality dispersion in mixing MWCNTs in the matrix due to the highly attractive Van der Waals force of MWCNT particles. A high aspect ratio strongly reduces the viscosity of the polymer such that a small amount of added MWCNTs cannot fully salvage the performance of the additive. In the case of fiber edition, metal catalysts can easily diffuse into substrates at high temperatures and different forms of carbon can be created on the surface of substrates due to the increasing temperature inside the chamber, such that a high quality fiber coating cannot be achieved. In addition, due to the limitation of size, CVD and PVD are difficult to apply to mass production and they can only be used to locally grow nanoparticles on the surface of fibers. Moreover, pure carbon nanotube fibers were recommended to overcome the problems encountered by processing CNTs and these fibers showed extremely high mechanical, thermal, and electrical properties, whereas creating a laminate is still challenging [86, 87]. Furthermore, carbon nanotubes were also used to solve the out-of-plane weakness problem [88, 89].

As can be seen from the literature review, so many researchers have been focusing on developing the mechanical properties of thermosetting composite materials. Mostly, the studies considered epoxy resin and carbon fiber. Several researches evaluated UPR [11, 56, 58] and glass fibers [11-13, 71, 75, 76, 78, 79, 84], especially not any topic related to the combination of chopped strand mat (CSM) and woven reinforced MWCNTs modified UPR, although UPR, CSM and woven are also well-known members in the composite world. In addition, dispersion methods of modified UPR and grown fibers by MWCNTs

have been applied well only in laboratory scale. Thus, further investigation of applying MWCNTs in mass production environments is very important. From chapter 3, the optimum ratio of MWCNTs (0.1 wt.%) was obtained by the higher tensile properties and dispersion quality. Two optimum conditions from chapter 2 were applied for the simple dispersion method of MWCNTs into UPR including mixing temperature and hardener ratio. Motivated by above discussion, this study aims to obtain higher mechanical properties of conventional fibers/ modified polymer composites based on some other optimum conditions in composite fabrication as well as in mixing MWCNTs into UPR. Therefore, other factors from chapter 2 such as reasonable initial curing temperatures of UPR, vacuum, and the best ratio and quality of MWCNTs from chapter 3 finally were applied to access tensile properties of various glass fibers/ edited UPR composites.

## **4.2 Experiment**

### **4.2.1 Materials**

Reinforcement components including glass fiber woven and glass fiber chopped strand mats were made by Kimchon Plant Company.

Unsaturated polyester resin (EC-304) and methyl ethyl ketone peroxide (MEKP) were made by Aekyung Chemical Company, South Korea.

The multi-walled carbon nanotubes (CM-130) with an outside diameter of 10-15 nm, an inside diameter of 5-10 nm, and length of 10-30  $\mu\text{m}$  were supplied by Hanwha Chemical Company, South Korea.

## **4.2.2 Fabrication**

### ***4.2.2.1 Matrix modification***

According to our previous results (chapter 3), a higher tensile strength and higher dispersion quality can be obtained when mixing MWCNTs and UPR at a high temperature. In this study, MWCNTs were mixed with UPR by a Hot and Stir machine at 60 °C and 2,000 rpm for 1 hour. Then, the mixing temperature was reduced to room temperature. This step is very important because at a high temperature, the curing time will be very short (section 2.4.3.1), which obstructs the fabrication procedure.

### ***4.2.2.2 Composite structure fabrication***

Generally, the composite laminate was fabricated with 4 layers of the fiber and matrix using a roller in a hand lay-up fabrication method. The ratio of fiber and matrix was kept as a constant (Table 4-1) to survey the effect of fiber changes and adding MWCNTs. Here, the chopped strand mat (CSM) weight fraction was 0.25 (25%) and woven weight fraction was 0.5 (0.5%). Meanwhile, the neat or modified UPR was quickly mixed at an optimum hardener ratio (1 wt.%) for 30 seconds by hand. After fabrication, the curing process was started at a certain temperature (from 25 to 35 °C) for 24 hours. Then, an oven was used for the post-curing process at 80 °C for 2 hours to remove air voids and improve cross-linking of the matrix and fiber. Finally, five tensile specimens in rectangular shape were cut by a diamond cutter for each plate (the length was 200 mm, the width was 20 mm, the thickness was varied in each plate) without a tab.

In case of applying vacuum, bleeder, peel ply and vacuum bag were used for packing specimens and mold after laminating. The high vacuum pump (W2V10) was connected by a hose to assist fabrication process for 5 hours to ensure UPR cured fully.

Table 4-1: Fiber weight fraction in different cases.

No.	Components	Weight fraction (%)			
		CSM	Woven	MWCNTs	UPR
1	MWCNTs+UPR			0.1	100
2	CSM+UPR	25			75
3	Woven+UPR		50		50
4	CSM+Woven+UPR	12.5	25		62.5
5	CSM+MWCNTs+UPR	25		0.075	75
6	Woven+MWCNTs+UPR		50	0.05	50
7	CSM+Woven+MWCNTs+UPR	12.5	25	0.0625	62.5

#### 4.2.3 Measurements

The tension test was conducted using an universal testing machine (DTU-900MHN) at a test speed of 2 mm/min according to ASTM D 3099. An extensometer with a 50 mm gauge length was used. The tensile properties were analyzed to evaluate the effects of the adding MWCNTs on the various composite structures.

#### 4.3 Results and discussion

Based on the optimized conditions such as initial curing temperature, fiber changes and vacuum, the tensile properties of the various fibers composite structures were continuously investigated by adding 0.1 wt.% MWCNTs. The good effects of MWCNTs are clear due to the good tensile properties of all fibers composite structures were obtained (Figure 4-1 and 4-2). The tensile strength of CSM/UPR increased from 71.31 to 77.72 MPa and Young's modulus increased from 6.70 to 7.34 GPa. Similarly, the tensile strength and elastic modulus of woven/UPR increased by 9.48% and 14.63%, respectively. Finally, the

strength and modulus of combination/UPR were enhanced by 25.29 MPa (14.63%) and 1.39 GPa (17.46%), respectively. In comparison, combination/UPR exhibits a little bit higher tensile properties after adding MWCNTs than woven composite, while CSM reproduces the lowest impact. Indeed, the raise of tensile properties in fibers composite expresses the important role of the appearance of MWCNTs. Previously, the adding 0.1 wt.% into UPR represented the good dispersion quality than other ratios of MWCNTs without any agglomerations of MWCNTs in field emission scanning electron microscope (FE-SEM) results, that means there were no stress concentration in modified UPR. Consequently, the tensile stress transferred well from UPR to MWCNTs, then the higher of 42.14% tensile strength and 14.33% elastic modulus were achieved in chapter 3. Compare to the improvement of tensile properties and the weight fraction of all components of various fibers/ modified UPR composite in the current results, we can see that the performance of 0.1 wt.% MWCNTs is almost conserved.

As we observed, composite structures, especially polyester, are very sensitive to the environment. In addition, the composite fabrication procedure is complicated involving many steps such as stacking several fiber layers, especially applying bleeder, peel ply and vacuum bag before employing vacuum pump. That may take much time while curing already occurred in previous step. Therefore, choosing the appropriate moment and initial temperature for fabrication was the biggest difficulty in the experiments to get a better effect of using vacuum before the UPR cured. In comparison, the results discussed in the section 2.6.3.3, the tensile properties of the nanocomposite structures were lower. The main reason may be attributed to the difference of the initial curing temperature and the time to start vacuum (section 2.4.3.1) that affect on the vacuum pressure applied.



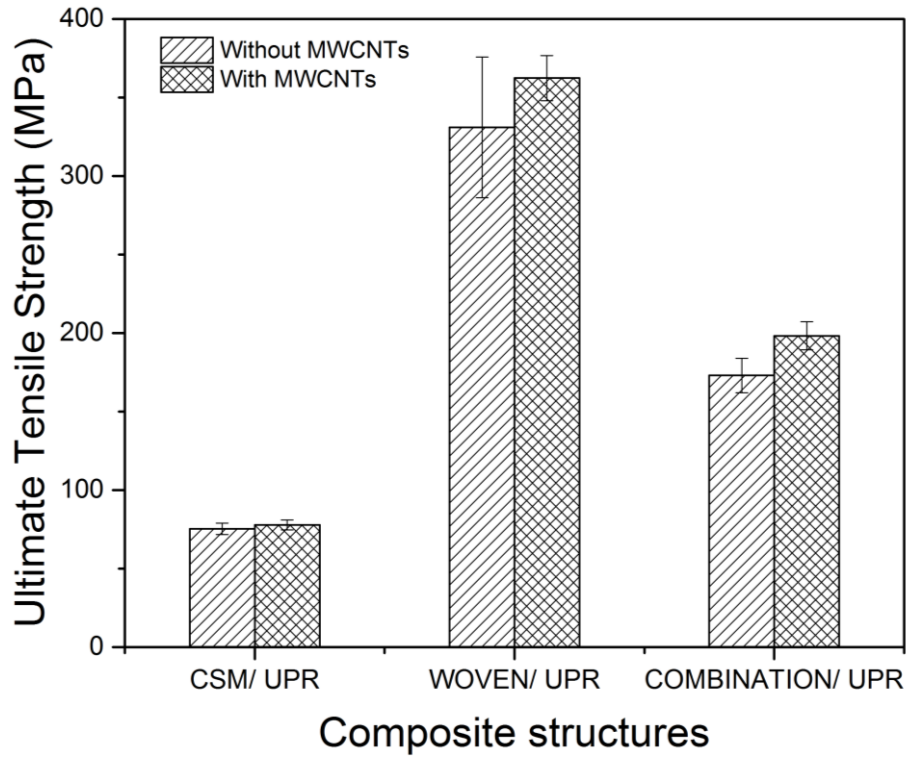


Figure 4-1: Effects of MWCNTs on the tensile strength of various fibers composite

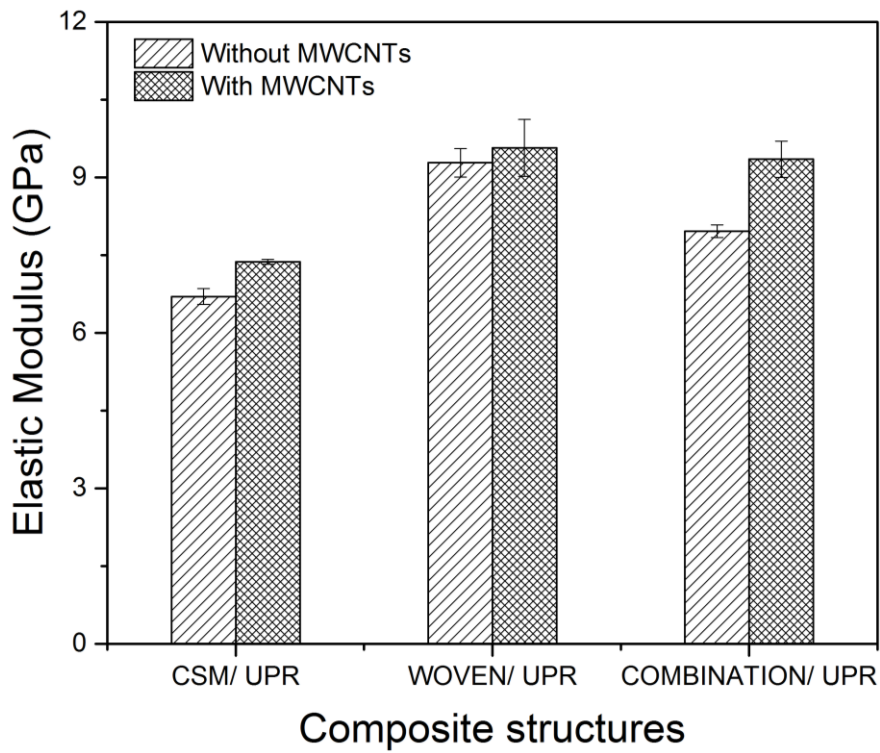


Figure 4-2: Effects of MWCNTs on the elastic modulus of various fibers composite

#### **4.4 Conclusions**

In this study, all of the optimum conditions were applied to evaluate the effect of adding MWCNTs on tensile properties of various glass fibers composite. Finally, MWCNTs possessed a positive influence on the tensile properties of the composite structure under these optimum conditions mentioned in chapter 2. Additionally, mixing conditions of the simple modification object (UPR) and dispersion method (stir method) are close to the realistic processes used in the industry. They not only indicate the enhanced mechanical properties of composite materials, but also realize the safe working conditions (less harmful, lower exothermic temperature and shorter time in fabrication). Combining other good effect factors, therefore, the results in this study could be widely applied for mass production in glass fiber reinforced unsaturated polyester resin composites involving MWCNTs.

## **CHAPTER 5:**

# **Fracture toughness of neat UPR and various glass fibers composites**

## 5.1 Introduction

GFRP composites have been known as good in-plane strength materials, that is a good choice for specific reinforced orientation. However, their out-of-plane behavior is much lower than in-plane characteristics. Indeed, the laminated composites are anisotropic materials and stacked by some laminas. Therefore, the out-of-plane strength or delamination resistance is significantly dependent on the strength of resin, bridging fiber, or interfacial strength of fiber and matrix [90]. Moreover, the flaws during fabrication or after working for a long time cannot be perfectly prevented and estimated the same as other materials. That causes sudden failures and may cause the serious disasters.

The theory of fracture mechanics has been proposed to deal with this kind of risk. Basically, three modes of fracture were introduced including opening (mode I), in-plane shear (mode II), and out-of plane (mode III) [91]. The extended modes were also known as mixed-modes that combine at least two of above three modes. There are many types of specimen that can be used to investigate fracture toughness, such as compact tension (CT), single-edge-notch bending (SENB), double cantilever beam (DCB), end-notched flexural (ENF), etc. Based on the different loading conditions, each mode will be taken into account. Besides, the linear elastic fracture mechanics (LEFM) is normally applied for brittle composite materials due to their own elastic behaviors.

Besides the improvement of mechanical properties, the fracture toughness of GFRP composites also need to enhance in order to avoid the critical risk of their applications while in service. Fundamentally, fracture toughness of GFRP can be improved if tougher resin and/or fiber and their interfacial strength. There are several results that have been focused on raising fracture toughness of resin and/or fiber reinforced polymer composites.

Carbon nanotubes with their various forms (single-walled, double-walled, or multi-walled) have been used potentially to rise fracture toughness of UPR as well as GFRP. For example, The 0.1 wt.% single-walled CNTs were used to obtain the increase of 13% in mode I fracture toughness and 28% in mode II fracture toughness of carbon/epoxy laminate composites [92]. A. Tuğrul Seyhan et al. [93] achieved higher fracture toughness of neat polymer using the pristine and functionalized MWCNTs and DWCNTs; Volkan Eskizeybek et al [94] grafted CNTs chemically onto plain weave glass fabric mats to improved mode I interlaminar fracture toughness of composite structures. MWCNTs were also used to modified resin and enhance delamination fatigue resistance of glass fiber plain weave composites [95]. Adding MWCNTs also can increase 94% interfacial shear stress (IFSS) [73] and 80% fracture toughness [77] of carbon fiber/epoxy composites. Beside carbon nanotubes, other nanomaterials were introduced to increase mode I and mode II interlaminar fracture toughness of woven carbon fabric such as graphene nanoplatelets (GnPs) and carbon blacks (CBs) [96]. In addition, mode I, mode II, and mixed-mode I/II interlaminar fracture toughness of GFRP also can be raised by fiber treatment [97]. Fracture behavior of GFRP can be changed by the fiber volume fraction [98] as well as environment [99].

The resin is homogeneous material and CSM is assumed as homogeneous one. That mean the fracture mechanics can be applied by create initial crack using razor blade and/or sawing for those materials. Additionally, the initial crack of laminated composite can be generated by adding non-adhesive film at the mid-plane of plate during fabrication. However, the pre-crack method can be strongly affected fracture toughness value of homogeneous materials [100]. A new method was proposed by Nithiananthan Kuppusamy [101], that can release almost residual strain, and obtain consistent, sharp pre-crack. Thus

the fracture toughness value could be naturally accurate. Although the initial crack can be produced better than tapping razor blade and does not depend on the skill of technician using the apparatus introduced in this research, but the procedure is quite complicated due to the calculation of mechanical properties and additional tools. Individually, UPR has gelation state that may be easier to generate initial crack in compare to the rigid state. Therefore, in this chapter, the prototype of initial crack generation is introduced. Furthermore, in our best knowledge, pre-crack of CSM laminated composite has not been generated by insert thin film at mid-plane to investigate the energy release rate. Besides, the fracture behavior of CSM and woven have not studied as well. Consequently, this chapter aims to find the good process of pre-crack of UPR and investigate the fracture toughness of various glass fibers reinforced UPR composites. It is a preparation step to enhance fracture toughness of those composites by adding some good fracture toughness nanoparticles in the future works.

## **5.2 Experiment**

### **5.2.1 Materials**

Reinforcement components including glass fiber woven and glass fiber chopped strand mats were made by Kimchon Plant Company.

Unsaturated polyester resin (EC-304) and methyl ethyl ketone peroxide (MEKP) were made by Aekyung Chemical Company, South Korea.

### **5.2.2 Fabrication**

#### ***5.2.2.1 Single-edge-notch bending (SENB) specimen for UPR***

As mentioned in the reference [100], in plane strain fracture toughness was not influenced by the notch geometry. Additionally, according to ASTM D 5045-99 [102],

single-edge-notch bending specimen was chosen to investigate the effect of initial crack creation method on the toughness ( $K_{IC}$ ) of UPR in this experiment. The aluminum mold was designed and fabricated based on the ASTM D 5045-99, that can be seen at Figure 5-1 and 5-2 with 10 mm in thickness of specimen.



Figure 5-1: Aluminum mold for casting UPR

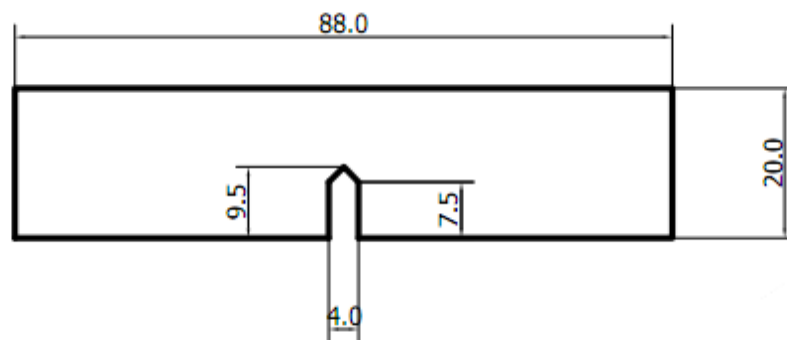


Figure 5-2: The shape and parameter of SENB specimen

The UPR was mixed with 1% hardener for 30 seconds before pouring into the mold (Figure 5-3). Then, the curing was happened at room temperature for 24 hours. The post-curing was also held after curing in an oven at 80 °C in 2 hours. The SENB specimens can be obtained easily when the temperature of oven reduced to room temperature due to the volume shrinkage of UPR. Finally, the specimens were polished before create the crack.

Three different pre-crack methods were used including tapping razor blade, sawing, and bending the specimen in gelation stage of UPR (current method). Obviously, the initial crack length was measured after create crack and the crack tip already identify.



Figure 5-3: UPR after casting in aluminum mold



### 5.2.2.2 Double cantilever beam (DCB) and end-notched flexural (ENF) specimen for composites

The composite plates were fabricated by laminate 8 layers of different glass fibers reinforced UPR using hand lay-up method. The size of plates is 250 mm in length and 220 mm in width. The Teflon film with 25  $\mu\text{m}$  in thickness was inserted at the mid-plane of all plate to create the initial crack. The weight fraction of CSM and woven were 25% and 50% in composite fabrication, respectively. The curing was occurred at room temperature for 24 hours, then post-curing was in an oven at 80  $^{\circ}\text{C}$  for 2 hours. Then, the plates were cut by diamond cutter to obtained DCB and ENF specimens with the same parameters (200 mm in length and 20 mm in width), while the thickness was varies with the different of fibers (Figure 5-4). The fiber changes are the same as Chapter 4, where CSM, Woven, and their combination were utilized.

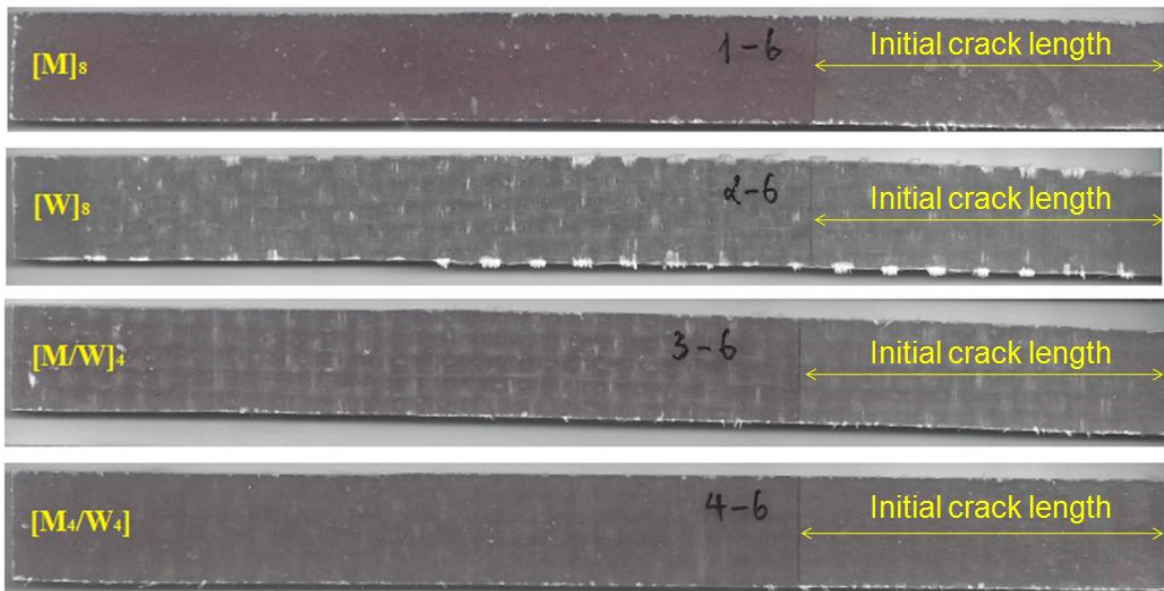


Figure 5-4: Configuration of mode I and mode II specimens

The parameters of DCB and ENF specimens were strictly followed ASTM D5528-3 [103] and ASTM D7905/D7905M-14 [104], respectively. Therefore, piano hinges were

purchased for attachment at mode I specimens. The hinges and pre-crack ends were crashed by rough sand paper, then cleaned by acetone before using rabbit bond to attach them together. The DCB specimens were then marked the crack tip position and crack propagation length with 5 mm interval. Meanwhile, non-precracked (NPC) method was applied for ENF specimens. Thus, 3 different crack length (20 mm, 30 mm, and 40 mm) and applied load positions were marked on the specimen. NPC toughness means an interlaminar fracture toughness value that is determined from the pre-implanted insert [104].

### **5.2.3 Testing**

Confocal microscope was used to monitor the crack shape and parameters of SENB specimen before fracture test. Besides, surface roughness of initial crack surface and morphology of initial crack surface and fracture surface of SENB specimen after fracture test were also determined by 2D and 3D images from confocal microscope.

The SENB specimens were tested by 3 point bending method with speed of 15 revolution per minute (rpm) (or 12 mm/min). The span length was determined by 4\*width of specimen (80 mm); ENF was also tested by 3 point bending method with speed of 1 rpm (0.8 mm/min). The span length was fixed by 100 mm; while DCB was test by tension loading with 4 rpm (3.2 mm/min). It was continuously tested to record load, displacement, and crack propagation. While crack propagation was visually recorded by necked-eyes and stopwatch timer then matched with load and displacement by time. All of tests were conducted by EUN SUNG universal testing machine (Figure 5-5). The load and displacement were recorded by DT board (DAQ DT9838) with 200 Hz of frequency.



Figure 5- 5: Configuration of mode I and mode II specimens

### 5.3 Calculations

#### 5.3.1 Plane-strain fracture toughness $K_{IC}$ of UPR (ASTM D5045-99)

$$K_Q = \left( \frac{P_Q}{BW^{\frac{3}{2}} \cdot 1} \right) f(x) \quad (5-1)$$

$$f(x) = 6x^{1/2} \frac{[1.99 - x(1-x)(2.15 - 3.93x + 2.7x^2)]}{(1+2x)(1-x)^{3/2}} \quad (5-2)$$

Here:

- $K_Q$  is the trial critical stress intensity factor  $K_{IC}$  value,  $\text{MPa}\cdot\text{m}^{1/2}$
- $P_Q$  is determined load, kN

- B is thickness, cm
- W is width, cm
- $x = a/W$  (a is crack length, cm)

The relation between load and displacement of UPR can be seen at the Figure 5-6 as the following:

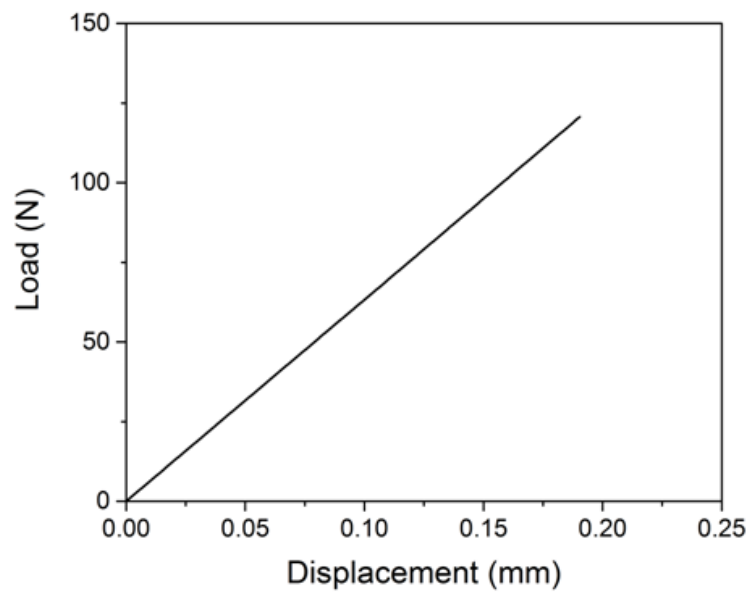


Figure 5-6: Load-displacement curve of UPR

Thus,  $P_Q$  is  $P_{max}$  in this situation.

From the linear behavior of load and displacement of UPR (Figure 5-6), the energy release rate  $G_{IC}$  ( $\text{kJ/m}^2$ ) can be calculated by applying the linear elastic fracture mechanics (LEFM) formula as:

$$G_{IC} = \frac{(1 - \nu)K_{IC}^2}{E} \quad (5 - 3)$$

While, E is Young's modulus (MPa) and  $\nu$  is Poisson's ratio of UPR that were also obtained from tensile test. In the experiment, tensile test was performed at the same time and temperature condition as the fracture test using Rosette strain gauge to record strain in 2 directions that helped to calculate Elastic modulus and Poisson's ratio.

### **5.3.2 Mode I interlaminar fracture toughness of various glass fibers reinforced UPR composites (ASTM D5528-13)**

The modified beam theory (MBT) method was chosen for calculation.

$$G_I = \frac{3P\delta}{2b(a + |\Delta|)} \quad (5 - 4)$$

Here:

- $G_I$  is mode I interlaminar fracture toughness,  $\text{kJ/m}^2$
- P is load, N
- $\delta$  is load point displacement, mm
- b is specimen width, mm
- a is delamination length, mm
- $\Delta$  is correcting delamination length due to the rotation of beam during loading, mm. It can be calculated by linear relation of the cube root of compliance  $C^{1/3}$  and delamination length a (Figure 5-7). Where compliance  $C = \delta/P$ .

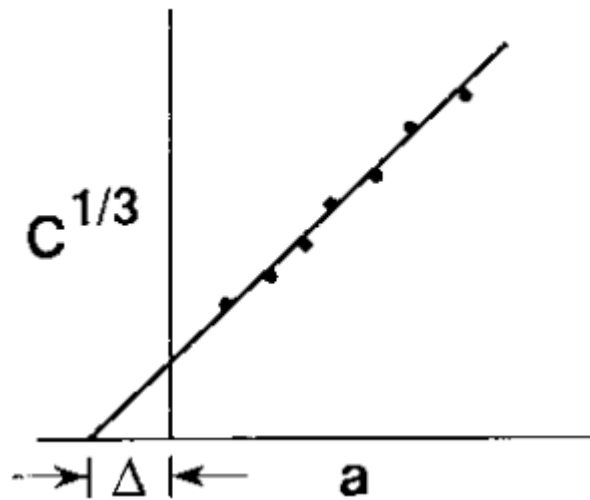


Figure 5-7: Determination of correcting delamination length (Figure 4, Ref. 103)

Using Microsoft Excel, we can obtain  $\Delta$  easily as the following procedure: Plot the curve of  $a$  and  $C^{1/3}$ , then using linear regression function ( $C^{1/3} = ba + d$ , here  $b$  and  $d$  are arbitrary) to fit that curve. The accurate of linear function can be evaluated by the coefficient of determination  $R^2$  that should be closed to 1. Finally, solving the obtained linear equation we can achieve  $\Delta$ .

Figure 5-8 shows an example of this procedure. The red curve describes the true relation of  $C^{1/3}$  and  $a$ , while black one is linear regression function.  $R^2 = 0.988$  means the fitting curve is reasonable, thus  $b = 0.011$  and  $d = 0.079$  while  $y$  is  $C^{1/3}$  and  $x$  is  $a$ . Solving the equation:  $y = 0.011x + 0.079 = 0$ , then  $x = -7.18$  mm. That is expected value  $\Delta$ .

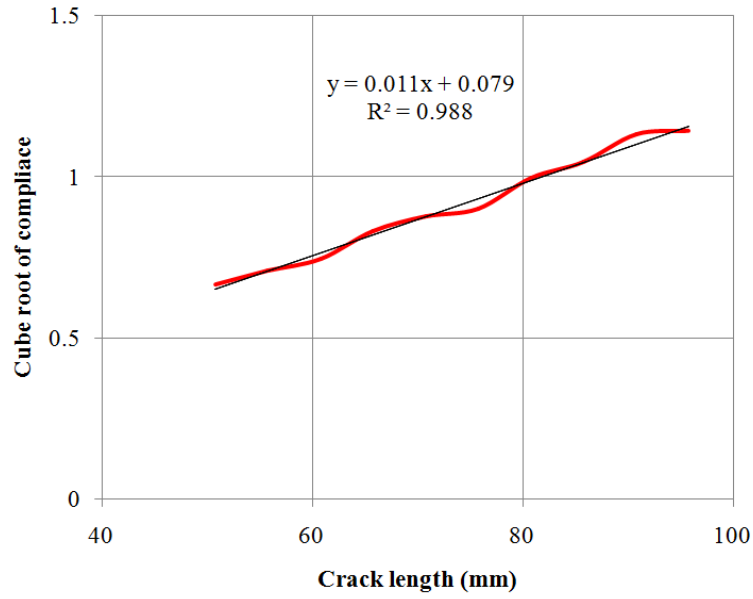


Figure 5-8: Linear regression function of cube root of compliance and delamination length

In addition, the compliance values can be extracted from the load-displacement curve for each specimen. That curve includes the recorded delamination length (Figure 5-9).

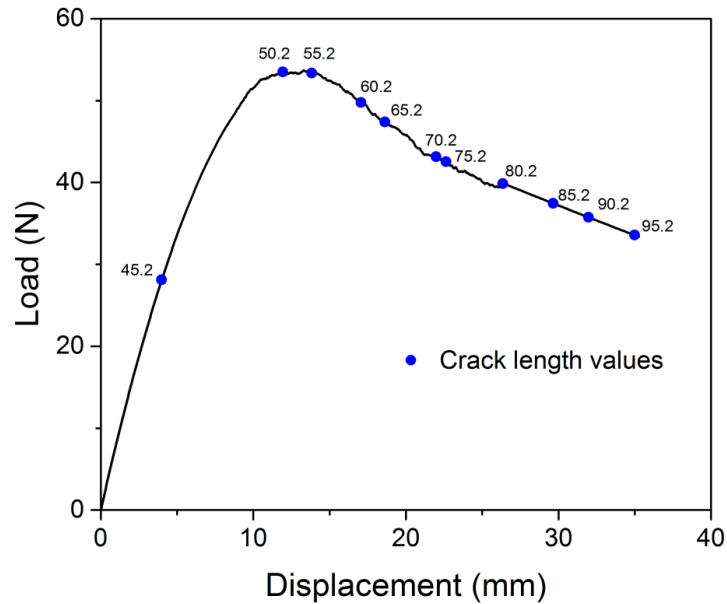


Figure 5-9: Load, displacement, and delamination length of mode I test

### 5.3.3 Mode II interlaminar fracture toughness of various glass fibers reinforced UPR composites (ASTM D7905/D7905M-14)

From the crack tip, 3 different of crack length values were determined by 20, 30 and 40 mm. At 20 mm and 40 mm of crack length, about 50% of maximum force was applied to find the compliant values, while the test was performed until reaching the maximum force at  $a_0 = 30\text{mm}$  (Figure 5-10).

The compliance calibration (CC) method was chosen for calculation:

$$G_Q = \frac{3mP_{max}^2 a_0^2}{2B} \quad (5 - 5)$$

Here:

- $G_Q$  is the condition, it will be  $G_{IIC}$ ,  $\text{kJ/m}^2$
- $P_{max}$  is the maximum force from fracture test, N
- $a_0$  is crack length using in the fracture test,  $a_0 = 30 \text{ mm}$ .
- B is specimen width, mm
- m is the CC coefficient, it can be determined by solving the equation:

$$C = A + ma^3 \quad (5 - 6)$$

As the specimen procedure in section 5.3.3, linear regression function can be found to fit the compliance (C) and crack length cubed ( $a^3$ ) using Microsoft Excel. There are only three values of a and C from the curve (Figure 5-11).



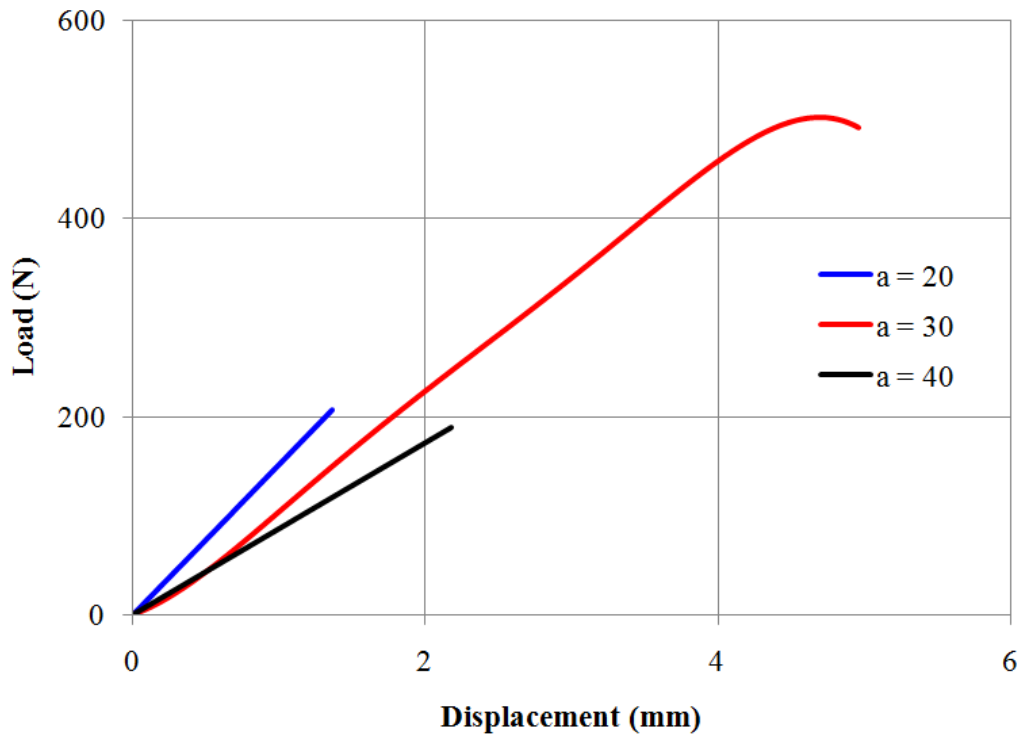


Figure 5-10: Load - displacement curve of different crack length in fracture test

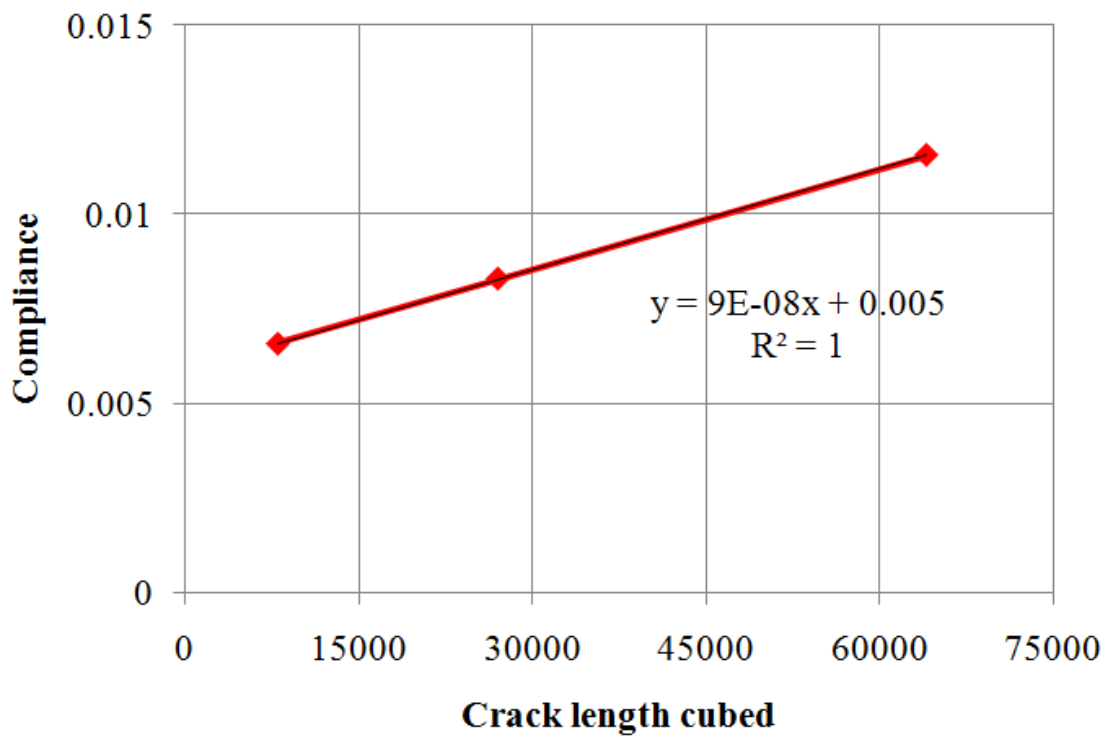


Figure 5-11: Linear regression function of compliance and delamination length cubed

$R^2 = 1$  means the fitting curve of compliance and delamination length cubed is completely matched by linear function. Compare with the (5-6) equation, thus,  $A = 0.005$  and  $m = 9E-08$ .

## **5.4 Results and discussion**

### **5.4.1 Effect of pre-crack method on the behavior of UPR**

#### **5.4.1.1 Morphology**

The notch of specimen after curing was obtained as Figure 5-12. Normally, the shape of specimen was kept as the shape of mold.

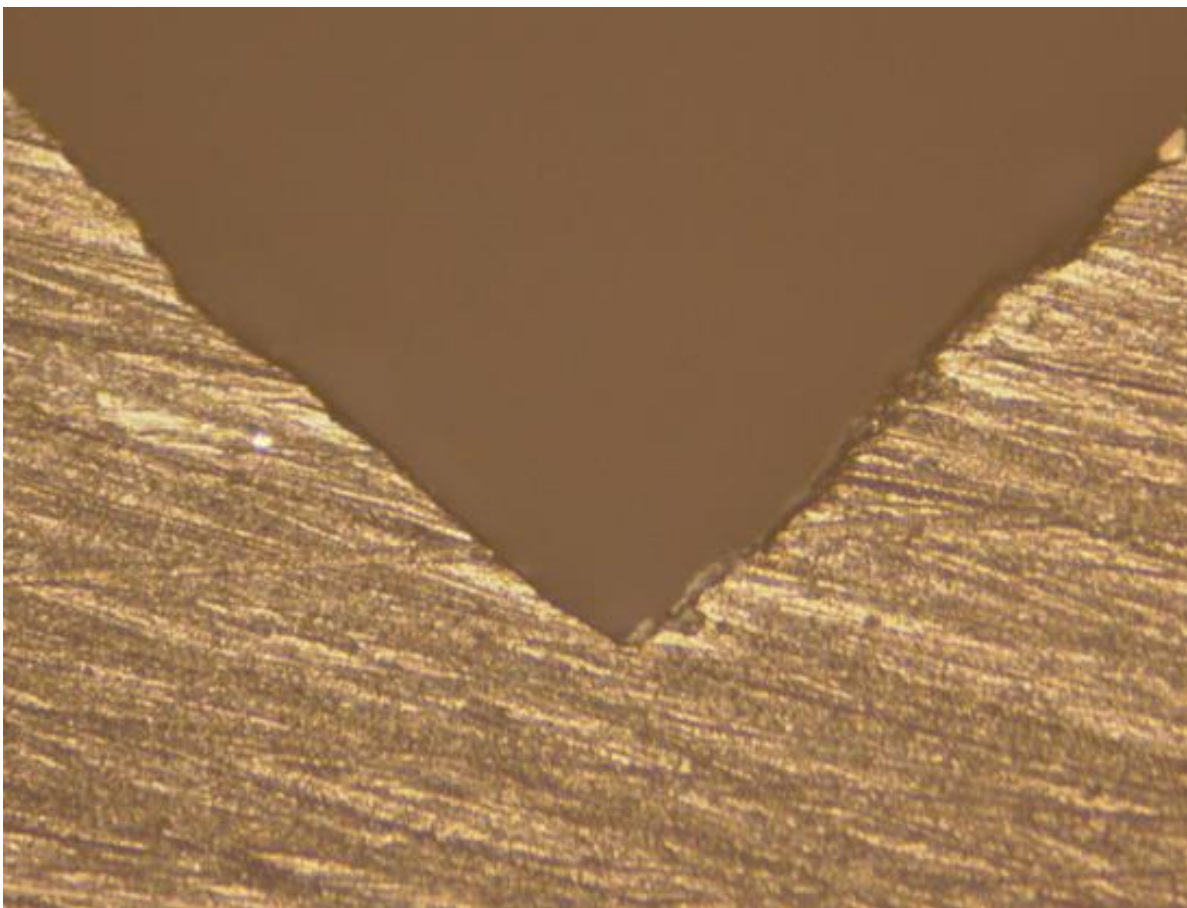


Figure 5-12: The notch of SENB specimen after curing

However, the shape of crack was different based on the different pre-crack methods. The width and length of crack was kept as the criteria from ASTM D 5045-99 where the crack length should be 2 times higher than the width of crack. Table 5-1 shows detail the shape and parameters of cracks. Where V shape crack was observed by Razor blade, U shape by Sawing, and current method showed sharper crack.

In addition, the different of pre-crack methods were also investigated after fracture test by fracture surface and initial crack surface (Figure 5-13). The fracture surface of UPR was not changed by different initial crack creation method (Figure 5-14). Meanwhile, the initial crack surfaces were much different and their surface roughness values were also different (Table 5-2). The higher average surface roughness (17  $\mu\text{m}$ ) and smaller width of crack represented more natural crack surface in compare to other methods.

Table 5-1: The shape of pre-crack with different methods.

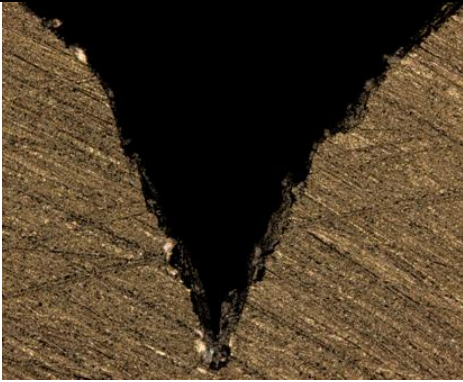


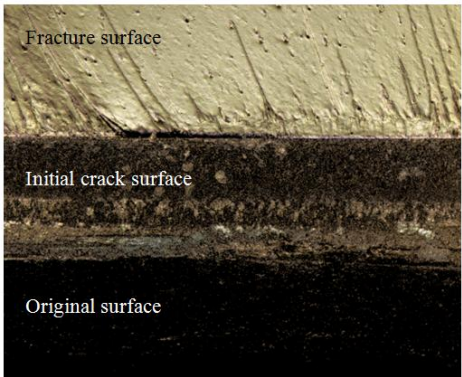
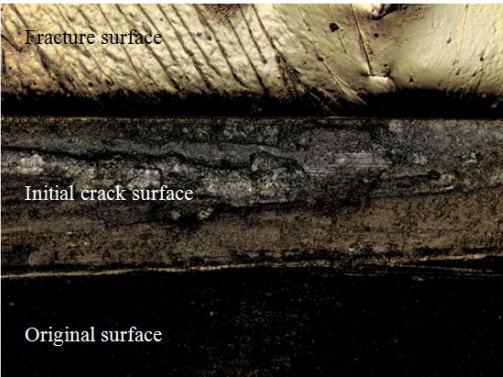
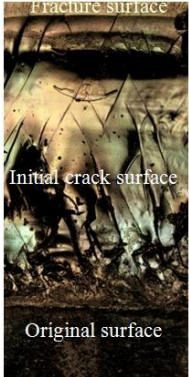
Razor blade	Sawing	Current method
		
Length: 560 $\mu\text{m}$ Average width: 334 $\mu\text{m}$	Length: 1,753 $\mu\text{m}$ Average width: 736 $\mu\text{m}$	Length: 2,218 $\mu\text{m}$ Average width: 108.4 $\mu\text{m}$

Table 5-2: The surface of pre-crack after fracture test.

2D images from confocal microscope		
Razor blade	Sawing	Current method
		
Surface roughness (Ra) of initial crack surface		
3 $\mu\text{m}$	7 $\mu\text{m}$	17 $\mu\text{m}$

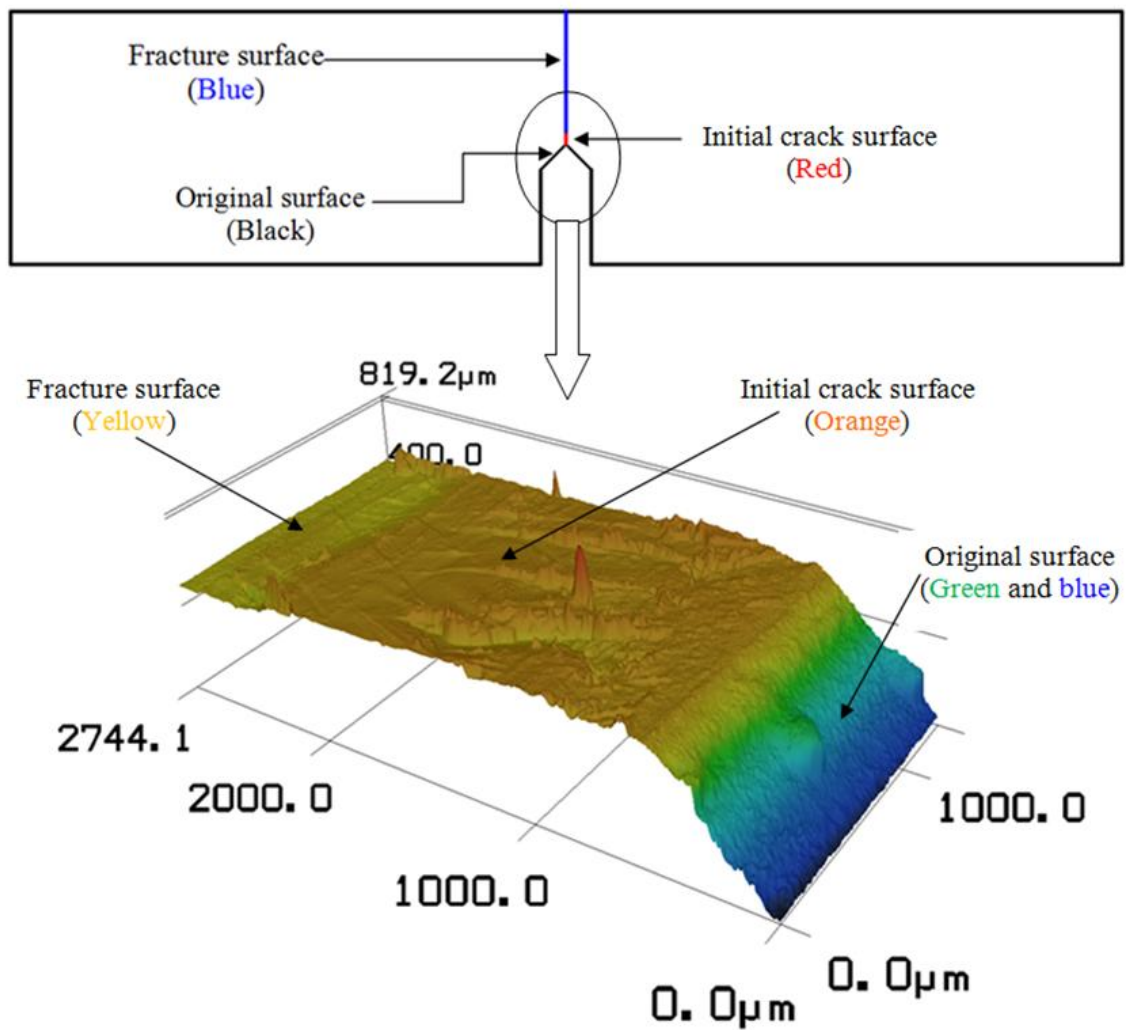


Figure 5-13: The configuration and surfaces of specimen after fracture test

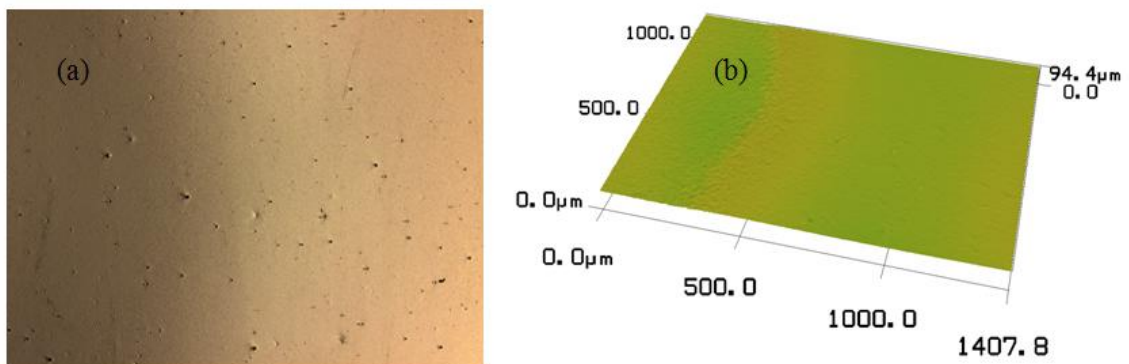


Figure 5-14: Fracture surface of UPR after fracture test: (a) 2D model and (b) 3D model

#### 5.4.1.2 Plane-strain fracture toughness $K_{IC}$ and $G_{IC}$ of UPR

The critical stress intensity factor was obtained based on the different initial crack methods. The test was also performed for the specimen without initial crack. Because of the notched edge, the SENB specimens were fractured in a straight line consistent with loading direction. The comparison of fracture toughness of those pre-crack methods can be seen at Figure 5-15. Generally, the new crack method showed the lowest stress intensity factor value and sawing method presented the highest value. Razor blade tapping method is the traditional pre-crack method that mentioned even in ASTM [102]. Although, the stress intensity factor of this method indicated a little bit lower value than no initial crack case. The different results also can be seen more detail at the Table 5-3. The current results agree well with the tendency in [100] where the natural crack possessed the lowest fracture toughness value. The reason of the difference can be attributed to the residual strain from each method [101]. Therefore, combining the morphology result in section 5.4.1.1, the current method can be concluded as the better pre-crack method.

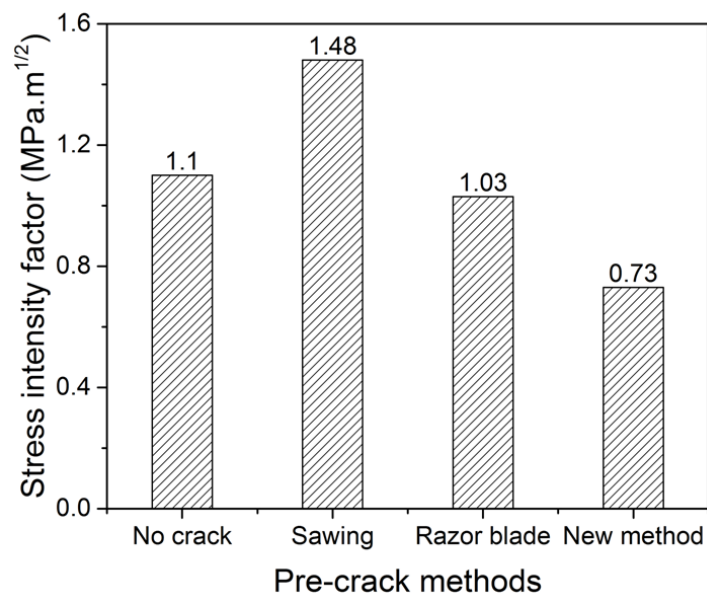


Figure 5-15: Critical stress intensity factor of different pre-crack methods

Table 5-3: The difference in pre-crack method.

Pre-crack methods	Difference (%)
No initial crack	50.88
Sawing	102.74
Razor blade	41.10
Current method	0

The strain energy release rate was calculated by equation (5-3). Similar with stress intensity factor,  $G_{IC}$  value was changed by the different initial crack creation methods (Table 5-4).

Table 5-4:  $G_{IC}$  of the different pre-crack methods.

Pre-crack methods	Elastic modulus (MPa)	Poisson's ratio	$G_{IC}$ (kJ/m <sup>2</sup> )
No initial crack	4,698	0.4045	0.1961
Sawing			0.3500
Razor blade			0.1889
Current method			0.0942

## 5.4.2 Effect of different fibers on interlaminar fracture toughness of composites

### 5.4.2.1 Mode I

The crack propagation was recorded simultaneously with load and displacement of DCB specimen (Figure 5-9), thus the mode I interlaminar fracture toughness was also calculated equally in each crack propagation length by formula (5-4). As a consequence, the delamination resistance curve (Figure 5-16) also generated by the calculated values accordingly. Initially, the crack were observed visually including the sound. From the

Figure 1-16, the initial fracture toughness was very small in compare to other crack propagation positions. It may be the behavior of UPR at the crack tip [92] and it is also evidenced by the strain energy release rate values are almost the same as the value at Table 5-4 (without initial crack) except the case of  $[M]_8$ . Some other neighbor crack tip positions, the delamination resistance was also small that may be attributed to the effect of Teflon film thickness that make the laminates around crack tip cannot bond well together. The higher crack length showed almost stable delamination resistance.

Practically, 5 specimens of each plate were tested and 11 crack propagation positions of one specimen were recorded. Then, the average interlaminar fracture toughness were summarized except the initial crack values (because of the UPR behavior) for each fiber composite (Figure 5-17). Interestingly, the different fibers can bring the different interlaminar fracture toughness values. Therefore, the combination of CSM and woven possessed the higher resistance than each pristine fiber. While, CSM indicated smallest ability in the open mode and  $[M_4/W_4]$  specimen showed the highest value.

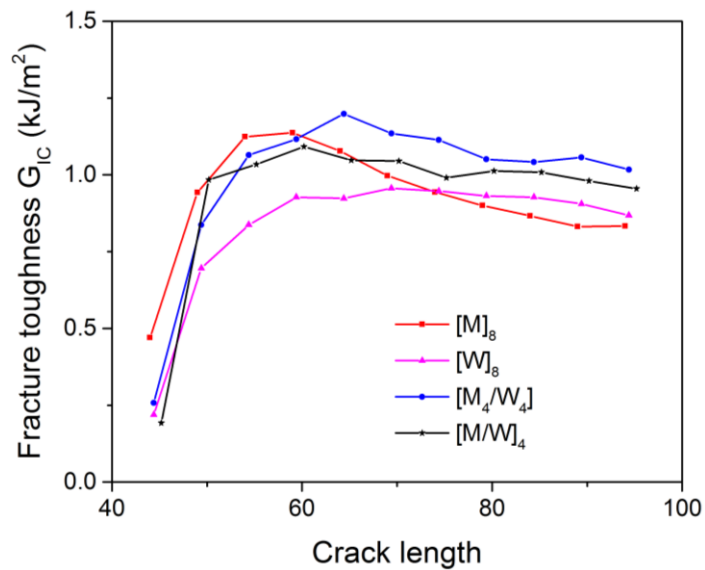


Figure 5-16: Delamination resistance curves with different fibers composites



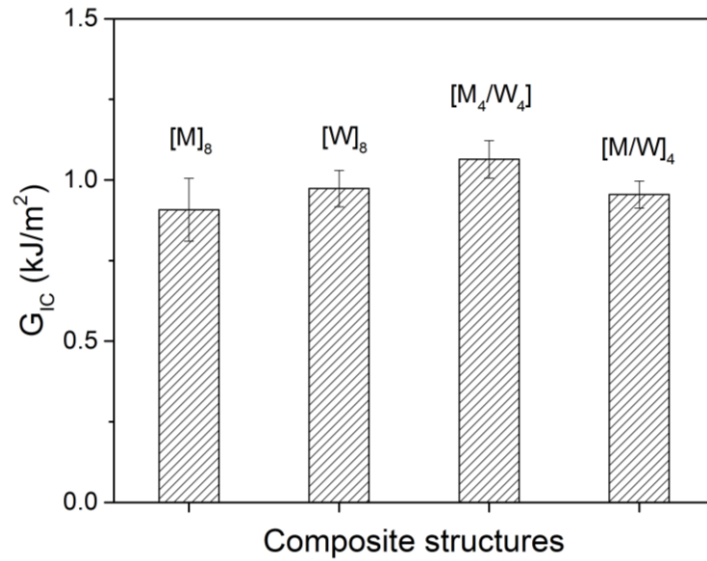


Figure 5-17: Mode I interlaminar fracture toughness of various glass fibers composite

We can see the fracture resistance order of CSM and woven at Figure 5-17 and 5-18 is changed because Figure 5-18 represents the average value but Figure 5-17 shows the specific specimen value. The reason of higher fracture toughness of composite materials than pure UPR can be attributed to the fiber bridging. And, the different fibers and their stacking sequence also represented the different amount of fiber bridging (Figure 5-18). The difference of fiber bridging also distinguishes fracture toughness values.

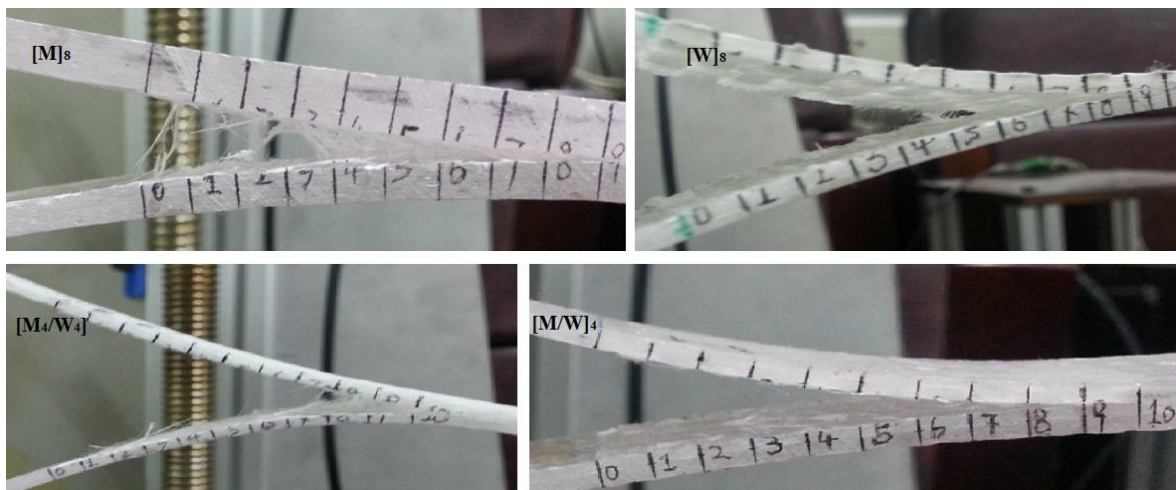


Figure 5-18: Fiber bridging of different glass fibers composite

### 5.4.2.2 Mode II

Almost the same tendency was also achieved from mode II fracture test for different glass fibers composite (Figure 5-19). Thus,  $[M_4/W_4]$  specimen still described the toughest materials, but woven had smallest in-plane shear resistance ability instead of CSM. In comparison with mode I interlaminar fracture toughness, all of glass fibers can relatively undergo higher mode II fracture loading.

However, the mode II fracture test did not considered the crack propagation. Thus, after the test, the specimens were only broken locally (Figure 5-20).

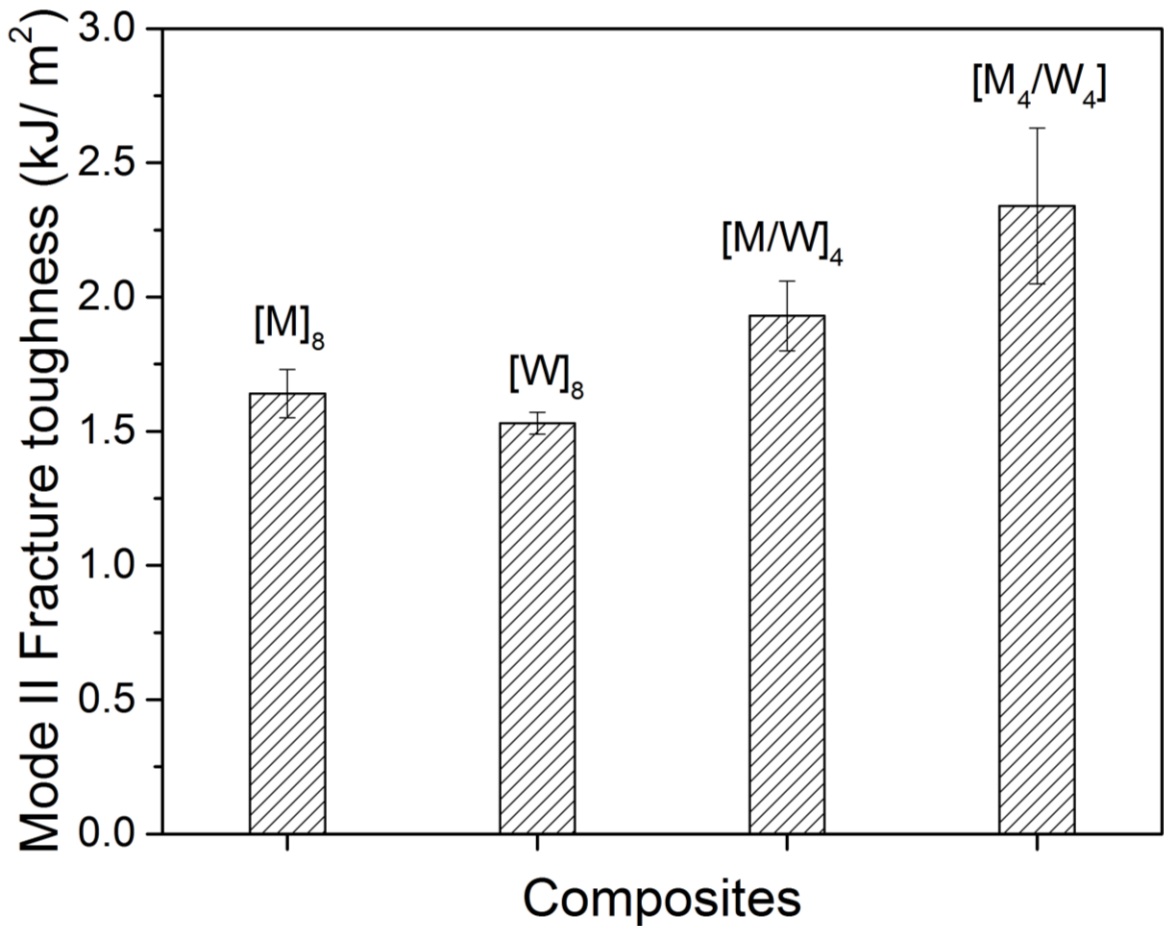


Figure 5-19: Mode II fracture toughness of different glass fibers composite

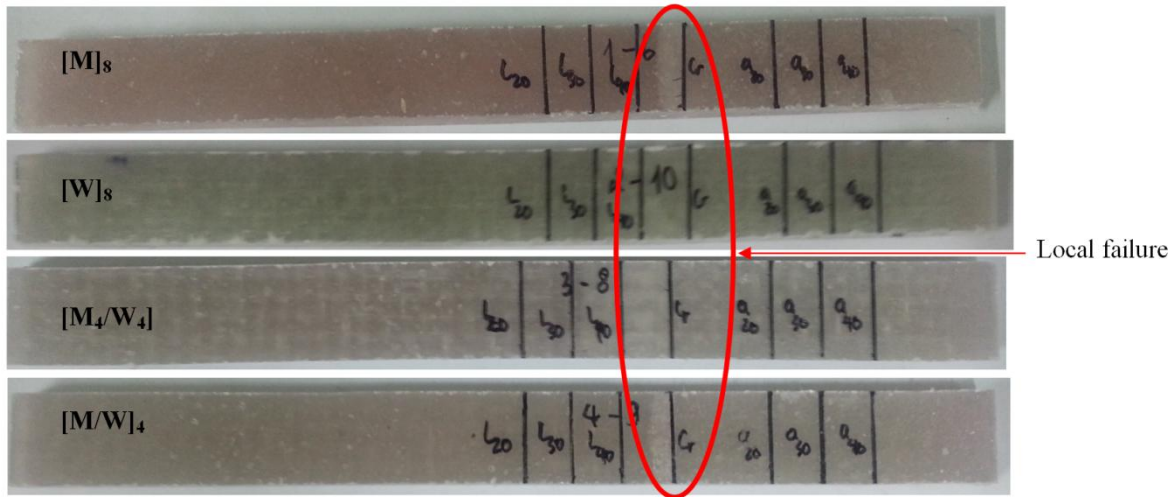


Figure 5-20: The specimens after mode II fracture test

## 5.5 Conclusions

A new pre-crack method was proposed in this study. It can be a better method due to the natural crack with sharper and smaller gap of initial crack geometry and lower residual strain. Thus, the critical stress intensity factor of natural initial crack of UPR was resulted in smaller value.

The mode I and mode II fracture behavior of different glass fibers reinforced UPR composite were investigated. The higher delamination resistance in both mode I and mode II was obtained for the glass fiber combination of CSM and woven. The bonding between 4 separated CSM and woven (M<sub>4</sub>/W<sub>4</sub>) showed the best quality and higher than [M/W]<sub>4</sub> although they have the same component but they have different stacking sequence. CSM and woven represented a little bit different in 2 mode fracture. In all case of fiber changes, NPC mode II fracture toughness is higher than in mode I delamination.

## **CHAPTER 6:**

### **Conclusions and future works**

## 6.1 Conclusions

The optimum conditions of dispersion of MWCNTs and UPR were found based on the mixing temperature, hardener ratio, and initial curing temperature. Most of conditions could improve the quality of dispersion and the mechanical properties of modified UPR.

The glass fiber changes could bring different mechanical properties of each fiber composite. Based on the rule of mixture (ROM), the combination of CSM and woven could be average properties of each fiber if their volume fraction is similar. Besides, the fabrication method using vacuum also have positive effect of the properties of various glass fibers composite.

From the optimum conditions, adding 0.1 wt.% MWCNTs into UPR can achieve higher mechanical properties of not only UPR but also various glass fibers composite reinforced modified UPR.

Current method of create initial crack of UPR was proposed and better results were obtained by sharper crack tip and smaller crack width, less residual strain. They were all resulted in smaller critical stress intensity factor value.

Finally, the glass fiber changed were also investigated by mode I and mode II interlaminar fracture toughness. The combination of CSM and woven possessed as the highest delamination resistance in both types of loading.

## 6.2 Future works

The new pre-crack method could bring a more natural initial crack, that could be used for further study the effect of MWCNTs on fracture toughness of UPR.

The main mechanism of delamination resistance was found, applying MWCNTs may improve the fracture toughness of various glass fibers composite as well. That may be the solution of the current challenging that is improving the weak out-of-plane behavior of laminated composite.

All of results in this thesis are experimental results. Therefore, using numerical method should be considered to verify the current results and to emphasize the role of MWCNTs in modified resin as well as modified GFRP composites. Nowadays, the materials normally include various compositions in different scales. For instance, composite materials involve CNTs (in nano-scale), UPR and fiber (in macro- or micro-scale). Therefore, the multi-scale simulation could be a high potential to solve the problems through nano-scale to macro-scale.

## REFERENCES

- [1] Jones RM. Mechanics of composite materials. *CRC press*; 1998 July 01.
- [2] History of Composites. The evolution of lightweight composite materials, *ThoughtCo., Science*; 2017 April 02.
- [3] Sathishkumar TP, Satheeshkumar S, Naveen J. Glass fiber-reinforced polymer composites—a review. *Journal of Reinforced Plastics and Composites*. 2014 Jul; 33 (13):1258-75.
- [4] Scheirs J, Long TE, editors. Modern polyesters: chemistry and technology of polyesters and copolyesters. *John Wiley & Sons*; 2005 Sep 1.
- [5] Ashby MF. Materials selection in mechanical design. *MRS Bull*; 2005 Dec 30.
- [6] Carl Z, Zweben C, Devon P. Composite materials, Mechanical Engineers' Handbook, chapter 10, 4th edition, *John Wiley&Sons, Inc.*; 2015.
- [7] Michael GB, Wilburn S, Allan BI, Albeert RL, Arthur BM. Processing and fabrication technology. *Technomic publication*; 1990.
- [8] Kelly A, Zweben C, editors. Comprehensive composite materials. Elsevier. The Boulevard, Langford Lane, Kidlington, Oxford, UK: *Elsevier Science Ltd.*; 2000. Volume 2. pp 1-57.
- [9] Campbell FC. Structural composite materials, chapter 1. *ASM International*; 2010.
- [10] S. Iijima, Helical Microtubules of Graphitic Carbon, *Nature*, 354 (1991) 56-58.
- [11] Erden S, Sever K, Seki Y, Sarikanat M. Enhancement of the mechanical properties of glass/polyester composites via matrix modification glass/polyester composite siloxane matrix modification. *Fibers and Polymers*. 2010; 11: 732-737.
- [12] Warriar A, Godara A, Rochez O, Mezzo L, Luizi F, Gorbatiikh L, Lomov SV, VanVuure AW, Verpoest I. The effect of adding carbon nanotubes to glass/epoxy composites in the fibre sizing and/or the matrix. *Composites Part A: Applied Science and Manufacturing*. 2010; 41: 532-538.
- [13] Godara A, Gorbatiikh L, Kalinka G, Warriar A, Rochez O, Mezzo L, Luizi F, Van Vuure AW, Lomov SV, Verpoest I. Interfacial shear strength of a glass fiber/epoxy bonding in composites modified with carbon nanotubes. *Composites Science and Technology*. 2010; 70: 1346-1352.
- [14] Du J, Bai J, Cheng H. The present status and key problems of carbon nanotube based polymer composites. *Express Polymer Letters*. 2007; 1: 253-273.
- [15] Allaoui A, Bai S, Cheng HM, Bai JB. Mechanical and electrical properties of a MWNT/epoxy composite. *Composites Science and Technology*. 2002; 62: 1993-1998.
- [16] Yeh MK, Tai NH, Liu JH. Mechanical behavior of phenolic-based composites

reinforced with multi-walled carbon nanotubes. *Carbon*. 2006; 44: 1-9.

[17] Montazeri A, Javadpour J, Khavandi A, Tcharkhtchi A, Mohajeri A. Mechanical properties of multi-walled carbon nanotube/epoxy composites. *Materials & Design*. 2010; 31: 4202-4208.

[18] Xie XL, Mai YW, Zhou XP. Dispersion and alignment of carbon nanotubes in polymer matrix: A review. *Materials Science & Engineering R-Reports*. 2005; 49: 89-112.

[19] Ma PC, Siddiqui NA, Marom G, Kim JK. Dispersion and functionalization of carbon nanotubes for polymer-based nanocomposites: a review. *Composites Part A: Applied Science and Manufacturing*. 2010; 41: 1345-1367.

[20] Hwang SH, Bang DS, Yoon KH, Park YB. Smart materials and structures based on carbon nanotube composites: *INTECH Open Access Publisher* (2011).

[21] Qian D, Dickey EC, Andrews R, Rantell T. Load transfer and deformation mechanisms in carbon nanotube-polystyrene composites. *Applied physics letters*. 2000; 76: 2868-2870.

[22] Battisti A, Skordos AA, Partridge IK. Monitoring dispersion of carbon nanotubes in a thermosetting polyester resin. *Composites Science and Technology*. 2009; 69: 1516-1520.

[23] Seyhan AT, Gojny FH, Tanoğlu M, Schulte K. Critical aspects related to processing of carbon nanotube/unsaturated thermoset polyester nanocomposites. *European polymer journal*. 2007; 43: 374-379.

[24] Sandler J, Shaffer M, Prasse T, Bauhofer W, Schulte K, Windle A. Development of a dispersion process for carbon nanotubes in an epoxy matrix and the resulting electrical properties. *Polymer*. 1999; 40: 5967-5971.

[25] Li J, Ma PC, Chow WS, To CK, Tang BZ, Kim JK. Correlations between percolation threshold, dispersion state, and aspect ratio of carbon nanotubes. *Advanced Functional Materials*. 2007; 17: 3207-3215.

[26] Ramanathan T, Abdala A, Stankovich S, Dikin D, Herrera-Alonso M, Piner R, et al. Functionalized graphene sheets for polymer nanocomposites. *Nature nanotechnology*. 2008; 3: 327-331.

[27] Ureña-Benavides EE, Kayatin MJ, Davis VA. Dispersion and rheology of multiwalled carbon nanotubes in unsaturated polyester resin. *Macromolecules*. 2013; 46: 1642-1650.

[28] Sahoo NG, Rana S, Cho JW, Li L, Chan SH. Polymer nanocomposites based on functionalized carbon nanotubes. *Progress in polymer science*. 2010; 35: 837-867.

[29] Bensadoun F, Kchit N, Billotte C, Trochu F, Ruiz E. A comparative study of dispersion techniques for nanocomposite made with nanoclays and an unsaturated polyester resin. *Journal of Nanomaterials*. 2011 (2011) 6.

[30] Shokrieh MM, Saeedi A, Chitsazzadeh M. Mechanical properties of multi-walled carbon nanotube/polyester nanocomposites. *Journal of Nanostructure in Chemistry*. 2013; 3: 1-5.



- [31] Beg MDH, Alam AM, Yunus RM, Mina MF. Improvement of interaction between pre-dispersed multi-walled carbon nanotubes and unsaturated polyester resin. *Journal of Nanoparticle Research*. 2015; 17: 1-13.
- [32] Alam AKM, Beg MDH, Yunus RM. Micro structure and fractography of multiwalled carbon nanotube reinforced unsaturated polyester nanocomposites. *Polymer Composites*. (2016).
- [33] Toorkey RF, Rajanna KC, Prakash PKS. Curing of unsaturated polyester: Network formation. *Journal of Chemical Education*. 1996; 73: 372-373.
- [34] d'Almeida JRM and Monteiro SN. The influence of the amount of hardener on the tensile mechanical behavior of an epoxy system. *Polymers for Advanced Technologies*. 1998; 9: 216-221.
- [35] Huang YJ, Leu JS. Curing of unsaturated polyester resins. Effects of temperature and initiator: 1. Low temperature reactions. *Polymer*. 1993; 34: 295-304.
- [36] Belloul N, Ahmed-Benyahia A, Serier A, Ouali N. Effect of Temperature and Initiator on Glass Fibre/Unsaturated Polyester Composite: Cross-linking, Mechanical Properties. In: Boukharouba T., Elboujdaini M., Pluvinage G. (eds) *Damage and Fracture Mechanics*. Springer, Dordrecht. 2009; 497-504.
- [37] Zhang J, Xu YC, Huang P. Effect of cure cycle on curing process and hardness for epoxy resin. *Express Polymer Letters*. 2009; 3: 534-541.
- [38] Kelly A, Zweben C, editors. Comprehensive composite materials. Elsevier. The Boulevard, Langford Lane, Kidlington, Oxford, UK: *Elsevier Science Ltd.*; 2000. Volume 2. pp 1-57.
- [39] Budai Z, Sulyok Z, Vargha V. Glass-fibre reinforced composite materials based on unsaturated polyester resins. *Journal of thermal analysis and calorimetry*. 2012; 109: 1533-1544.
- [40] Miwa M, Ohsawa T, Tahara K. Effects of fiber length on the tensile strength of epoxy/glass fiber and polyester/glass fiber composites. *Journal of Applied Polymer Science*. 1980; 25.5: 795-807.
- [41] Kim DW, Hennigan DJ, Beavers KD. Effect of fabrication processes on mechanical properties of glass fiber reinforced polymer composites for 49 meter (160 foot) recreational yachts. *International Journal of Naval Architecture and Ocean Engineering*. 2010; 2.1: 45-56.
- [42] Kim SY, Shim CS, Sturtevant C, Kim DW, Song HC. Mechanical properties and production quality of hand-layup and vacuum infusion processed hybrid composite materials for GFRP marine structures. *International Journal of Naval Architecture and Ocean Engineering*. 2014; 6.3: 723-736.
- [43] Petrova I, Ivanov E, Kotsilkova R, Tsekov Y, Angelov V. Applied study on mechanics of nanocomposites with carbon nanofillers. *Journal of Theoretical and Applied Mechanics*. 2013; 43: 67-76.

- [44] Guo P, Chen X, Gao X, Song H, Shen H. Fabrication and mechanical properties of well-dispersed multiwalled carbon nanotubes/epoxy composites. *Composites science and Technology*. 2007; 67: 3331-3337.
- [45] Song YS and Youn JR. Influence of dispersion states of carbon nanotubes on physical properties of epoxy nanocomposites. *Carbon*. 2005; 43: 1378-1385.
- [46] ASTM D638-03, Standard test method for tensile properties of plastics, *ASTM international, West Conshohocken, PA*; 2003.
- [47] Pan ZW, Xie SS, Lu L, Chang BH, Sun LF, Zhou WY, Wang G, Zhang DL. Tensile tests of ropes of very long aligned multiwall carbon nanotubes. *Applied Physics Letters*. 1999; 74: 3152-3154.
- [48] Yu MF, Lourie O, Dyer MJ, Moloni K, Kelly TF, Ruoff RS. Strength and breaking mechanism of multiwalled carbon nanotubes under tensile load. *Science*. 2000; 287: 637-640.
- [49] Shan Z, Qin S, Liu Q, Liu F. Key manufacturing technology & equipment for energy saving and emissions reduction in mechanical equipment industry. *International Journal of Precision Engineering and Manufacturing*. 2012; 13: 1095-1100.
- [50] Song X. Vacuum assisted resin transfer molding (VARTM): model development and verification. Blacksburg, Virginia, USA: Doctoral dissertation, *Virginia Polytechnic Institute and State University*. 2003.
- [51] Allaoui A, Bai S, Cheng HM, Bai JB. Mechanical and electrical properties of a MWNT/epoxy composite. *Composites science and technology*. 2002; 62: 1993-1998.
- [52] Montazeri A, Javadpour J, Khavandi A, Tcharkhtchi A, Mohajeri A. Mechanical properties of multi-walled carbon nanotube/epoxy composites. *Materials & Design*. 2010; 31: 4202-4208.
- [53] Coleman JN, Khan U, Blau WJ, Gun'ko YK. Small but strong: a review of the mechanical properties of carbon nanotube-polymer composites. *Carbon*. 2006; 44: 1624-1652.
- [54] Yeh MK, Tai NH, Liu JH. Mechanical behavior of phenolic-based composites reinforced with multi-walled carbon nanotubes. *Carbon*. 2006; 44: 1-9.
- [55] Shokrieh MM, Saeedi A, Chitsazzadeh M. Mechanical properties of multi-walled carbon nanotube/polyester nanocomposites. *Journal of Nanostructure in Chemistry*. 2013; 3: 1-5.
- [56] Ma PC, Siddiqui NA, Marom G, Kim JK. Dispersion and functionalization of carbon nanotubes for polymer-based nanocomposites: a review. *Composites Part A: Applied Science and Manufacturing*. 2010; 41: 1345-1367.
- [57] Seyhan AT, Gojny FH, Tanoğlu M, Schulte K. Critical aspects related to processing of carbon nanotube/unsaturated thermoset polyester nanocomposites. *European Polymer Journal*. 2007; 43: 374-379.
- [58] Li WZ, Wang DZ, Yang SX, Wen JG, Ren ZF. Controlled growth of carbon nanotubes

- on graphite foil by chemical vapor deposition. *Chemical Physics Letters*. 2001; 335: 141-149.
- [59] Zhu S, Su CH, Lehoczky SL, Muntele I, Ila D. Carbon nanotube growth on carbon fibers. *Diamond and Related Materials*. 2003; 12: 1825-1828.
- [60] De Riccardis MF, Carbone D, Makris TD, Giorgi R, Lisi N, Salernitano E. Anchorage of carbon nanotubes grown on carbon fibres. *Carbon*. 2006; 44: 671-674.
- [61] Laachachi A, Vivet A, Nouet G, Doudou BB, Poilane C, Chen J, Ayachi MH. A chemical method to graft carbon nanotubes onto a carbon fiber. *Materials Letters*. 2008; 62: 394-397.
- [62] Gong QJ, Li HJ, Wang X, Fu QG, Wang ZW, Li KZ. In situ catalytic growth of carbon nanotubes on the surface of carbon cloth. *Composites Science and Technology*. 2007; 67: 2986-2989.
- [63] Zhao J, Liu L, Guo Q, Shi J, Zhai G, Song J, Liu Z. Growth of carbon nanotubes on the surface of carbon fibers. *Carbon*. 2008; 46: 380-383.
- [64] De Greef N, Zhang L, Magrez A, Forró L, Locquet JP, Verpoest I, Seo JW. Direct growth of carbon nanotubes on carbon fibers: Effect of the CVD parameters on the degradation of mechanical properties of carbon fibers. *Diamond and Related Materials*. 2015; 51: 39-48.
- [65] Thostenson ET, Li WZ, Wang DZ, Ren ZF, Chou TW. Carbon nanotube/carbon fiber hybrid multiscale composites. *Journal of Applied physics*. 2002; 91: 6034-6037.
- [66] Mathur RB, Chatterjee S, Singh BP. Growth of carbon nanotubes on carbon fibre substrates to produce hybrid/phenolic composites with improved mechanical properties. *Composites Science and Technology*, 2008; 68: 1608-1615.
- [67] Kepple KL, Sanborn GP, Lacasse PA, Gruenberg KM, Ready WJ. Improved fracture toughness of carbon fiber composite functionalized with multi walled carbon nanotubes. *Carbon*. 2008; 46: 2026-2033.
- [68] Sager RJ, Klein PJ, Lagoudas DC, Zhang Q, Liu J, Dai L, Baur JW. Effect of carbon nanotubes on the interfacial shear strength of T650 carbon fiber in an epoxy matrix. *Composites Science and Technology*. 2009; 69: 898-904.
- [69] Kar KK, Rahaman A, Agnihotri P, Sathiyamoorthy D. Synthesis of carbon nanotubes on the surface of carbon fiber/fabric by catalytic chemical vapor deposition and their characterization. *Fullerenes, Nanotubes and Carbon Nanostructures*. 2009; 17: 209-229.
- [70] Dai J, Soliman E, Safdari M, Al-Haik M, Reda Taha MM. Effect of carbon nanotube growth conditions on strength and stiffness of carbon and glass fiber polymer composites. In Proceedings of 51st AIAA/ASME/ASCE/AHS/ASC Structures. *Structural Dynamics, and Materials Conference*. 2010.
- [71] Sharma SP, Lakkad SC. Effect of CNTs growth on carbon fibers on the tensile strength of CNTs grown carbon fiber-reinforced polymer matrix composites. *Composites Part A: Applied Science and Manufacturing*. 2011; 42: 8-15.

- [72] An F, Lu C, Li Y, Guo J, Lu X, Lu H, He S, Yang Y. Preparation and characterization of carbon nanotube-hybridized carbon fiber to reinforce epoxy composite. *Materials & Design*. 2012; 33: 197-202.
- [73] Zu M, Li Q, Zhu Y, Dey M, Wang G, Lu W, Deitzel JM, Gillespie JW, Byun JH, Chou TW. The effective interfacial shear strength of carbon nanotube fibers in an epoxy matrix characterized by a microdroplet test. *Carbon*. 2012; 50: 1271-1279.
- [74] Jamnani BD, Hosseini S, Rahmanian S, Rashid SA, Balavandy SK. Grafting carbon nanotubes on glass fiber by dip coating technique to enhance tensile and interfacial shear strength. *Journal of Nanomaterials*. 2015; 16: 1-7.
- [75] Lili S, Yan Z, Yuexin D, Zuoguang Z. Interlaminar shear property of modified glass fiber-reinforced polymer with different MWCNTs. *Chinese Journal of Aeronautics*. 2008; 21: 361-369.
- [76] Godara A, Mezzo L, Luizi F, Warriar A, Lomov SV, Van Vuure AW, Gorbatikh L, Moldenaers P, Verpoest I. Influence of carbon nanotube reinforcement on the processing and the mechanical behaviour of carbon fiber/epoxy composites. *Carbon*. 2009; 47: 2914-2923.
- [77] Rahman MM, Zainuddin S, Hosur MV, Malone JE, Salam MB, Kumar A, Jeelani S. Improvements in mechanical and thermo-mechanical properties of e-glass/epoxy composites using amino functionalized MWCNTs. *Composite Structures*. 2012; 94: 2397-2406.
- [78] Rahman MM, Zainuddin S, Hosur MV, Robertson CJ, Kumar A, Trovillion J, Jeelani S. Effect of NH<sub>2</sub>-MWCNTs on crosslink density of epoxy matrix and ILSS properties of e-glass/epoxy composites. *Composite Structures*. 2013; 95: 213-221.
- [79] Shokrieh MM, Saeedi A, Chitsazzadeh M. Evaluating the effects of multi-walled carbon nanotubes on the mechanical properties of chopped strand mat/polyester composites. *Materials & Design*. 2014; 56: 274-279.
- [80] Taraghi I, Fereidoon A, Mohyeddin A. The effect of MWCNTs on the mechanical properties of Woven Kevlar/epoxy composites. *Steel and Composite Structures*. 2014; 17: 825-834.
- [81] Genedy M, Daghash S, Soliman E, Taha MM. Improving fatigue performance of GFRP composite using carbon nanotubes. *Fibers*. 2015; 3: 13-29.
- [82] Tarfaoui M, Lafdi K, El Moumen A. Mechanical properties of carbon nanotubes based polymer composites. *Composites Part B: Engineering*. 2016; 103: 113-121.
- [83] Mahato KK, Rathore DK, Prusty RK, Dutta K, Ray BC. Tensile behavior of MWCNT enhanced glass fiber reinforced polymeric composites at various crosshead speeds. *InIOP Conference Series: Materials Science and Engineering*. 2017; 178: 1-7.
- [84] Warriar A, Godara A, Rochez O, Mezzo L, Luizi F, Gorbatikh L, Lomov SV, VanVuure AW, Verpoest I. The effect of adding carbon nanotubes to glass/epoxy composites in the fibre sizing and/or the matrix. *Composites Part A: Applied Science and Manufacturing*. 2010; 41: 532-538.
- [85] Haque A, Ramasetty A. Theoretical study of stress transfer in carbon nanotube

reinforced polymer matrix composites. *Composite Structures*. 2005; 71: 68-77.

[86] Behabtu N, Green MJ, Pasquali M. Carbon nanotube-based neat fibers. *Nano today*. 2008; 3: 24-34.

[87] Wu AS, Chou TW. Carbon nanotube fibers for advanced composites. *Materials Today*. 2012; 15: 302-310.

[88] Veedu VP, Cao A, Li X, Ma K, Soldano C, Kar S, Ajayan PM, Ghasemi-Nejhad MN. Multifunctional composites using reinforced laminae with carbon-nanotube forests. *Nature materials*. 2006; 5: 457-462.

[89] Bhanushali H, Bradford PD. Woven glass fiber composites with aligned carbon nanotube sheet interlayers. *Journal of Nanomaterials*. 2016; 1-9.

[90] Ding W. Delamination analysis of composite laminates. *University of Toronto*; 2000.

[91] Anderson TL. Fracture mechanics: Fundamentals and applications. *CRC press*; 2017.

[92] Ashrafi B, Guan J, Mirjalili V, Zhang Y, Chun L, Hubert P, Simard B, Kingston CT, Bourne O, Johnston A. Enhancement of mechanical performance of epoxy/carbon fiber laminate composites using single-walled carbon nanotubes. *Composites science and technology*. 2011 Sep 9; 71 (13): 1569-78.

[93] Seyhan AT, Tanoğlu M, Schulte K. Tensile mechanical behavior and fracture toughness of MWCNT and DWCNT modified vinyl-ester/polyester hybrid nanocomposites produced by 3-roll milling. *Materials Science and Engineering: A*. 2009 Oct 15; 523 (1-2): 85-92.

[94] Eskizeybek V, Avci A, Gülce A. The Mode I interlaminar fracture toughness of chemically carbon nanotube grafted glass fabric/epoxy multi-scale composite structures. *Composites Part A: Applied Science and Manufacturing*. 2014 Aug 1; 63: 94-102.

[95] Grimmer CS, Dharan CK. Enhancement of delamination fatigue resistance in carbon nanotube reinforced glass fiber/polymer composites. *Composites Science and Technology*. 2010 Jun 1; 70 (6): 901-8.

[96] Srivastava VK, Gries T, Veit D, Quadflieg T, Mohr B, Kolloch M. Effect of nanomaterial on mode I and mode II interlaminar fracture toughness of woven carbon fabric reinforced polymer composites. *Engineering Fracture Mechanics*. 2017 Jul 1; 180: 73-86.

[97] Rikards R, Buchholz FG, Bledzki AK, Wacker G, Korjakin A. Mode I, mode II, and mixed-mode I/II interlaminar fracture toughness of GFRP influenced by fiber surface treatment. *Mechanics of composite materials*. 1996 Sep 1; 32 (5): 439-62.

[98] Leonard LW, Wong KJ, Low KO, Yousif BF. Fracture behaviour of glass fibre-reinforced polyester composite. *Proceedings of the Institution of Mechanical Engineers, Part L: Journal of Materials: Design and Applications*. 2009 Apr 1; 223 (2): 83-9.

[99] Masud AK, Zaman AK, Al-Khaled A. Effects of environment on fracture toughness of glass fiber/polyester composite. *Journal of Mechanical Engineering*. 2007; 38: 38-44.

[100] De Souza JM, Yoshimura HN, Peres FM, Schön CG. Effect of specimen pre-cracking method and notch geometry in plane strain fracture toughness tests as applied to a PMMA resin. *Polymer Testing*. 2012 Sep 1; 31 (6): 834-40.

[101] Kuppasamy N, Tomlinson RA. Repeatable pre-cracking preparation for fracture testing of polymeric materials. *Engineering Fracture Mechanics*. 2016 Feb 1; 152: 81-7.

[102] ASTM D5045-99, Standard Test Methods for Plane-Strain Fracture Toughness and Strain Energy Release Rate of Plastic Materials. *Annual Book of ASTM Standards*. 8; 2007.

[103] ASTM D5528-13. Standard test method for mode I interlaminar fracture toughness of unidirectional fiber-reinforced matrix composites. *ASTM International, West Conshohocken, PA*; 2013.

[104] ASTM D7905-14. Standard test method for determination of the mode II interlaminar fracture toughness of unidirectional fiber-reinforced polymer matrix composites. Space simulation; aerospace and aircraft; composite materials. *ASTM International, West Conshohocken, PA*; 2015.

## RESEARCH ACTIVITIES

### Journal papers

1. Pham-Thanh Nhut, **Van-Tho Hoang** and Young Jin Yum. "Evaluation of cavitations erosion of a propeller blade surface made of composite materials". *Journal of Mechanical Science and Technology*, Vol. 29, Issue 4, pp. 1629-1636, (2015).
2. **Van-Tho Hoang** and Young-Jin Yum. "Optimization of mixing process and effect of multi-walled carbon nanotubes on tensile properties of unsaturated polyester resin in composite materials". *Journal of Mechanical Science and Technology*, Vol. 31, Issue 4, pp. 1621-1627, (2017).
3. Huu-Duc Nguyen-Tran, **Van-Tho Hoang**, Ta Van Do, Doo-Man Chun and Young-Jin Yum. "Effect of multi-walled carbon nanotubes on the mechanical properties of carbon fiber reinforced polyamide-6/polypropylene composites for light weight automotive parts". *Materials 2018*, 11, 429.
4. **Van-Tho Hoang** and Young-Jin Yum. "Optimization of the fabrication conditions and effects of multi-walled carbon nanotubes on the tensile properties of various glass fibers/unsaturated polyester resin composite structures". *e-Polymers*, accepted (April 2018).
5. Rui Li, Soon Yong Yang, Young Jin Yum, Yong Seok Kim, **Van-Tho Hoang**, Won Jun Kim. "A study on the Additive Manufacturing (AM) of Piercing Punch by the PBF Method of Metal 3D Printing Using the Mold Steel Powder Materials". *Journal of Mechanical Science and Technology*, submitted (2018).

## **Conference papers**

1. Nguyen Tran Huu Duc, Chi-Vinh Ngo, **Van-Tho Hoang**, Young-Jin Yum and Doo-Man Chun, “Fabrication of Light Weight Composite using Carbon Nanotube (CNT) and Carbon Fiber for Automotive Applications”, *The Korean Society of Mechanical Engineers*, 2014.4, 150-151.
2. Nguyen Tran Huu Duc, Chi-Vinh Ngo, **Van-Tho Hoang**, Young-Jin Yum and Doo-Man Chun, “Carbon nanotube and carbon fiber reinforced polymer composite for light weight automotive part”, *The Korean Society of Mechanical Engineers*, 2014.5, 11-11.
3. **Van-Tho Hoang** and Young-Jin Yum, “Effect of stacking sequence on deformation of laminated composite structures”, *The Korean Society of Mechanical Engineers*, 2014.5, 10-10.
4. D. M. Chun, H. S. Oh, Mohammad Nur E AlamAl Nasim, Chi-Vinh Ngo, **Van-Tho Hoang** and Young-Jin Yum , “Study of Carbon Deposition using Nano-Particle Deposition System”, *The Korean Society of Mechanical Engineers*, 2014.5, 571-571.
5. **Van-Tho Hoang** and Young-Jin Yum, “Effect of stacking sequence and fiber volume fraction on deformation of laminated composite structures”, *The Korean Society of Mechanical Engineers*, 2014.11, 2158-2161.
6. Young-Jin Yum and **Van-Tho Hoang**, “The Effect of Carbon Nanotubes and Graphene Oxide on Mechanical Properties of Polyester Resin”, *The Korean Society of Mechanical Engineers*, 2015.02, 45-45.
7. Nguyen Tran Huu Duc, **Van-Tho Hoang**, Young-Jin Yum and Doo-Man Chun, “Injection molding of carbon nanotube and carbon fiber reinforced hierarchical polymer composite for light weight automotive part”, *International conference on Advances in Composite materials and Structures*, 2015.4, 36-36 (Istanbul, Turkey).
8. **Van-Tho Hoang** and Young-Jin Yum, “The Effect of Multiwalled Carbon Nanotubes and Graphene Oxide on the Tensile Properties of Unsaturated Polyester Resin in Composite Materials”, *The Korean Society of Mechanical Engineers*, 2015.11, 2537-2542.
9. P.T. Nhut, **Van-Tho Hoang** and Young-Jin Yum, “Mechanical Properties of Alkali Treated Coconut Trunk Particles in Composite Materials”, *The Korean Society of precision Engineers*, 2015.12, 116-116.
10. Jin-Young Kim, **Van-Tho Hoang**, Vo Quoc Truong, Bo-Hung Kim and Young-Jin Yum, “Study on the Deformation of Casting Part”, *The Korean Society of Mechanical Engineers*, 2016.04, 384-385.
11. **Van-Tho Hoang**, Jin-Young Kim and Young-Jin Yum, “Tensile Properties of Multi-walled Carbon Nanotubes/Unsaturated Polyester Resin Mixing by Stir Method”, *The Korean Society of Mechanical Engineers*, 2016.12, 2416-2418.



12. **Van-Tho Hoang** and Young-Jin Yum, “Effect of Multi-walled Carbon Nanotubes on the tensile properties of Glass fiber chopped strand mat /Unsaturated Polyester Resin”, *The Korean Society of Mechanical Engineers*, 2017.04, 305-306.
13. Young Jin Yum, Soon Yong Yang, Yong Seok Kim, **Van-Tho Hoang**, Jin Young Kim, Seong Woong Choi and Jong Won Kum, “A Study on the Fabrication of Punch for the Post Processing of Ultra High Strength Part by Hot Stamping Using 3D Printing Technology”, *The Korean Society of Mechanical Engineers*, 2017.04, 307-308.
14. Li Rui, Yong Seok Kim, Soon Yong Yang, **Van-Tho Hoang**, Young Jin Yum and Jong Won Kum, “A study on Analytical Prediction of Punch Strength required for Ultra high strength parts in piercing process after hot stamping”, *International forum on strategic technology*, 2017.05, 70-71.
15. Li Rui, **Van-Tho Hoang**, Jong Won Kum, Yong Seok Kim, Young Jin Yum and Soon Yong Yang, “A study on the Prediction of Punch shape range for improving Punch strength by partial semi-additive method using metal 3D printing technique”, *21<sup>st</sup> International conference on Mechatronics technology*, 2017.10, 350-354.
16. **Van-Tho Hoang** and Young-Jin Yum, “Effect of Multi-walled Carbon Nanotubes and fabrication method on the tensile properties of glass fiber/polyester composite materials”, *21<sup>st</sup> International conference on Mechatronics technology*, 2017.10, 358-361.
17. Ta Van Do, **Van-Tho Hoang** and Doo-Man Chun, “Effect of water absorption on mechanical properties of PA6/PP composite materials”, *21<sup>st</sup> International conference on Mechatronics technology*, 2017.10, 362-365.
18. Yong Seok Kim, Li Rui, **Van-Tho Hoang**, Jong Won Kum, Young Jin Yum and Soon Yong Yang, “A study on the Production of full-additive manufacturing Punch fabricated of high-strength mold steel powder materials using 3DP technique”, *21<sup>st</sup> International conference on Mechatronics technology*, 2017.10, 366-371.
19. **Van-Tho Hoang** and Young-Jin Yum, “Effect of Multi-walled Carbon Nanotubes and fabrication method on Flexural properties of Glass fiber/ Polyester composite materials”, *The Korean Society of Mechanical Engineers*, 2017.11, 207-207.
20. **Van-Tho Hoang** and Young-Jin Yum, “Effect of fibers and stacking sequence on mode II fracture toughness of glass fiber reinforced unsaturated polyester resin composites”, *The Korean Society of Mechanical Engineers*, spring conference (CAE and Applied Mechanics Division), 2018.04, 280-281.
21. Li Rui, Yong Seok Kim, **Van-Tho Hoang**, Young Jin Yum, Soon Yong Yang, and Won Jun Kim, “A study on the Mechanical properties of HWS high Wear resistance Steel powder Material deposited by directed Energy deposition process”, *The Korean Society of Mechanical Engineers*, spring conference (CAE and Applied Mechanics Division), 2018.04, 284-285.

## **R&D Projects**

- 1.** Numerical simulation (ABAQUS) the behavior of shape memory implant devices in human body.
  - Funded by: Kang&Park medical Company.
  - Principle Investigator: Prof. Young-Jin Yum.
  
  - *Role: statics simulation by ABAQUS (main contribution).*
  
- 2.** Sunroof frame development of light weight with high stiffness using carbon-nano composite.
  - Funded by: Ministry of Industry and Commercial, South Korea.
  - Principle Investigator: Prof. Young-Jin Yum and Prof. Doo-Man Chun.
  
  - *Role: Fabrication and mechanical tests (main contribution).*
  
- 3.** Experimental and numerical (ABAQUS) investigation tensile and fatigue behavior of shape memory alloys (SMA) implant devices in human body.
  - Funded by Kang&Park medical Company.
  - Principle Investigator: Prof. Young-Jin Yum.
  
  - *Role: Test and simulation (main contribution).*
  
- 4.** Development of Structural Analysis Technology for the Casting Using Different Analysis Tools.
  - Funded by: Hyundai Motor Company.
  - Principle Investigator: Prof. Young-Jin Yum and Prof. Bo-Hung Kim.
  
  - *Role: statics simulation by ABAQUS (main contribution).*
  
- 5.** Fundamental research for cutting-process of ultra high strength product (1,500 MPa) and development of hot-stamping mold with 3D printing method.
  - Funded by Korea Research Foundation.
  - Principle Investigator: Prof. Soon-Young Yang and Prof. Young-Jin Yum.
  
  - *Role: Material testing includes tensile, compressive, hardness, impact, density and wear (main contribution).*
  
- 6.** Structure and CFD analysis of desulfurization equipment stirrer of thermal power plant.
  - Funded by SungWoo Corporation.
  - Principle Investigator: Prof. Young-Jin Yum and Prof. Kyung-Sik Chang
  
  - *Role: statics simulation by ABAQUS (main contribution).*